

MOLECULARLY IMPRINTED POLYMER SENSOR SYSTEMS FOR ENVIRONMENTAL ESTROGENIC ENDOCRINE DISRUPTING CHEMICALS



By

NOMAPHELO NTSHONGONTSI

(MSc Nanoscience)

UNIVERSITY of the
WESTERN CAPE

A thesis submitted in fulfilment of the requirements for the degree of

PHILOSOPHIAE DOCTOR

In the

**Department of Chemistry
Faculty of Science
University of the Western Cape, South Africa**

Supervisor: Prof Emmanuel I. Iwuoha

January 2018

ABSTRACT

There is growing concern on endocrine disrupting compounds (EDCs). The presence of drugs in water supplies was first realized in Germany in the early 1990s when environmental scientists discovered clofibric acid. Clofibric acid has the ability to lower cholesterol in ground water below a water treatment plant. Endocrine disrupting compounds can be defined as those chemicals with the ability to alter daily functioning of the endocrine system in living organisms. There are numerous molecules that are regarded or referred to as EDCs such as but not limited to organochlorinated pesticides, industrial chemicals, plastics and plasticizers, fuels, estrogens and many other chemicals that are found in the environment or are in widespread use. 17β -estradiol is the principal estrogen found in mammals during reproductive years. Estriol is produced in large quantities during pregnancy. 17β -estradiol is the strongest, estriol the weakest. Estriol is water soluble, estrone and estradiol are not. Although estrogen is produced in women they are also at risk of over exposure to estrogen. Pesticides are extensively used today in agricultural settings to prevent and control pests. Various pesticides, including banned organochlorines (OCs) and modern non-persistent pesticides, have shown the ability to disrupt thyroid activity, disturbing the homeostasis of the thyroid system. Because these EDCs have adverse effects on health of both human and wildlife, it is imperative to develop viable cost-effective analytical methods for the detection of these EDCs in complicated samples and at very low concentrations. Very high selectivity towards particular compounds is a very important property for the suitability of a detection method. This is because these compounds mostly coexist in complex matrices which makes the detection of a specific compound very challenging. It is paramount to develop highly sensitive and selective methods for the detection of these estrogens and phosphoric acid-based pesticides at trace levels. Generally the methods used include immunological methods, chemiluminescence, high performance liquid

chromatography (HPLC), liquid chromatography-mass spectrometry (LC-MS) and gas chromatography-mass spectrometry (GC-MS), which combined with sample pretreatment methods, such as liquid-liquid extraction (LLE), solid-phase extraction (SPE), pressurised liquid extraction (PLE) and accelerated solvent extraction (ASE), etc., are the techniques of choice when it comes to the detection of endogenous EDCs and eEDCs. These processes were considered complicated, time consuming, to have low selectivity, and use large amounts of organic solvents. Therefore, choosing a suitable sample pretreatment method is very important. Molecularly imprinted polymers (MIPs) offer a tailor made methodology for the fabrication of electrochemical sensors, by the polymerization (both chemically and electrochemically) of functional monomers in the presence of the target analyte or analyte of interest and an interaction between the target analyte and functional monomer usually occurs through non-covalent interactions. Conducting polymers can be applied in the fabrication of the MIP sensors to ensure good conductivity. They can be applied on their own or can form composites with metals or through homo/heteropolymerization with other polymers. In this study conducting polymers were used in the fabrication of molecularly imprinted polymer sensors. Polypyrrole was used as the conducting polymer electrodeposited on the surface of a glassy carbon electrode for the detection of dimethoate, an organophosphorus pesticide. Using cyclic voltammetry (CV) pyrrole was electrochemically polymerized to form a film of polypyrrole. CV and square wave voltammetry (SWV) were used to characterize the thin polymer film deposited on the electrode surface. It was determined to be a suitable material for the mediation of electron transfer from the solution to the electrode and was characterised by a D_0 of $4.1 \times 10^{-5} \text{ m}^2 \cdot \text{s}^{-1}$ showing a relatively fast electron transfer. The dimethoate had a dynamic linear range (DLR) of 0.01 nM – 0.14 nM. The limit of detection (LOD) of the sensor was found to be 0.035 nM, thus showing that the sensor can detect concentrations of acetylthiocholine chloride (ATCl) even at low concentration as 0.035 nM dimethoate that may be present and sensitivity

of 0.32 $\mu\text{A/nM}$. The development of an AuNPs nanocomposite is reported in this study for the detection of estrone. The results obtained showed the successful synthesis of AuNPs with particle shapes ranging from spherical to triangle and undefined prism-like structures, the other shapes arose from the aggregation of the spherical structures. The particle sizes ranging between 51.37-56.48 nm. Furthermore, the optical absorption spectrum from UV-Vis of AuNPs showed the intrinsic band at about 528.5 nm which further indicates the successful fabrication of AuNPs. The narrow band demonstrates the excellent dispersed state of gold nanoparticles. From the absorbance spectrum, the $E = h \times C/\lambda_{\text{onset}}$ equation was used to determine the band gap of the particles and it was found that the energy band gap was 1.98 eV characteristic of material with conductive properties. The AuNPs were used to enhance the conductive properties of poly(3,4-ethylenedioxythiophene) a known conducting polymer selected for the fabrication of the MIP sensor. The use of the nanocomposite in the sensor development showed good electrochemical properties. In CV there was an observable decrease in the analytical signal of the redox probe $[\text{Fe}(\text{CN})_6]^{-3/-4}$ with an increase in the concentration of the analyte of interest. There was also a decrease in the semi-circle obtained from the Nyquist plot with an increase in concentration. The phenomenon in both techniques can be attributed to the occupation of the analyte into the cavities that were formed during MIP formation. The study of the successful chemical synthesis of a poly(methacrylic-co-3,4-ethylenedioxythiophene) copolymer P(MAA-co-EDOT) from methacrylic acid and 3,4-ethylenedioxythiophene monomers through oxidation using ammonium persulfate was also reported. High resolution scanning electron microscopy (HRSEM) was used for the determination of the surface morphologies the polymers, and which exhibited packed coral and irregular coral-like structures of the P(MAA-co-EDOT) and around poly(methacrylic acid) (PMAA) surface due to the hardening of the material after the drying in the oven. Optical properties investigated using UV-Vis spectroscopy showed maximum absorption band at

approximately 280 nm which can be attributed to the π - π^* transition of the thiophene ring for poly(3,4-ethylenedioxythiophene) (PEDOT). Maximum absorption band for PMAA at 250 nm which was attributed to the π - π^* transition that is due to the C=O. While the band at 218 nm due to the transitions n- σ^* is associated to the interaction between carbon and oxygen (C-O) characteristic bands. The band at 227 nm can be attributed to n- σ^* transition, whilst that at 252 nm can be assigned to the n- π^* transitions. The wavelengths were used to determine the energy band gaps of PMAA, PEDOT and P(MAA-co-EDOT) and were found to be 4.96, 4.32 and 4.92 eV, respectively. The application of the P(MAA-co-EDOT) in the fabrication of a MIP sensor for the detection of 17 β -estradiol is also reported in this thesis. The structural properties of the MIP were determined by Fourier transform infrared spectroscopy (FTIR) which showed the decrease in the intensity of the band for the C-O-H functionality that occurs by the hydrogen bonding between the copolymer and 17 β -estradiol. The high resolution scanning electron microscopy (HRSEM) images of the MIP showed the presence of cavities on the MIP surface caused by the removal of the template from the polymer matrix. The electrochemical behaviour of the MIP sensor was explored using differential pulse voltammetry (DPV) by comparing the current response between the MIP-target analyte complex, MIP (after removal of the analyte) and MIP after the rebinding of target analyte. The MIP sensor had a limit of detection (LOD) of 0.006 nM, a dynamic linear range (DLR) of 0.001-0.01 nM and sensitivity of $1,25 \times 10^{-7}$ μ A/nM with a good selectivity for 17 β -estradiol detection. Based on a study done by the world health organization (WHO) there are about 800 chemicals suspected and known to be capable of being endocrine disruptors, however as much as there are a number of such chemicals known only a small fraction of them have been investigated and tested to determine the overt endocrine effects on organisms. Thus it is important to fabricate a sensor with a low LOD and a wide DLR such as the one in this study. So that even at lowest concentrations estrogens can be detected in samples.

KEY WORDS

Molecularly imprinted polymers

Conducting polymers

Estrogens

Pesticides

Dimethoate

Endocrine disrupting compounds

Differential pulse voltammetry

Limit of detection

Copolymerization

Acetylcholinesterase enzyme

Gold nanoparticles

Multichannel detection system



DECLARATION

I declare that “**Molecularly imprinted polymer sensor systems for environmental estrogenic endocrine disrupting chemicals**” is my own work, that it has not been submitted before for any degree or examination in any other university, and that all the sources I have used or quoted have been indicated or acknowledged as complete references.



Nomaphelo Ntshongontshi

January 2018

Signed N. Ntshongontshi

ACKNOWLEDGEMENTS

To the Lord almighty thank you for granting me strength and the courage to complete my work through the difficult times, thank you for the constant protection.

To my supervisor, Prof Emmanuel Iwuoha a big and special thanks for the encouraging words when I had no hope, for the support that you gave me and assuring me that I can do better than what I thought I could. Also thank you for the supervision and guidance that you have given me throughout my work and for never giving up on me.

To my co-supervisor Prof Vernon Somerset, I would like to express my words of thanks for the guidance and support you've shown me during my PhD.

To the staff of the Chemistry department and SensorLab members, thank you for the patience, the love and the support you have given me. Your help is highly appreciated.

To my family thank you for being patient with me through all these years. Knowing that I have your endless support and that you are with me through the good and the worst times, I am where I am today because of you. I appreciate the love you have always shown and given me without expecting anything in return, well this one is for you, and this is what you are getting in return.

To all my friends thank you for all the shoulders you provided for me to cry on. You are sincerely appreciated. Thank you.

To Ayanda Jack you have always been by my side since we were young, thank you for all your patience and for always giving me the ear when I was complaining, thank you for the never ending love and support you have always offered me without any expectations.

To Nomxolisi Dywili, thank you for always being my friend, my pillar of strength for being there for me even though we were sharing the same struggle.

To Wonderboy Ntuthuko Hlongwa, our journey started years ago, we have been through ups and downs together, and together we have come up strong.

To Naledi Raleie thank you for being a good friend and for your constant encouragement.

To Dr Sidwaba, you have been nothing but inspirational to me, your strength and wisdom has had great impact on me.

To Dr Usisipho Feleni, the friendship, love and support you have shown me will always be remembered.

To Sisa Maqubela thank you for the constant encouragement, for always being there lifting me up when I was in the verge of giving up. No amount of words would be enough to express my gratitude.

Thank you to the National Research Foundation South Africa for the opportunity and the funding you gave me throughout the completion of the study.

Thank you to the Coimbra group for funding my project during my international stay.



DEDICATION

This thesis is dedicated to:

My late brother Lusindiso Ntshongontshi

May your wonderful and gentle soul rest in eternal peace.

My Parents

Nothembisile and Qinisile Ntshongontshi

My siblings

Lwandile Ntshongontshi, Akhona Ntshongontshi, Tembisa Ntshongontshi, Veliswa
Ntshongontshi, Tembela Ntsimango



LIST OF PUBLICATIONS

N. Ntshongontshi, A.A.A. Baleg, R.F. Ajayi, C. Rassie, E. Nxusani, L. Wilson, U. Feleni, U. Sidwaba, S. Qakala, S.F. Douman, P.G.L. Baker and E.I. Iwuoha. Cytochrome P450-3A4/Copper-Poly(Propylene Imine)-Polypyrrole Star Co-Polymer Nanobiosensor System for Delavirdine - A Non-Nucleoside Reverse Transcriptase Inhibitor HIV Drug. *Journal of Nano Research*, **40** (2016), 265-280.

R.F. Ajayi, E. Nxusani, S.F. Douman, A. Jonnas, **N. Ntshongontshi**, U. Feleni, K. Pokpas, L. Wilson and E.I. Iwuoha. Silver Nanoparticle-Doped Poly(8-Anilino-1-Naphthalene Sulphonic Acid)/CYP2E1 Nanobiosensor for Isoniazid - A First Line Anti-Tuberculosis Drug. *Journal of Nano Research*, **40** (2016), 229-251.

S. Duoman, U. Feleni, X. Fuku, R. Ajayi, E. Nxusani, **N. Ntshongontshi**, Emmanuel Iwuoha. New Generation Nanoelectrochemical Biosensors for Disease Biomarkers: 1. Indium Telluride Quantum Dots Signaling of Telomerase Cancer Biomarker. *Journal of Nanoscience and Nanotechnology* **16**, *12* (2016), 12844-12850.

M.P. Bilibana, A.R. Williams, C. Rassie, C.E. Sunday, H. Makelane, L. Wilson, **N. Ntshongontshi**, A.N. Jijana, M. Masikini, P.G.L. Baker and E.I. Iwuoha. Electrochemical Aptatoxisensor Responses on Nanocomposites Containing Electro-Deposited Silver Nanoparticles on Poly(Propyleneimine) Dendrimer for the Detection of Microcystin-LR in Freshwater. *Sensors*, **16** (2016), 1901.

C. Rassie, J. Van Wyk, L. Wilson, **N. Ntshongontshi**, A. Jonnas, U. Feleni, R. F. Ajayi, P. Baker and E. Iwuoha. Electrochemical Ultra-Low Detection of Isoniazid Using a

Salicyldamine Functionalised G1-DAB-(NH₂)₄ Dendritic Sensor vs. UV-VIS Spectrophotometric Detection. *Journal of Nano Research*, **45** (2016), 164-174.

D. Capoferri, M. Del Carlo, **N. Ntshongontshi**, E.I. Iwuoha, M. Sergi, F. Di Ottavio, D. Compagnone. MIP-MEPS based sensing strategy for the selective assay of dimethoate. Application to wheat flour samples. *Talanta*, **174** (2017), 599–604.



LIST OF CONFERENCE PRESENTATION

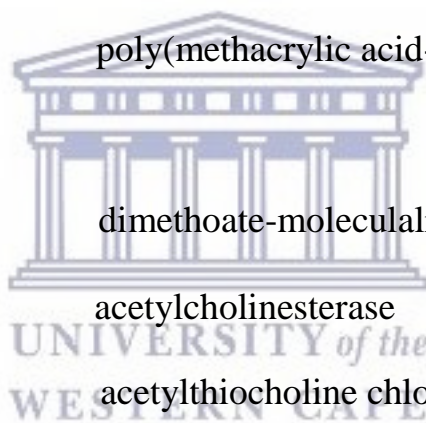
Poster presentation at the 14th International Symposium on Macro- and Supramolecular Architectures and Materials (MAM-14), 25 November, 2014, Johannesburg, South Africa.

Poster presentation at the 3rd International Symposium on Electrochemistry - Materials, Analytical and Physical Electrochemistry Today (MAPET-15), 26-28 May 2015, Bellville, South Africa.



LIST OF ABBREVIATIONS AND ACRONYMS

EDCs	Endocrine Disruptors
eEDCs	estrogenic endocrine disruptors
MIP	Molecularly imprinted polymer
PPy	poly(pyrrole)
MAA	methacrylic acid
EDOT	3,4-ethylenedioxythiophene
PEDOT	poly(3,4-ethylenedioxythiophene)
P(MAA-co-EDOT) ethylenedioxythiophene)	poly(methacrylic acid-co-3,4- dimethoate-molecularly imprinted polymer
Dim-MIP	
AchE	acetylcholinesterase
ATChCl	acetylthiocholine chloride
E2	17 β -estradiol
EE2	ethinylestradiol
E1	estrone
E3	estriol
CV	cyclic voltammetry
DPV	differential pulse voltammetry
SWV	square wave voltammetry
LOD	limit of detection



DLR	dynamic linear range
NIP	non imprinted polymer
HR-TEM	high resolution transmission microscopy
HR-SEM	high resolution scanning electron microscopy
XRD	x-ray diffraction
FTIR	Fourier transform infrared spectroscopy
EIS	electrochemical impedance spectroscopy
OPs	organophosphates
PBS	phosphate buffer
AuNPs	gold nanoparticles

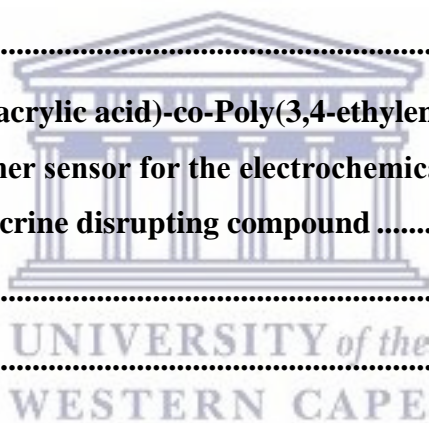


TABLE OF CONTENTS

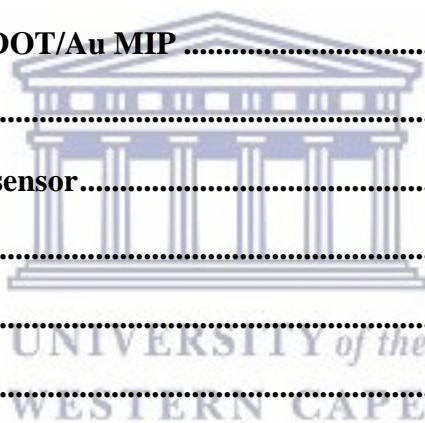
ABSTRACT.....	2
KEY WORDS.....	6
DECLARATION.....	7
ACKNOWLEDGEMENTS	8
DEDICATION.....	10
LIST OF PUBLICATIONS	11
LIST OF CONFERENCE PRESENTATION	13
LIST OF ABBREVIATIONS AND ACRONYMS	14
LIST OF FIGURES	20
CHAPTER ONE	28
Introduction.....	28
1.1 Background.....	29
1.1.1 Prevalence of estrogenic endocrine disrupting compounds and their mechanism of action.	29
1.1.2 Prevalence of pesticide based endocrine disrupting compounds and their mechanism.....	34
1.2 Problem statement.....	38
1.3 Rationale and Motivation	38
1.4 Aims and objectives.....	40
1.5 The specific objectives of this study include:	40
1.6 Thesis outline	42
1.7 References	43
CHAPTER TWO	54

Literature review	54
Abstract	55
2.0 Introduction	56
2.1 Conducting polymers	56
2.2 Synthesis of conducting polymers	58
2.3 Copolymers Based on 3,4-Ethylenedioxythiophene	66
2.4 Applications of conducting polymers.....	67
2.5 Gas sensors	71
2.6 Molecularly imprinted polymers.....	72
2.7 Estrogens	75
2.8 Acetylcholinesterase	77
2.9 Organophosphate pesticides	78
2.11 References	80
CHAPTER THREE	99
Electrochemical synthesis of a polypyrrole based molecularly imprinted polymer sensor on surfaces of glassy carbon electrodes sensitive to dimethoate- an acetylcholinesterase inhibitor organophosphate pesticide.	99
Abstract	101
3.0 Introduction	102
3.1 Experimental section.....	106
3.1.1 Chemicals	106
3.1.2 Instrumentation and procedure	107
3.1.3 Preparation of MIP and NIP film electrodes and electrochemical measurements.....	107
3.2 Results and discussion	109
3.3 Conclusion.....	122
3.4 References	123
CHAPTER FOUR.....	129

Chemical synthesis and characterization of a novel conductive poly(methacrylic acid-co-3,4-ethylenedioxythiophene) copolymer.	129
Abstract.....	130
4.0 Introduction.....	131
4.1 Experimental.....	133
4.1.1 Chemicals	133
4.1.2 Instrumentation and procedure	134
4.1.3 Cleaning of electrodes	135
4.1.4 Preparation of polymer materials	135
4.3 Conclusion.....	154
4.4 References	155
CHAPTER FIVE	161
Development of a Poly(methacrylic acid)-co-Poly(3,4-ethylenedioxythiophene) molecularly imprinted polymer sensor for the electrochemical detection of 17β-estradiol-An estrogenic endocrine disrupting compound	161
Abstract.....	163
5.0 Introduction.....	164
5.1 Experimental.....	167
5.1.1 Chemicals	167
5.1.2 Instrumentation and procedure	167
5.1.3 Cleaning of electrodes	168
5.1.4 Preparation of NIP and MIP electrodes	168
5.2 Results and discussion.....	170
5.2.1 Selectivity and reproducibility of MIP sensor	178
5.3 Conclusion.....	181
5.4 References	182
CHAPTER SIX	188



Electrochemical molecularly imprinted polymer sensor using a 96-well screen-printed microplate for 17α-estradiol detection.	188
<i>Summary</i>	189
Abstract	189
6.0 Introduction	190
6.1 Methodology	191
6.1.1 Chemicals	191
6.1.2 Instrumentation and procedure	192
6.1.3 Cleaning of electrodes	192
6.1.4 Synthesis of gold nanoparticles	193
6.1.5 Electrochemical polymerization of PEDOT	193
6.1.6 Preparation of PEDOT/Au MIP	193
6.3 Results and discussion	195
6.3.3 Selectivity of MIP sensor	202
6.4 Conclusion	202
6.5 References	203
CHAPTER SEVEN	206
Conclusion and recommendations	206
7.1 Conclusions	207
7.2 Recommendations and future work	209



LIST OF FIGURES

FIGURE 1. 1: REPRESENTING POSSIBLE MECHANISMS INVOLVED IN CELLULAR ACTIONS OF NATURAL OSTROGENS (PINTO ET AL. 2014).	33
FIGURE 1. 2: STRUCTURE OF 17B-ESTRADIOL	34
FIGURE 1. 3: STRUCTURE OF DIMETHOATE	36
FIGURE 1. 4: SCHEMATIC OF EDC AND PPCP LEAKAGE INTO DRINKING WATER (WWW.EUSEM.COM) (J. LINTELMANN, A. KATAYAMA, N. KURIHARA, L. SHORE, A. WENZEL, ENDOCRINE DISRUPTORS IN THE ENVIRONMENT (IUPAC TECHNICAL REPORT), PURE APPL. CHEM. 75 (2003) 631–681.)	36
FIGURE 2. 1: POSSIBLE POLYMERIZATION MECHANISM FOR EDOT	62
FIGURE 2. 2: GALVANOSTATIC POLYMERIZATION OF EDOT AT 1 MA/CM². THE EDOT MONOMER DISSOLVED IN ACETONITRILE TOGETHER WITH A SUPPORTING SALT (LITHIUM PERCHLORATE) WAS POLYMERISED UNTIL A	

SIGNIFICANT INCREASE OF POTENTIAL INDICATING THE END OF POLYMERIZATION WAS OBSERVED (SCROSATI 1989).....	64
FIGURE 2. 3: TYPICAL POTENTIODYNAMIC EXPERIMENT OF CONDUCTING POLYMER GROWTH. POTENTIODYNAMIC GROWTH OF A POLYPYRROLE FILM IN ACETONITRILE (+1% H₂O)/0.1 M TBAPF₆, V) 100 mV s⁻¹, T 298 K (ROAD ET AL. 1979).....	65
FIGURE 3.1: ACETYLCHOLINE IN CHOLIGENIC SYNAPSES.	105
FIGURE 3.2: PREPARATION OF PPY MODIFIED ELECTRODE	108
FIGURE 3.3: PREPARATION OF MIP ELECTRODE	109
FIGURE 3.4: CYCLIC VOLTAMMOGRAMS OF (A) GCE, (B) POLYPYRROLE (PPY), (C) PPY AND DIMETHOATE AND (D) MIP IN 0.1 M PBS pH 7 0.1 M KCL, , KCL AND 1 mM K₃Fe(CN)₆.....	110
FIGURE 3.5: STRUCTURE OF DIMETHOATE	111
FIGURE 3.6: CYCLIC VOLTAMMOGRAMS OF 1 mM K₃[Fe(CN)₆] AT 10 mV/S IN 0.1 M PBS SOLUTIONS CONTAINING 0.1 M KCL AT BARE GCE, PPY, DIM- PPY FILM, MIP AND DIMETHOATE REBINDING MIP FILM.....	112
FIGURE 3.7: (A) CYCLIC VOLTAMMOGRAM, (B) SQUARE WAVE VOLTAMMOGRAM OF 1 mM K₃[Fe(CN)₆] AT 10 mV/S IN 0.1 M PBS SOLUTIONS CONTAINING 0.1 M KCL, (C) SHOWS PLOT OF I_{PA} VS pH TO 0.1 NM SUBSTRATE EFFECT OF pH AT MIP ELECTRODE.....	114

FIGURE 3.8: CYCLIC VOLTAMMOGRAMS (A), SQUARE WAVE VOLTAMMOGRAM (B) OF MIP AFTER REBINDING OF DIMETHOATE AT DIFFERENT CONCENTRATIONS (0.01, 0.02, 0.03, 0.04, 0.06, 0.08, 0.1, 0.12, 0.14, 0.16, 0.18, 0.2, 0.3, 0.4, 0.5, 0.6, 0.7, 0.8, 0.9 AND 1 nM) IN 0.1 M PBS pH 7, 0.1 M KCl, AND 1 mM $K_3[Fe(CN)_6]$115

FIGURE 3.9: (A) CV, (B) SWV OF ACETYLTHIOCHOLINE AT MIP AT DIFFERENT CONCENTRATIONS (0.01, 0.02, 0.03, 0.04, 0.06, 0.08, 0.1, 0.12, 0.14, 0.16, 0.18, 0.2, 0.3, 0.4, 0.5, 0.6, 0.7, 0.8, 0.9 AND 1 nM) IN THE PRESENCE OF AChE, 0.1 M PBS pH 7, 0.1 M KCl, AND 1 mM $K_3[Fe(CN)_6]$. (D) LINEAR RANGE OF THE CALIBRATION CURVE FOR THE RESPONSE OF THE MIP ELECTRODE TO HYDROLYSIS OF ATCl BY AChE.117

FIGURE 3.10: MECHANISM OF ATCl HYDROLYSIS CATALYZED BY AChE...118

FIGURE 3.11: (A) CV, (B) SWV OF INHIBITION OF AChE IN THE PRESENCE OF DIMETHOATE AT MIP ELECTRODE AT DIFFERENT CONCENTRATIONS (0.01, 0.02, 0.03, 0.04, 0.06, 0.08, 0.1, 0.12, 0.14, 0.16, 0.18, 0.2, 0.3, 0.4, 0.5, 0.6, 0.7, 0.8, 0.9 AND 1 nM) IN THE PRESENCE OF 0.1nM ACETYLTHIOCHOLINE, 0.1 M PBS pH 7, 0.1 M KCl, AND 1 mM $K_3 Fe(CN)_6$. (C) LINEAR RANGE OF THE CALIBRATION CURVE FOR THE RESPONSE OF THE MIP ELECTRODE TO INHIBITION OF ATCl BY DIMETHOATE.....119

FIGURE 3.12: PHOSPHORILATION OF AChE BY DIMETHOATE.....120

FIGURE 3.13: (A) CV, (B) ANODIC SWV OF INHIBITION OF AChE IN THE PRESENCE AND ABSENCE OF DIMETHOATE AT MIP ELECTRODE AT DIFFERENT IN THE PRESENCE OF 0.1nM ACETYLTHIOCHOLINE, 0.1 M PBS PH 7, 0.1 M KCL, AND 1 MM K₃Fe(CN)₆]......121

FIGURE 4. 1: REPRESENTATION OF THE CHEMICAL SYNTHESIS OF PMAA, PEDOT AND P(MAA-CO-EDOT)......137

FIGURE 4. 2: STRUCTURE OF (A) PMAA, (B) PEDOT AND (C) P(MAA-CO-EDOT)......138

FIGURE 4. 3: FTIR OF (A) PMAA AND (B) PEDOT......139

FIGURE 4. 4: FTIR SPECTRA OF P(MAA-CO-EDOT)......140

FIGURE 4. 5: HRSEM IMAGES AND ELEMENTAL ANALYSIS OF PMAA, PEDOT AND P(MAA-CO-EDOT)......142

FIGURE 4. 6: UV-VIS SPECTRA OF PMAA......143

FIGURE 4. 7: UV-VIS SPECTRA OF PEDOT......144

FIGURE 4. 8: UV-VIS OF P(MAA-CO-EDOT)......145

FIGURE 4. 9: XRD SPECTRA OF PMAA, PEDOT AND P(MAA-CO-EDOT). 147

FIGURE 4. 10: RAMAN SPECTRA OF A) PMAA, B) PEDOT.149

FIGURE 4. 11: P(MAA-CO-EDOT)......150

FIGURE 4. 12: CV OF A) PMAA, B) PEDOT, P(MAA-CO-PEDOT) IN 0.1 M PH 7 PHOSPHATE BUFFER AT SCAN RATES (0.01 V/s – 0.1 V/s). (A', B', AND

C') RANDLE SEVČIK PLOTS OF PMAA, PEDOT AND P(MAA-co-PEDOT) RESPECTIVELY IN 0.1M PHOSPHATE BUFFER AT (0.01 V/s – 0.1 V/s) FOR THE DETERMINATION OF THE DIFFUSION CO-EFFICIENT.151

FIGURE 5. 1: PREPARATION OF MOLECULARLY IMPRINTED POLYMER SENSOR.169

FIGURE 5. 2: FTIR SPECTRA OF (A) P(MAA-co-EDOT)-E2 (RED LINE), (B) 17B ESTRADIOL (BLACK LINE) AND (C) MIP (GREEN LINE).....170

FIGURE 5. 3: HRSEM IMAGES OF A) NIP AND B) MIP.....172

FIGURE 5. 4: (A) AND (C) CYCLIC VOLTAMMOGRAMS OF NIP/AU AND MIP/AU ELECTRODES RESPECTIVELY (0.01 V/s – 0.1 V/s) AND (B) AND (D) RANDLE SEVČIK PLOTS OF NIP/AU AND MIP/AU RESPECTIVELY IN 0.1 M PHOSPHATE BUFFER AT (0.01 V/s – 0.1 V/s) FOR THE DETERMINATION OF THE DIFFUSION CO-EFFICIENT.....173

FIGURE 5. 5: (A) DPV AND (B) CV OF P(MAA-co-PEDOT)-E2 (BLACK LINE), MIP (RED LINE) AND MIP AFTER DETECTION OF E2 AT A CONCENTRATION OF 0.01 nM AT A POTENTIAL OF 0.25-1 V.....175

FIGURE 5. 6: (A) DPV AND (B) CV OF THE DETECTION OF 17B-ESTRADIOL FROM 0 nM-1 nM FROM 0.5-1 V (C) NYQUIST PLOTS FOR THE FARADAIC IMPEDANCE MEASUREMENTS IN THE PRESENCE OF 5.0 mM $[\text{Fe}(\text{CN})_6]^{3-/4-}$ (D) CALIBRATION CURVE AND LINEAR RANGE OF THE CALIBRATION FOR

THE DETECTION OF 17 β -ESTRADIOL USING MIP (0-0.01 nM) (E) LINEAR RANGE OF THE NON-IMPRINTED POLYMER (NIP) (RED LINE) AND MIP (BLACK LINE) SENSORS.....	176
FIGURE 5. 7: CHEMICAL STRUCTURES OF THE COMPETING MOLECULES.....	180
FIGURE 5. 8: INTERFERENCE STUDIES USING MIP BASED ON 17 B-ESTRADIOL (0-0.01 nM).....	181
FIGURE 6.1: STRUCTURE OF AuNPs/PEDOT FILM. AuNPs/PEDOT/GCE.	195
FIGURE 6.2: (A) TEM OF AuNPs AND (B) SEM OF AuNPs, (C) EIS OF BARE ELECTRODE (BLACK), AuNPs (RED) AND PEDOT (GREEN) AND (D) BARE ELECTRODE (BLACK), AuNPs (RED) AND PEDOT (GREEN) USING [Fe(CN) ₆] ^{-3/-4} REDOX PROBE IN PBS.	196
FIGURE 6.3: CV OF (A) MIP FABRICATED WITH PEDOT POLYMER ON THE SURFACE OF THE ELECTRODE AND MIP FABRICATED USING THE AuNPs/PEDOT COMPOSITE AND (B) CYCLIC VOLTAMMOGRAMS OF NANOCOMPOSITE WITH ANALYTE (BLACK VOLTAMMOGRAM), MIP AFTER REMOVAL OF ANALYTE (RED VOLTAMMOGRAM), AND MIP AFTER REBINDING OF ANALYTE (ESTRONE) USING [Fe(CN) ₆] ^{-3/-4} REDOX PROBE IN PBS pH 7.	197
FIGURE 6.4: (A) CV AND (B) EIS AuNPs/PEDOT MIP FOR THE DETECTION OF ESTRONE USING [Fe(CN) ₆] ^{-3/-4} AS THE REDOX PROBE IN PBS PH 7....	199

FIGURE 6.5: REPRESENTATION OF THE MULTICHANNEL 96-WELL SYSTEM...199

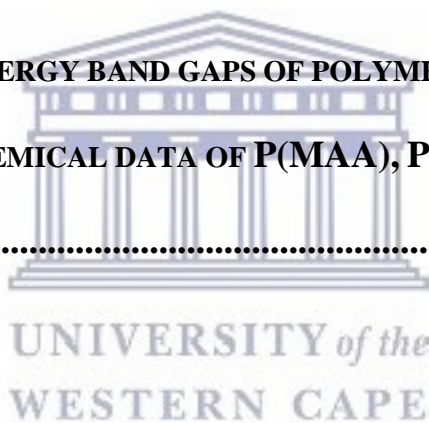
FIGURE 6.6: (A) CV OF COMPARISON BETWEEN 6 ELECTRODES OF THE 12 ELECTRODES OF THE SCREEN PRINTED CARBON MICROPLATE, (B) CV OF PMAA-CO-PEDOT-E2 (BLACK LINE), MIP (RED LINE) AND MIP AFTER DETECTION OF E2 AT A CONCENTRATION OF 0.2 nM, (C) DETECTION OF 17A-ESTRADIOL IN PBS AND (D) LINEAR RANGE OF THE CALIBRATION CURVE INSET.200

FIGURE 6.7: INTERFERENCE STUDIES USING MIP BASED ON 17 A-ESTRADIOL (0-0.14 nM).....201

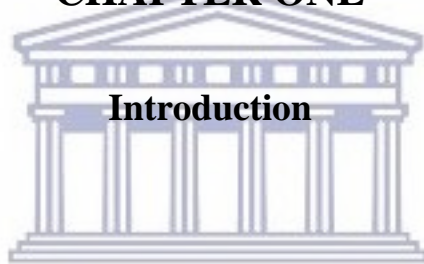


LIST OF TABLES

TABLE 3.1: CYCLIC VOLTAMMETRIC PARAMETERS FOR GCE, PPY, DIM-MIP AND MIP	110
TABLE 3.2: COMPARISON OF DETECTION METHODS TO THE PRESENT STUDY	122
TABLE 4. 1: TABLE OF ENERGY BAND GAPS OF POLYMERS	145
TABLE 4. 3: ELECTROCHEMICAL DATA OF P(MAA), P(EDOT) AND P(MAA-co-EDOT).....	154
TABLE 5.1: COMPARISON OF THE MIP WITH OTHER SENSORS.....	178



CHAPTER ONE

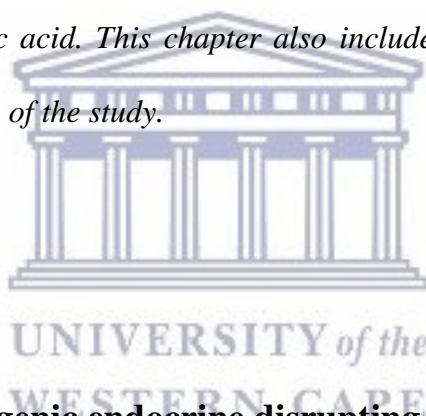


Introduction

UNIVERSITY *of the*
WESTERN CAPE

Summary

Over the years concern over the occurrence of endocrine disrupting compounds in the environment has seen a tremendous increase. There are several natural and man-made chemical compounds, they possess the ability to evoke estrogen-like responses. There have been reports of exposure to these endocrine disruptors. The lack of reliable detection methods means that most of exposure to these chemicals will go unnoticed. In this chapter the background on the endocrine system, its disruption and the chemicals that have the effect on the system focusing mainly on estrogenic endocrine disrupting compounds and on pesticides based on esters of phosphoric acid. This chapter also includes the problem statement and motivation, aim and objectives of the study.



1.1 Background

1.1.1 Prevalence of estrogenic endocrine disrupting compounds and their mechanism of action.

Since the mid-1990s there has been an increase in the awareness and great concern for the exposure to chemicals that are known for their potential to interact with the endocrine system (Kar *et al.* 2017) of both human and wildlife (Pinto *et al.* 2017) thus resulting in adverse effects (Hecker & Hollert 2011; Casado-Carmona *et al.* 2016; Di Donato *et al.* 2017). The human endocrine system is responsible for the control of various processes in the body (Sifakis *et al.* 2017), including early processes such as cell differentiation during organ formation and development, most tissue and organ function through adulthood (Roy & Kalita 2011). The endocrine system produces hormones, hormones which can be defined as molecules that are

produced by endocrine glands that travel through the body producing effects on distant cells and tissues through integrated complex interacting pathways usually involving hormone receptors (Sun *et al.* 2014). There are over 50 different hormones and related molecules responsible for controlling the normal functions of the human body across and within tissues and organs (Auriol *et al.* 2006). Hormones and their signalling pathways are important in functioning of the tissues and organs in both vertebrates and invertebrates and are similar in different species (Blumberg *et al.* 2011). Both pharmaceuticals and endocrine disruptors are categorized as subclasses of organic contaminants (Benotti *et al.* 2009) which can be defined as carbon-based chemicals, solvents and pesticides that get into the environment resulting in contamination or pollution (Elibariki & Maguta 2017). Contamination is one of the problems with global relevance, one of nine “planetary boundaries” (Anetor *et al.* 2008) (1) Stratospheric ozone depletion, (2) Loss of biosphere integrity (biodiversity loss and extinctions), (3) Climate Change, (4) Ocean acidification, (5) Freshwater consumption (Xu *et al.* 2016) and the global hydrological cycle, (6) Land system change, (7) Nitrogen and phosphorus flows to the biosphere and oceans, (8) Atmospheric aerosol loading, Chemical pollution and the release of novel entities, which should not be transgressed in order to avoid unacceptable global changes (Kümmerer 2007; Collins *et al.* 2015). The release of toxic and long-lived substances including synthetic pollutants (R. Liu *et al.* 2015), heavy metals and radioactive materials are some of the key human-driven changes to the environment (Diaconu *et al.* 2017; Carvalho *et al.* 2015). These compounds potentially have irreversible effects on both living organisms and the environment at large (Chen *et al.* 2017). Even when chemical pollution is at low levels and exposure to animals is of minute quantities (Pieper & Rotard 2011), the result of the exposure can have dire consequences including reduced fertility and permanent genetic damage can have severe effects on ecosystems far removed from the source of the pollution (Gmurek *et al.* 2017). Endocrine disrupting compounds (EDCs) are chemicals with the potential to bring about

negative effects of the endocrine system of humans and wildlife (Wee & Aris 2017). Several natural and synthetic chemical compounds have been identified that have the ability to evoke estrogen-like responses including pharmaceuticals, pesticides (Gómez-Pastora *et al.* 2017), industrial chemicals and heavy metals (Campbell *et al.* 2006; Rodriguez-Narvaez *et al.* 2017). The United States Environmental Protection Agency (USEPA) defines EDCs as endogenous agents that affect normal bodily functions such as synthesis, secretion, transport, binding, action and/or excretion of natural hormones. The primary functions of these hormones include development, reproduction and maintenance of homeostasis hormones (Kiyama *et al.* 2014; Combarous 2017; Xu *et al.* 2017; Dodson *et al.* 2012). These endocrine disruptors can be either man-made or natural, with the ability to interact with the estrogen receptors, other hormones, or transcription factors in the biochemical pathway of hormone activity (Nagpal & Meays 2009; Sornalingam *et al.* 2016). These EDCs can either act as antagonists or agonistic in affecting the functioning of the endogenous hormones. In certain target tissues some of the substances or chemicals can have both agonistic and antagonistic effects. Cross talk may occur between different systems and may result in systems being affected other than the anticipated one (Burks *et al.* 2016; Teles-Grilo Ruivo *et al.* 2017; Keiler *et al.* 2017). It is therefore imperative to be cautious in extrapolating in vitro hormone activity detected to the in vivo situation (WHO, 2002). The concept of crosstalk describes the way in which signal integration from multiple inputs within a response network affects a common biological output (Vert & Chory 2011). Through the discovery of the importance of signalling pathways controlling growth and development it is generally accepted that the response to a particular signal is not only due to a single pathway but rather shows pathway integration (Landini 2009). This discovery is what led to the cross talk phenomenon (Qian *et al.* 2016; Benedek *et al.* 2017; G. Li *et al.* 2017) which means that even when an environmental pollutant is known to have steroidal hormone activity, it can also have other effects since it is not limited to only one

activity (Genthe & Steyn n.d.). A good example for such a phenomena are isomers of DDT and some phthalates which not only have anti-androgenic but also estrogenic effects (Genthe & Steyn n.d.). According to a report by the World Health Organisation (WHO) in association with United Nations Environment Program (UNEP) there are approximately 800 known or suspected chemicals capable of interfering with hormone receptors, hormone synthesis and hormone conversion. However, only a small percentage of those chemicals have been investigated using tests that are able to identify evident endocrine effects in intact organisms.

Fig 1.1 shows the simplified scheme for the possible mechanisms involved in the cellular actions of natural estrogens (e.g., 17β -estradiol represented in fig 1.2, E2) and estrogenic endocrine disrupting compounds (EDCs). In the conventional mode of action (A), an estrogenic ligand binds and activates intracellular estrogen receptors (in fish, ER α , ER β a or ER β b) (Hamilton *et al.* 2014; Thornton 2002; Kiyama 2017), which dimerize in the nucleus, bind to estrogen-response elements in the promoters of target genes and regulate their transcription, through the recruitment of a range of possible cell-specific co-regulators (Burks *et al.* 2016; Tam & Giguère 2016). Other methods of action include: (B) indirect regulation of gene expression by interaction of ligand-bound Ers with other transcription factors (TF); (C,D) estrogen actions instigated by binding to membrane receptors (Ers or G-protein combined receptors, such as the GPER) and activation of protein kinase cascades or modifications in the levels of secondary messengers (Dworatzek & Mahmoodzadeh 2017; Guo *et al.* 2014; Zhang *et al.* 2017), resulting in (C) the activation of transcription factors that regulate gene expression or (D) rapid non-genomic effects, such as the activation of specific enzymes (Burgos-Aceves *et al.* 2016). While genomic actions can take hours to days, non-genomic effects occur in seconds or minutes. In addition, Ers can be activated and regulate gene expression in a ligand-independent manner through phosphorylation (P) in response to growth factor binding to their

membrane receptors (Labandeira-Garcia *et al.* 2016). Natural estrogens may compete with several EDCs (represented by different colours and shapes) for multiple receptors and pathways, resulting in a complex response that depends on the cellular context in terms of receptors and interacting proteins and, thus, may differ between tissues and circumstances (Romano & Gorelick 2016). cAMP, cyclic AMP; PKA, protein kinase A; PLC, phospholipase C; IP3, inositol 1,4,5-triphosphate; DAG, diacylglycerol; PKC, protein kinase C (Lazari *et al.* 2009; Patch *et al.* 2017; Tran *et al.* 2016b).

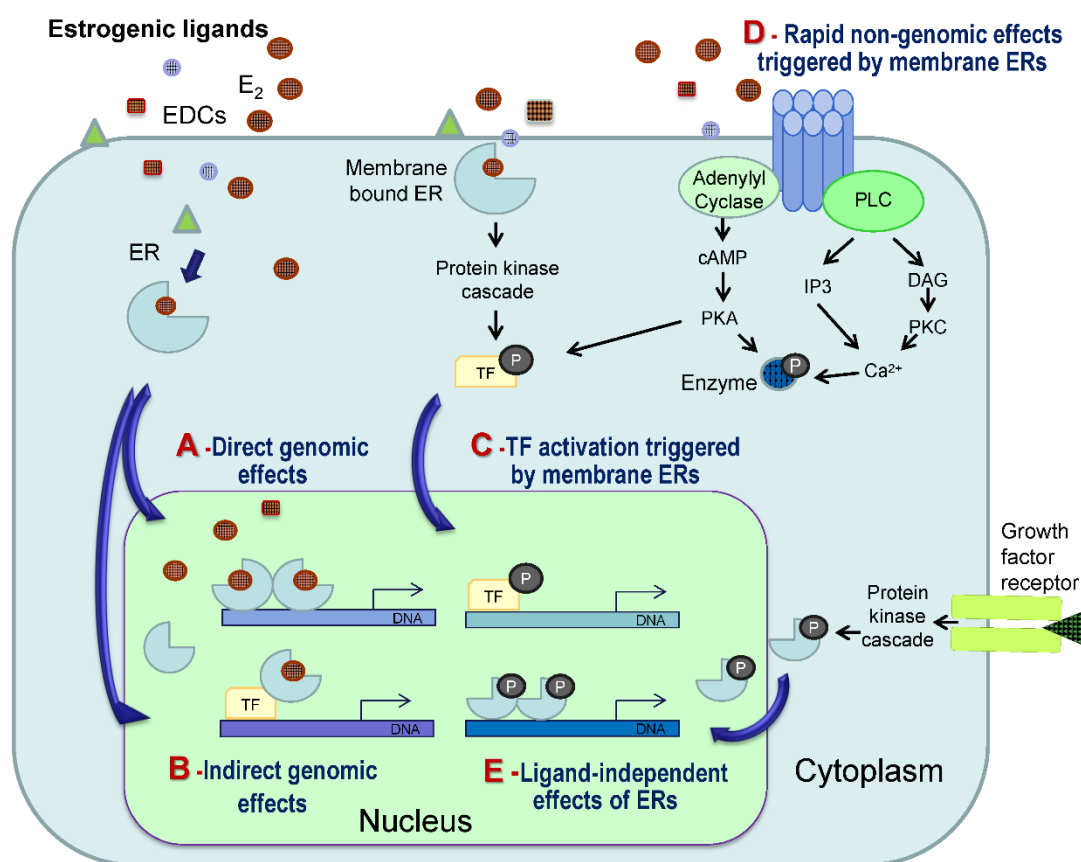


Figure 1. 1: representing possible mechanisms involved in cellular actions of natural estrogens (Pinto *et al.* 2014).

EDCs come from various sources such as, plastic bottles, metal food cans, flame retardants, toys, cosmetics, pesticides and detergents.

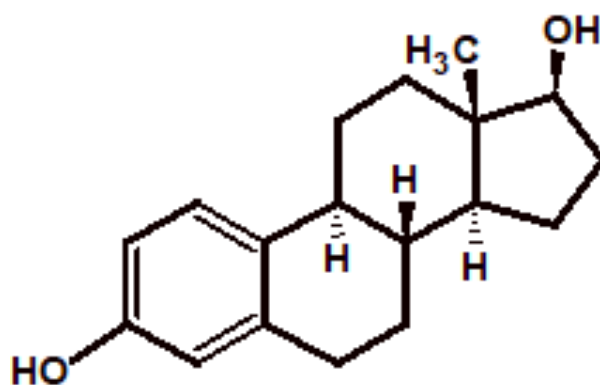


Figure 1. 2: Structure of 17 β -estradiol

1.1.2 Prevalence of pesticide based endocrine disrupting compounds and their mechanism

South Africa is home to more than 49 million people (Quinn *et al.* 2011). It has diverse climatic conditions ranging from semi-tropic to semi-arid regions. Majority of areas in the country receives rainfall in summer while some parts receive winter rainfall. The variation in environmental conditions allows growth and production of different kinds of crops from tropical fruit to maize and tree plantations. This means that some individual crops are susceptible to specific and various pests. Usage of pesticides is therefore imperative to ensure a high produce of these crops so as to accommodate and provide for the population which has been fast growing over the years. According to the Washington State University Urban IPM (Daniell 2012) and Pesticide Safety Education Program, pesticides can be defined as any substances or a combination of substances that are intended to mitigate a pest. Pests are any living organisms that can cause damage, can produce or transmit a disease. Insects, birds and/or mice are animals that can be considered as pests, plants such as weeds, microorganisms such as diseases and viruses can be referred to as pests. Pesticides are used in various sectors including agricultural, forestry, government, domestic, and industrial sectors (Naidoo & Buckley 2003; Sassolas 2012). The department of Agriculture, Forestry and Fisheries (DAFF)

is responsible for Fertilizers Feed, Agricultural Remedies and Stocks Remedies Act which governs the use of pesticides. The act was passed in Parliament in the year 1947, over the years the act has been amended but was never revised nor has it been scrutinized by the DAFF. There are more than 3000 pesticides and their products are approved for use in South Africa, many of those pesticides have not been re-evaluated, thus the risks that they might carry have not been reassessed to bring them in line with today's more severe standards of assessment. Organophosphates (Ops) are one of the widely used pesticides, thus the interest in their detection has seen an increase over the years, this is owed to their wide-ranging biological activity and reasonably low persistence when compared to organochlorine pesticides (Pogačnik & Franko 2003). Organophosphates are esters of phosphoric acid, they are known to be highly neurotoxic and disrupt the cholinesterase enzyme that regulates acetylcholine, a neurotransmitter needed for proper nervous system function (Pohanka 2014; Quinn 1987). Because of their high neurotoxicity, the OPs are widely used as pesticides and as nerve agents as part of chemical and biological warfare agents (Anetor *et al.* 2008; Liu & Lin 2005). Some of the commonly known organophosphorous pesticides include but not limited to dimethoate, malathion, chlorpyrifos, parathion, methyl parathion, diazinon, dichlorvos, phosmet and fenitrothion. Dimethoate ([O,O-Dimethyl S-(N-methylcarbamoylmethyl) phosphorodithioate]) depicted in fig 1.3 is an organophosphorous insecticide that is rapidly environmentally degradable, it is highly effective in the mitigation of pests.. This has led to it being used worldwide for agricultural purposes. Since its registration in the year 1962 it has been applied to various crops and insects including fruits, vegetables, grains, mites, flies, aphids, and plant hoppers. Because it is water soluble with low soil persistence, its potential to be present in running off and ending up into surface water and ground water is high.

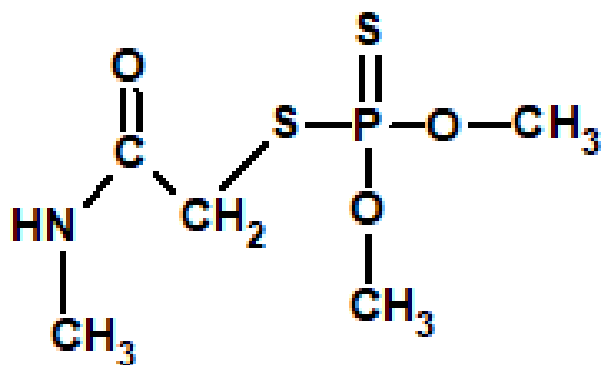


Figure 1. 3: Structure of dimethoate



Figure 1. 4: Schematic of EDC and PPCP leakage into drinking water (www.eusem.com) (J. Lintelmann, A. Katayama, N. Kurihara, L. Shore, A. Wenzel, Endocrine disruptors in the environment (IUPAC technical report), Pure Appl. Chem. 75 (2003) 631–681.).

As depicted in fig 1.4 the main sources of endocrine disruptors are the health facilities, residential areas and agriculture. Municipal waste travels from the health facilities and households to the treatment facilities, where some of the waste water is treated and some of the purified water is reused while some ends up on the ground (Sun *et al.* 2014; Coscollà *et al.* 2017). The sludge is reused for agricultural purposes as fertilizer. Through agricultural runoff the water ends up on the purified water system (treated effluent) (Ye *et al.* 2017). This increases the risks of exposure to not only humans but also animals who will ingest the water assuming that it has been rid of contaminants that might threaten their health and may have detrimental effects (Johnson & Chen 2017; Grimalt *et al.* 2017). Organophosphates such as dimethoate are known as acetylcholinesterase inhibitors (Akinbo & Pharm n.d.) because of their ability to interfere with functioning of acetylcholinesterase an enzyme that is responsible for the termination of impulse transmission at cholinergic synapses by the rapid hydrolysis of the neurotransmitter acetylcholine (ACh) to yield acetic acid and choline as shown in the mechanism below (Sussman & Silman 1992):



This inhibition is achieved through formation of a complex between the active site of the enzyme and the organophosphates (Kesik *et al.* 2014; Sussman & Silman 1992).

1.2 Problem statement

According to the South African department of environmental and water affairs, domestic water originates from various sources such as dams, rivers, streams or groundwater. There is variation in the water quality depending on whether it is supplied to the cities or rural areas, where the city receives water of better quality compared to that supplied to the rural areas. Water in rural areas often receives only partial or minimal treatment, while isolated communities and villages without access to electricity or other amenities often use water directly from rivers or streams without treatment. In the latter cases, both water quantity and quality may be affected by seasonal droughts or floods. Ground water, too, is frequently used with little or no treatment. Problems with water quality can be as a result of household water being obtained from shared/communal supply, it can also be compromised during transportation from the source to the household and also when it is stored in the home (Department of water Affairs 1996). In recent years there has been evidence of organic pollutants found in water in the environment worldwide. Yet their behaviour in drinking water and the impact they have on both human and the environment is still undetermined (Carvalho *et al.* 2015). Because they occur at fluctuating concentrations near analytical method determination limits (as most of these contaminants occur in the low ng/L range or even lower) could be part of the reasons why there is little knowledge on the occurrences of these compounds, their metabolites and products (Water *et al.* 1930).

1.3 Rationale and Motivation

There is an increase in the concern of endocrine disrupting chemicals (EDC) that are present in water (Smarr *et al.* 2016). There is a wide range of molecules that fall under EDCs, some of these molecules are organochlorinated pesticides and industrial chemicals, plastics, fuels,

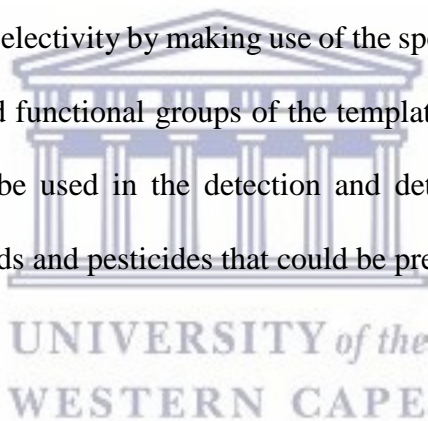
plasticizers and numerous other chemicals that exist in the environment or are in extensive use (Tahboub *et al.* 2017). These pollutants are chemicals that are capable of altering the regular functioning of the endocrine system of living organisms such as humans. EDs can also be demarcated based on their effects in the organism; even in minute quantities, they have the ability to alter the normal functions of the endocrine system, causing different types of cancer and damage to the reproductive systems of humans (Lazari *et al.* 2009). One of the main substances that has high endocrine disruptor activity is 17β -estradiol (Koç *et al.* 2011; Gansbeke *et al.* 2017; Smolarz *et al.* 2017; Ma *et al.* 2011). This hormone is a steroid that interferes with animals by causing abnormal development of thyroid function in birds and fish. The compound can also reduce fertility and lead to sexual disorders and immunological damage in crustaceans (Lafontaine *et al.* 2017), fish (Brown *et al.* 2018; Luigi *et al.* 2015), birds (Algae *et al.* 2013) and reptiles (Mingo *et al.* 2016). In humans, there is evidence that the development of certain diseases, such as breast and prostate cancer (Liu *et al.* 2012; Mansouri *et al.* 2017; Di Donato *et al.* 2017), has been caused by intense exposure to EDs. In addition, 17β -estradiol can reduce male fertility and can generate severe congenital malformations in children. Other EDCs including but not limited to pesticides.

Due to these potential carcinogenic properties and other antagonistic effects in human health, considerable interest was focused on developing cost-effective analytical methods for determining these compounds in complicated samples at low concentration levels (Therapy 2011; Perelo 2010; Hou *et al.* 2017). On the other hand, because their low concentrations commonly coexisted with the complexity matrices, it is paramount to develop highly sensitive and selective methods to determine these estrogens and phosphoric acid based pesticides at trace levels. The most commonly used methods include immunological methods, chemiluminescence (Kanso *et al.* 2017), HPLC (Haginaka 2002), LC-MS (Nieto *et al.* 2008), GC-MS (Dallüge *et al.* 2002), which combined with sample pretreatment methods, such as

liquid–liquid extraction (LLE), solid-phase extraction (SPE), pressurised liquid extraction (PLE) and accelerated solvent extraction (ASE), etc., are the most commonly used techniques for detecting endogenous EDCs and eEDCs. These processes were considered complicated, time consuming, to have low selectivity, and use large amounts of organic solvents. Therefore, choosing a suitable sample pretreatment method is very important.

1.4 Aims and objectives

This research projects aims at developing a molecularly imprinted polymer with the ability to recognise and bind estrogenic endocrine disrupting compounds used in the study as the template molecules with high selectivity by making use of the specific binding sites possessing complimentary size, shape and functional groups of the template molecule. This molecularly imprinted polymer will thus be used in the detection and determination of the estrogenic endocrine disruptive compounds and pesticides that could be present in water samples.

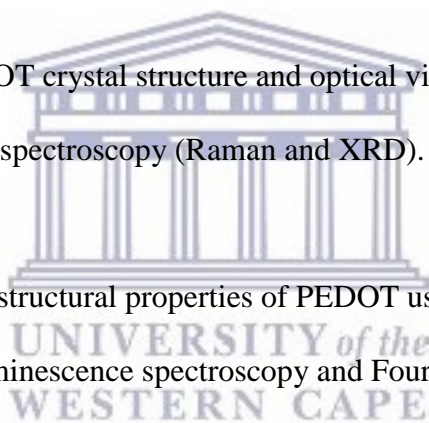


1.5 The specific objectives of this study include:

- 1) Fabrication of poly(pyrrole) molecularly imprinted polymer sensor: P(Py) MIP/GCE for dimethoate, an endocrine disrupting compound.
 - Surface modification of bare GCE by electrochemical deposition of thin layer of poly(pyrrole).
 - Determination of electrochemical properties of polymer material using cyclic voltammetry (CV) and square wave voltammetry (SWV).

2) Fabrication of poly(methacrylic acid-co-3,4-ethylenedioxythiophene) molecularly imprinted polymer sensor: P(MAA-co-PEDOT) MIP/GCE and P(MAA-co-PEDOT) MIP/Au for 17 β estradiol and 17 α estradiol.

- Chemical polymerization of 3,4-ethylenedioxythiophene in the presence of an oxidizing agent ammonium persulfate.
- Chemical polymerization of methacrylic acid (MAA) in the presence of oxidizing agents ammonium persulfate and iron (iii) chloride.
- Preparation of P(MAA-co-PEDOT) copolymer
- Determination of poly (3,4-ethylenedioxythiophene) (PEDOT) crystal structure and morphology using microscopic techniques (HR-TEM and HR-SEM).
- Determination of PEDOT crystal structure and optical vibrational modes using X-ray diffraction and Raman spectroscopy (Raman and XRD).
- Optical properties and structural properties of PEDOT using Ultraviolet-visible spectroscopy, photoluminescence spectroscopy and Fourier transformed infra-red spectroscopy (UV-Vis and FTIR).
- Surface modification of bare gold electrodes using poly (3,4-ethylenedioxythiophene) followed by determination of electrochemical properties of polymer material using cyclic voltammetry (CV), differential pulse voltammetry (DPV) and electrochemical impedance spectroscopy (EIS)
- Development, optimisation, evaluation and testing of



1.6 Thesis outline

The study consists of **seven chapters**

Chapter 1 gives information on the background on endocrine disrupting compounds from two sources; pesticides and estrogenic endocrine disruptors. This chapter also discussed are the rationale and motivation behind the study. Additionally the objectives and the outline of the thesis are discussed.

Chapter 2 introduces conducting polymers, how they differ and conventional over traditional material. Outlined is also the synthesis of the material, and the potential application fields giving particular emphasis on their applications in the field of sensors particularly imprinted polymer sensors.

Chapter 3 describes the fabrication of a molecularly imprinted polymer sensor based on polypyrrole on glassy carbon electrodes for the selective detection of dimethoate by electrochemical deposition. The PPy MIP-sensor was characterized electrochemically using CV and SWV, its response to dimethoate was investigated using both cyclic voltammetry and square wave voltammetry.

Chapter 4 describes the synthesis of a conductive copolymer based on the conducting polymer poly (3,4-ethylenedioxythiophene). The individual components ((poly) methacrylic acid and 3,4-ethylenedioxythiophene were characterized using FTIR, UV-Vis, SEM, TEM and electrochemical studies were performed using CV, SWV and DPV. The copolymer was chemically synthesized by the oxidation of the monomer materials, its properties were then investigated using SEM, TEM, Uv-Vis, FTIR, CV, SWV and DPV.

Chapter 5 describes the chemical synthesis and fabrication of a poly (methacrylic acid-3,4-ethylenedioxythiophene) molecularly imprinted polymer sensor. The sensor was prepared using 17 β -estradiol and estrogenic endocrine disruptor as the imprinted compound. Achieved

by the removal of the analyte molecule leaving cavities that are complimentary in shape and size. The properties of the MIP sensor were determined using FTIR, SEM, TEM, UV-Vis, CV, SWV, DPV and EIS. The sensor was used for the selective detection of 17 β -estradiol, the selectivity of the sensor was determined by the detection of interferences that are similar in structure and nature to the imprinted molecule using CV, SWV, DVP and EIS. The sensor showed very good selectivity to the target analyte.

Chapter 6 describes the detection of 17 α -estradiol, using a molecularly imprinted polymer sensor using multichannel instrument. It also describes the synthesis and characterization of AuNPs and preparation of a AuNPs/PEDOT composite and its application in molecularly imprinted polymer sensor, the determination of the differences in electrochemical signal when the polymer matrix is combined with the target/imprint molecule, when the imprint molecule is removed resulting in creation of cavities and when the target analyte is re-introduced and binds on the imprinted cavity sites.

Chapter 7 gives a summary of the work done as well as recommendations for future work.



1.7 References

Affairs, W., 1996. *Water Quality Guidelines Domestic*,

Akinbo, T. & Pharm, D., Organophosphates Poisoning.

Algae, A. et al., 2013. Aromatic amino acids and their derivatives as ligands for the isolation of aspartic proteinases. *The Communication of Ideas*, 3(2), pp.285–290.

Anetor, J.I. et al., 2008. Environmental chemicals and human neurotoxicity: Magnitude, prognosis and markers. *African Journal Biomedical Research*, 11(1), pp.1–12.

Auriol, M. et al., 2006. Endocrine disrupting compounds removal from wastewater, a new challenge. *Process Biochemistry*, 41(3), pp.525–539.

Benedek, G. et al., 2017. Estrogen protection against EAE modulates the microbiota and mucosal-associated regulatory cells. *Journal of Neuroimmunology*, 310(June), pp.51–59.

Benotti, M.J. et al., 2009. Pharmaceuticals and Endocrine Disrupting Compounds in U . S . Drinking Water. , 43(3), pp.597–603.

Blumberg, B., Iguchi, T. & Odermatt, A., 2011. *Endocrine disrupting chemicals*,

Brown, E. et al., 2018. Occurrence and levels of persistent organic pollutants (POPs) in farmed and wild marine fish from Tanzania. A pilot study. *Chemosphere*, 191, pp.438–449.

Burgos-Aceves, M.A. et al., 2016. Estrogen regulation of gene expression in the teleost fish immune system. *Fish & Shellfish Immunology*, 58, pp.42–49.

Burks, H. et al., 2016. Endocrine disruptors and the tumor microenvironment: A new paradigm in breast cancer biology. *Molecular and Cellular Endocrinology*, pp.1–7.

Campbell, C.G. et al., 2006. Biologically directed environmental monitoring, fate, and transport of estrogenic endocrine disrupting compounds in water: A review. *Chemosphere*, 65(8), pp.1265–1280.

Carvalho, A.R.M. et al., 2015. Occurrence and analysis of endocrine-disrupting compounds in a water supply system. *Environmental Monitoring and Assessment*, 187(3).

Casado-Carmona, F.A. et al., 2016. Magnetic nanoparticles coated with ionic liquid for the extraction of endocrine disrupting compounds from waters. *Microchemical Journal*, 128, pp.347–353.

Chen, L. et al., 2017. Transgenerational endocrine disruption and neurotoxicity in zebrafish larvae after parental exposure to binary mixtures of decabromodiphenyl ether (BDE-209) and lead. *Environmental Pollution*, 230, pp.96–106.

Collins, C.D. et al., 2015. “Towards a unified approach for the determination of the bioaccessibility of organic pollutants.” *Environment International*, 78, pp.24–31. Available at: <http://dx.doi.org/10.1016/j.envint.2015.02.005>.

Combarrous, Y., 2017. Endocrine Disruptor Compounds (EDCs) and agriculture: The case of pesticides. *Comptes Rendus Biologies*, (2017), pp.7–10.

Coscollà, C. et al., 2017. Human exposure and risk assessment to airborne pesticides in a rural French community. *Science of the Total Environment*, 584–585, pp.856–868.

Dallüge, J. et al., 2002. Comprehensive two-dimensional gas chromatography with time-of-flight mass spectrometric detection applied to the determination of pesticides in food extracts. *Journal of Chromatography A*, 965(1–2), pp.207–217.

Daniell, H., 2012. NIH Public Access. , 76(October 2009), pp.211–220.

Diaconu, A. et al., 2017. Researches regarding the reduction of pesticide soil pollution in vineyards. *Process Safety and Environmental Protection*, 108, pp.135–143.

Dodson, R.E. et al., 2012. Endocrine disruptors and asthma-associated chemicals in consumer products. *Environmental Health Perspectives*, 120(7), pp.935–943.

Di Donato, M. et al., 2017. Recent advances on bisphenol-A and endocrine disruptor effects on human prostate cancer. *Molecular and Cellular Endocrinology*.

Dworatzek, E. & Mahmoodzadeh, S., 2017. Targeted basic research to highlight the role of estrogen and estrogen receptors in the cardiovascular system. *Pharmacological Research*, 119, pp.27–35.

Elibariki, R. & Maguta, M.M., 2017. Status of pesticides pollution in Tanzania – A review. *Chemosphere*, 178, pp.154–164.

Gansbeke, K. Van et al., 2017. Regioselective monoalkylation of 17 β -estradiol for the synthesis of cytotoxic estrogens. *Steroids*, 124(June), pp.54–59.

Genthe, B. & Steyn, M., An Overview of Health Effects of Endocrine Disrupting Chemicals in Water - Where are we in South Africa?

Gmurek, M., Olak-Kucharczyk, M. & Ledakowicz, S., 2017. Photochemical decomposition of endocrine disrupting compounds ??? A review. *Chemical Engineering Journal*, 310, pp.437–456.

Gómez-Pastora, J. et al., 2017. Review and perspectives on the use of magnetic nanophotocatalysts (MNPCs) in water treatment. *Chemical Engineering Journal*, 310, pp.407–427.

Grimalt, J.O. et al., 2017. Comparative toxicity and endocrine disruption potential of urban and rural atmospheric organic PM 1 in JEG-3 human placental cells *. , 230, pp.378–386.

Guo, J. et al., 2014. Two natural products, trans-phytol and (22E)-ergosta-6,9,22-triene-3 β ,5 α ,8 α -triol, inhibit the biosynthesis of estrogen in human ovarian granulosa cells by aromatase (CYP19). *Toxicology and Applied Pharmacology*, 279(1), pp.23–32.

Haginaka, J., 2002. HPLC-based bioseparations using molecularly imprinted polymers. , (2), pp.337–351.

Hamilton, K.J., Arao, Y. & Korach, K.S., 2014. Estrogen hormone physiology: Reproductive findings from estrogen receptor mutant mice. *Reproductive Biology*, 14(1), pp.3–8.

Hecker, M. & Hollert, H., 2011. Endocrine disruptor screening: regulatory perspectives and needs. *Environmental Sciences Europe*, 23(1), p.15.

Hou, C. et al., 2017. Estrogenicity assessment of membrane concentrates from landfill leachate treated by the UV-Fenton process using a human breast carcinoma cell line. *Chemosphere*, 180, pp.192–200.

Johnson, A.C. & Chen, Y., 2017. Does exposure to domestic wastewater effluent (including steroid estrogens) harm fish populations in the UK? *Science of the Total Environment*, 589, pp.89–96.

Kanso, H. et al., 2017. Chemiluminescence immunoassays for estradiol and ethinylestradiol based on new biotinylated estrogen derivatives. *Analytical Biochemistry*, 537, pp.63–68.

Kar, S. et al., 2017. Endocrine-disrupting activity of per- and polyfluoroalkyl substances: Exploring combined approaches of ligand and structure based modeling. *Chemosphere*, 184, pp.514–523.

Keiler, A.M. et al., 2017. Evaluation of estrogenic potency of a standardized hops extract on mammary gland biology and on MNU-induced mammary tumor growth in rats. *Journal of Steroid Biochemistry and Molecular Biology*, 174(July), pp.234–241.

Kesik, M. et al., 2014. An acetylcholinesterase biosensor based on a conducting polymer using multiwalled carbon nanotubes for amperometric detection of organophosphorous pesticides. *Sensors and Actuators, B: Chemical*, 205, pp.39–49.

Kiyama, R. et al., 2014. Estrogen-responsive genes for environmental studies. *Environmental Technology and Innovation*, 1–2(C), pp.16–28.

Kiyama, R., 2017. Estrogenic terpenes and terpenoids: Pathways, functions and applications. *European Journal of Pharmacology*, 815(July), pp.405–415.

Koç, I. et al., 2011. Selective removal of 17 β -estradiol with molecularly imprinted particle-embedded cryogel systems. *Journal of Hazardous Materials*, 192(3), pp.1819–1826.

Kümmerer, P.K., 2007. Pharmaceuticals and the Environment. , (September), pp.1–10.

Labandeira-Garcia, J.L. et al., 2016. Menopause and Parkinson's disease. Interaction between estrogens and brain renin-angiotensin system in dopaminergic degeneration. *Frontiers in Neuroendocrinology*, 43, pp.44–59.

Lafontaine, A. et al., 2017. Proteomic response of *Macrobrachium rosenbergii* hepatopancreas exposed to chlordecone: Identification of endocrine disruption biomarkers? *Ecotoxicology and Environmental Safety*, 141(April), pp.306–314.

Landini, P., 2009. Cross-talk mechanisms in biofilm formation and responses to environmental and physiological stress in *Escherichia coli*. *Research in Microbiology*, 160(4), pp.259–266..

Lazari, M.F.M. et al., 2009. Estrogen receptors and function in the male reproductive system. *Arquivos brasileiros de endocrinologia e metabologia*, 53(8), pp.923–933.

Li, G. et al., 2017. Estrogen directly stimulates LHb expression at the pituitary level during puberty in female zebrafish. *Molecular and Cellular Endocrinology*, pp.1–11.

Liu, G. & Lin, Y., 2005. Electrochemical sensor for organophosphate pesticides and nerve agents using zirconia nanoparticles as selective sorbents. *Analytical Chemistry*, 77(18), pp.5894–5901.

Liu, L. et al., 2012. Discovery of estrogen receptor α modulators from natural compounds in Si-Wu-Tang series decoctions using estrogen-responsive MCF-7 breast cancer cells. *Bioorganic and Medicinal Chemistry Letters*, 22(1), pp.154–163.

Liu, R. et al., 2015. Residential Exposure to Estrogen Disrupting Hazardous Air Pollutants and Breast Cancer Risk. *Epidemiology*, 26(3), pp.365–373.

Luigi, V., Giuseppe, M. & Claudio, R., 2015. Emerging and priority contaminants with endocrine active potentials in sediments and fish from the River Po (Italy). *Environmental Science and Pollution Research*, 22(18), pp.14050–14066.

Ma, J. et al., 2011. The study of core-shell molecularly imprinted polymers of 17 β -estradiol on the surface of silica nanoparticles. *Biosensors and Bioelectronics*, 26(5), pp.2791–2795.

Mansouri, S. et al., 2017. Estrogen can restore Tamoxifen sensitivity in breast cancer cells amidst the complex network of resistance. *Biomedicine and Pharmacotherapy*, 93, pp.1320–1325.

Mingo, V., Lötters, S. & Wagner, N., 2016. Risk of pesticide exposure for reptile species in the European Union. *Environmental Pollution*, 215, pp.164–169.

Nagpal, N. & Meays, C., 2009. Water Quality Guidelines for Pharmaceutically-active-Technical Appendix. , pp.1–86.

Naidoo, V. & Buckley, C., 2003. Survey of Pesticide Wastes in South Africa and Review of Treatment Options. , (1128), pp.1–82.

Nieto, A. et al., 2008. Determination of natural and synthetic estrogens and their conjugates in sewage sludge by pressurized liquid extraction and liquid chromatography-tandem mass spectrometry. *Journal of Chromatography A*, 1213(2), pp.224–230.

Patch, R.J. et al., 2017. Indazole-based ligands for estrogen-related receptor α as potential anti-diabetic agents. *European Journal of Medicinal Chemistry*, 138, pp.830–853.

Perelo, L.W., 2010. Review: In situ and bioremediation of organic pollutants in aquatic sediments. *Journal of Hazardous Materials*, 177(1–3), pp.81–89.

- Pieper, C. & Rotard, W., 2011. Investigation on the removal of natural and synthetic estrogens using biofilms in continuous flow biofilm reactors and batch experiments analysed by gas chromatography/mass spectrometry. *Water Research*, 45(3), pp.1105–1114.
- Pinto, P.I.S. et al., 2017. In vitro screening for estrogenic endocrine disrupting compounds using Mozambique tilapia and sea bass scales. *Comparative Biochemistry and Physiology Part C: Toxicology & Pharmacology*, 199(June), pp.106–113.
- Pogačnik, L. & Franko, M., 2003. Detection of organophosphate and carbamate pesticides in vegetable samples by a photothermal biosensor. *Biosensors and Bioelectronics*, 18(1), pp.1–9.
- Pohanka, M., 2014. Inhibitors of acetylcholinesterase and butyrylcholinesterase meet immunity. *International Journal of Molecular Sciences*, 15(6), pp.9809–9825.
- Qian, S. wen et al., 2016. BMP4 Cross-talks With Estrogen/ER α Signaling to Regulate Adiposity and Glucose Metabolism in Females. *EBioMedicine*, 11, pp.91–100.
- Quinn, D.M., 1987. Acetylcholinesterase: enzyme structure, reaction dynamics, and virtual transition states. *Chemical Reviews*, 87(5), pp.955–979.
- Quinn, L.P. et al., 2011. *Pesticide use in South Africa: one of the largest importers of pesticides in Africa*,
- Rodriguez-Narvaez, O.M. et al., 2017. Treatment technologies for emerging contaminants in water: A review. *Chemical Engineering Journal*, 323, pp.361–380.
- Romano, S.N. & Gorelick, D.A., 2016. Crosstalk between nuclear and G protein-coupled estrogen receptors. *General and Comparative Endocrinology*.
- Roy, S. & Kalita, J.C., 2011. Determination of Endocrine Disrupting Compounds in Water Bodies Around Guwahati City , Assam , India through Gas Chromatography / Mass spectrometry. *International journal of chemtech research*, 3(4), pp.1840–1844.

Sassolas, A., 2012. Biosensors for Pesticide Detection: New Trends. *American Journal of Analytical Chemistry*, 3(3), pp.210–232.

Sifakis, S. et al., 2017. Human exposure to endocrine disrupting chemicals: effects on the male and female reproductive systems. *Environmental Toxicology and Pharmacology*, 51, pp.56–70.

Smarr, M.M., Kannan, K. & Buck Louis, G.M., 2016. Endocrine disrupting chemicals and endometriosis. *Fertility and Sterility*, 106(4), pp.959–966.

Smolarz, K. et al., 2017. Elevated gonadal atresia as biomarker of endocrine disruptors: Field and experimental studies using *Mytilus trossulus* (L.) and 17-alpha ethinylestradiol (EE2). *Marine Pollution Bulletin*, 120(1–2), pp.58–67.

Sornalingam, K., McDonagh, A. & Zhou, J.L., 2016. Photodegradation of estrogenic endocrine disrupting steroidal hormones in aqueous systems: Progress and future challenges. *Science of the Total Environment*, 550, pp.209–224.

Sun, Y. et al., 2014. Occurrence of estrogenic endocrine disrupting chemicals concern in sewage plant effluent. *Frontiers of Environmental Science and Engineering*, 8(1), pp.18–26.

Sussman, J.L. & Silman, I., 1992. Acetylcholinesterase: Structure and use as a model for specific cation-protein interactions. *Current Biology*, 2, p.612.

Tahboub, Y.R., Zaater, M.F. & Khater, D.F., 2017. Semi-volatile organic pollutants in Jordanian surface water. *Arabian Journal of Chemistry*, 10, pp.S3318–S3323.

Tam, I.S. & Giguère, V., 2016. There and back again: The journey of the estrogen-related receptors in the cancer realm. *Journal of Steroid Biochemistry and Molecular Biology*, 157, pp.13–19.

Teles-Grilo Ruivo, L.M. et al., 2017. Coordinated Acetylcholine Release in Prefrontal Cortex and Hippocampus Is Associated with Arousal and Reward on Distinct Timescales. *Cell Reports*, 18(4), pp.905–917.

Therapy, M., 2011. Combined estrogen-progestogen contraceptives. *IARC Monographs on the Evaluation of Carcinogenic Risks to Humans*, 100 A, pp.297–335.

Thornton, M.J., 2002. The biological actions of estrogens on skin. *Experimental dermatology*, 11(6), pp.487–502.

Tran, T.K.A. et al., 2016. Potential mechanisms underlying estrogen-induced expression of the molluscan estrogen receptor (ER) gene. *Aquatic Toxicology*, 179, pp.82–94.

Vert, G. & Chory, J., 2011. Crosstalk in Cellular Signaling: Background Noise or the Real Thing? *Developmental Cell*, 21(6), p.1179.

Water, R., Services, A. & Africa, S., 1930. Determination of Endocrine Disrupting Compounds such as Hormones in Environmental Water Samples by HPLC-MS.

Wee, S.Y. & Aris, A.Z., 2017. Endocrine disrupting compounds in drinking water supply system and human health risk implication. *Environment International*, 106(May), pp.207–233.

Xu, F. et al., 2017. Supported gold clusters as effective and reusable photocatalysts for the abatement of endocrine-disrupting chemicals under visible light. *Journal of Catalysis*, 354, pp.1–12.

Xu, M. et al., 2016. A research on application of water treatment technology for reclaimed water irrigation. *International Journal of Hydrogen Energy*, 41(35), pp.15930–15937.

Ye, M. et al., 2017. Pesticide exposures and respiratory health in general populations. *Journal of Environmental Sciences (China)*, 51, pp.361–370.

Zhang, H. et al., 2017. 4-Nitrophenol (PNP) inhibits the expression of estrogen receptor B and disrupts steroidogenesis during the ovarian development in female rats. *Environmental Pollution*, 229, pp.1–9.





Summary

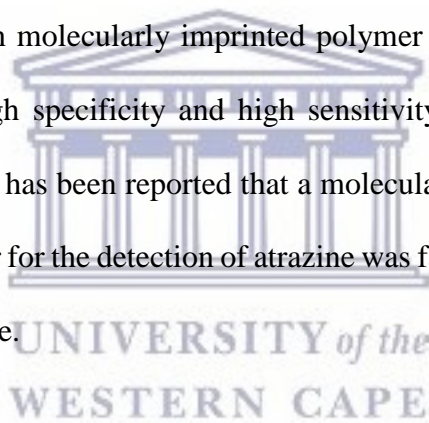
Over the years traditional polymers were used for their mechanical and insulating properties. The emergence of conducting polymers has gained a lot of interest in the scientific and technological world. Conducting polymers are characterized by the presence of conjugated double bonds which give rise to the electro conductive nature of the polymers. They have metal-like properties while retaining the properties of traditional polymers. They can be synthesized through both chemical and electrochemical polymerization of monomers of choice. Depending on the application for which the polymer is required, the method of preparation can be chosen. In this chapter the background on conducting polymers, their history, properties and applications have been described.



Abstract

Polymer materials commonly known as “plastics” have received a lot of interest over the years, their insulating, chemical and mechanical properties have seen them being applied in various fields. The emerging of conducting polymers has however shifted the interest. These polymer materials behave as hybrids between metals and polymers, making them “super material”. There are currently 25 reported conducting polymers and they all have the same structural feature of conjugated double bonds. This feature results in material with high electron affinity, low energy transitions and ionization potentials. They can be made both electrochemically and chemically. Electrochemical polymerization being the most attractive synthetic route as it has many advantages, including the fact that minute quantities of materials

are required resulting in low amounts of by-products and waste which could be potentially hazardous to the environment. The process is less time consuming and depending on the application, the polymer film thickness is controlled. They can be used in the preparation of nanocomposite material, including composites of metals and composites with other polymers which is known as copolymerization. They also have the potential of application in various fields such as sensors where they are used for the modification of electrode surfaces. This is due to their conducting ability, environment stability, low-cost fabrication process, light weight, and easy tailoring, to obtain the required performance. Polyaniline poly (3,4-ethylenedioxythiophene) (PEDOT) and poly pyrrole (PPy) have been used to improve the electrochemical performances of electrodes using several electrode modification techniques including electrodeposition. In molecularly imprinted polymer sensors conducting polymers (CPs) ensure that there is high specificity and high sensitivity by building highly specific recognition sites in the CPs. It has been reported that a molecularly imprinted polymer sensor based on a conducting polymer for the detection of atrazine was fabricated with high specificity and sensitivity towards atrazine.



2.0 Introduction

2.1 Conducting polymers

The exploration of the electrical conductivity of polymers dates back to the 1960's (Hu *et al.* 2017). Traditional polymers commonly known as plastics have been used because of the attractive chemical, electrically insulating (Lakshmi *et al.* 2009) and mechanical properties (Elahi *et al.* 2015). The use of conducting polymers as electronic material is fairly new. The properties of conducting polymers differ depending on whether they are in pristine form or doped form. In pristine form they tend to have insulating and semi-conducting properties while when they are doped their electrical conductivity resembles that of metals (Linko *et al.* 1999).

Since 1977, the dream of combining the processing and mechanical properties of polymers with the electrical and optical properties of metals has driven both the science and technology of conducting polymers. In 1977 it was found by Shirakawa, Heeger and McDiarmid that films of polyacetylene (PAC) increase their conductivity tremendously when they are exposed to iodine vapour, from a low value where they behave as semiconductors up to values equivalent to metals. In the year 2000 they jointly received a Nobel Prize in chemistry for their discovery and development of conducting polymers. Soon after this discovery, a series of stable conducting polymers, including **polypyrrole (PPy)** (Harraz *et al.* 2008; Ozcan 2007; Wang *et al.* 2001; Fall *et al.* 2006), **polyphenylene**, **polyaniline (PAn)** (Sen *et al.* 2016; Dhawan *et al.* 1997; Elahi *et al.* 2015; Tovide, Jaheed, *et al.* 2014), and **polythiophene (PTh)** (Anon 2004; Yurtsever & Yurtsever 2000; Zanardi *et al.* 2013; Hu *et al.* 2017), were reported from the end of the 1970s which led to the research on conducting polymers. They are applied in the development of batteries, electronic displays, sensors, functional electrodes to name a few. The conductivity of almost all conjugated polymers can reach the order of 10^{-3} – 10^3 S/cm after doping (Li 2015a). Currently there are 25 conducting polymers that have been reported (Ateh *et al.* 2006). All these polymers share a similar structural feature, a conjugation of double bonds (Zhao *et al.* 2014; Cheng *et al.* 2009). This structural feature is what brings about the properties, notably, low-energy optical transitions and ionization potentials as well as high-electron affinities. What makes conducting polymers materials of interest is their intrinsic properties making them behave as metals and inorganic semiconductors due to their good electronic and optical properties (Bitar, Maalouly, Chebib, Lerbret, Lee, *et al.* 2015). Not only do conducting polymers have good optical and electronic properties, they also have mechanical properties attributed to conventional polymers together with exceptional electrochemical redox activity, thus giving them an advantage over other materials. Obviously, conducting polymers, including doped conducting polymers and intrinsic semiconducting conjugated polymers, will

play a vital role in the future development of organic optoelectronic and electrochemical devices (Mousavi *et al.* 2008). Conducting polymers can be classified into two major groups depending on the synthetic method: these groups are chemically polymerized materials and electropolymerized. Chemical polymerization brings about a lot of advantages including the ability of mass production and low costs, this is almost difficult to achieve using the electrochemical polymerization synthetic methods (Kudoh *et al.* 1998; Alemayehu & Himariam 2014). On the other hand, electrochemical polymerization has the ability to directly produce conducting polymer films which are suitable for applications in electronic devices (Toshima & Hara 1995).

2.2 Synthesis of conducting polymers

2.2.1 Chemical polymerization

There are several methods and oxidants that can be used in the chemical polymerization of EDOT/EDT and its derivatives. The chemical polymerization techniques that are used for their synthesis include template synthesis, reverse microemulsion polymerization (Yao *et al.* 2014), pulsed electron beam synthesis and interfacial polymerization in the presence of an oxidant and/or surfactant. Reverse microemulsion is a complex method that involves radical addition polymerization that takes place in a heterogenous system (Selvaganesh *et al.* 2007). The emulsification of a hydrophobic monomer in water by an oil-in-water emulsifier followed an initiation reaction through the addition of a water or oil soluble free radical initiator. This process yields a milky fluid which is called “latex”, “polymer dispersion” or “synthetic latex” which is defined as colloidal dispersion of polymer particles in aqueous medium. Emulsion polymerization is one of the promising methods of oxidative polymerization of the EDOT monomer, however EDOT is quite insoluble in water and after the monomer is initiated it tends to react with water thus polymerization in the absence of an emulsifier results in low

production yields of the PEDOT polymer with poor conductivity (Pyshkina 2010; Lakouraj *et al.* 2014). To improve this problem, surfactants such as dodecyl sulfate (SDS) or polymeric surfactant, for example, poly (styrenesulfonate) were suggested as suitable molecules to improve the yield during polymerization of EDOT. Surfactants with sulfonate functional groups offer stability to colloids in one step during synthesis while on another step it aids in doping thus resulting in PEDOT with high electrical conductivity (Manisankar *et al.* 2007) in his work used this method to prepare PEDOT and PEDOT/Au nanocomposite whilst (Pyshkina & Kubarkov 2010) used the method to prepare PEDOT using sodium salt of 2-naphthalenesulfonic acid as dopant and emulsifier. (Kudoh *et al.* 1998) found that emulsion polymerization in the presence of an anionic surfactant as an emulsifier and an oxidant $\text{Fe}_2(\text{SO}_4)_3$ results in increased production of PEDOT while on the other hand an emulsifier-free emulsion polymerization of 3,4-ethylenedioxythiophene (EDOT) shows a decrease in the production of PEDOT with poor conductivity. In general, the conductivity of the latex particle increases with increasing doping level of PEDOT from the sulfonate groups of the surfactant. However, with excess amount of the nonconductive surfactants on the outer surface of conductive particles, the conductivity of the film made from the core-shell latex reaches a maximum and decreases with increasing surfactant amount. In order to solve this problem, it is necessary to use a typical oil-in-water emulsion polymerization of EDOT monomer in the presence of water soluble conductive oligomers or polymer. The typical method uses oxidizing agents such as iron (III) FeCl_3 or p-toluenesulfonate ($\text{Fe}(\text{OTs})_3$) and ammonium persulfate (APS) or sodium persulfate ($\text{Na}_2\text{S}_2\text{O}_8$). This method yields a black compound, PEDOT. These oxidants have been frequently used in conjunction with an additive such as an organic base or a surfactant. (Paradee & Sirivat 2013) synthesized PEDOT nanoparticles via chemical oxidation polymerization using ammonium peroxydisulfate (APS) as the oxidant, they investigated the effects of APS concentration, surfactant concentration and the type of

surfactant using dodecylbenzenesulfonic acid and sodium dodecylsulfate. They found that polymerization in the absence of surfactants results in formation of smaller particles sizes due to the large amount of initiator which induces lower molecular weights and smaller particle size. They also found that the smaller particles size results in an increase in electrical conductivity due to due to the large surface area. The type of surfactant and its concentration have an impact on the particle size and the shape of the nanoparticles. (Mohammad Reza Nabid, 2010) reported the development of a water soluble PEDOT by using transition metal presence of sulfonated polystyrene (SPS) is reported. The reactions were catalysed by various catalysts such as such as iron, cobalt and manganese phthalocyanine. When metallophthalocyanines were used they proved to have good activities for polymerization, their disadvantage was shown under oxidising conditions where they showed easy degradability. A study by (Pyshkina & Kubarkov 2010) described the use of high concentration emulsion polymerization of 3,4-ethylenedioxythiophene in the presence of sodium salt of 2- naphthalenesulfonic acid as dopant and emulsifier and ferrum(III) sulfate as oxidant. The influence of heat treatment at 125°C of poly(3,4-ethylenedioxythiophene) on its conductivity and morphology was studied. It was shown that the initial conductivity of poly(3,4-ethylenedioxythiophene) has an effect on the conductivity of the heat treated poly(3,4-ethylenedioxythiophene). The heating of poor conductive poly(3,4-ethylenedioxythiophene) results in decrease in its conductivity while the heating of the poly(3,4- ethylenedioxythiophene) with maximal conductivity of 160 S/cm leads to increase of its conductivity up to several thousand S/cm (Ouyang *et al.* 2004; Hernández *et al.* 2017).

2.2.2 Electrochemical polymerization

Besides the oxidative chemical polymerization method, there is another equally useful method; electrochemical oxidation of the monomer. Electrochemical polymerization refers to the

oxidation of the monomer onto the anode surface by the application of a positive potential that eliminates the use of an oxidant which is used in the chemical polymerization (Waenkaew *et al.* 2011; Florea, Cristea, Vocanson, Robert, *et al.* 2015). To date the mechanism of electropolymerization of conducting polymers is still not fully understood and remains subject to controversial discussion (Sharma *et al.* 2012). Diaz was the first to present the mechanistic concept for the formation of conducting polymers. He suggested, in resemblance with radicalic or ionic polymerization processes, that in the polymerization of pyrrole the monomers dimerize at the R-position after oxidation at the electrode and that proton elimination occurs from the doubly charged σ -dimer, forming an aromatic neutral dimer. As this dimer, on account of its greater conjugation, is more easily oxidized than the monomer, it is immediately oxidized to its cation, undergoing a next coupling step with a monomeric radical cation, and then from the resulting charged trimer again protons are eliminated. The proposed mechanism of the electropolymerization shown in fig 2.1 begins with the formation of primary cation radicals by monomer oxidation at the anode (Tovide, Jaheed, *et al.* 2014). After cation radical formation dimers are formed through deprotonation and rearomatization. Further oxidation and reaction of the formed cation radicals and monomer result in the polymer growth. After the dimer formation process, deposition which includes nucleation, growth and other processes take place.

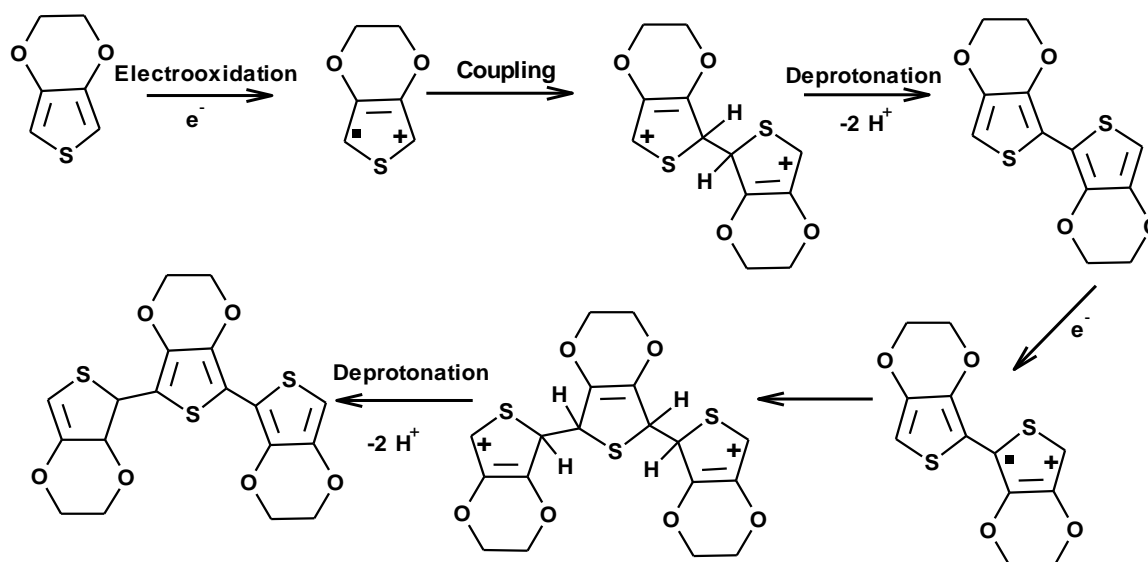


Figure 2. 1: Possible polymerization mechanism for EDOT

The use of this method is advantageous on the basis that it requires minute amounts of monomer, short polymerization times and can yield both electrode-supported and free-standing films. The polymer films can be deposited on a small surface area with a high degree of geometrical conformity and a controllable thickness which can be achieved by the number of cycles resulting in film growth in potentiodynamic cycling. This approach allows for the preparation of smooth conducting polymers on conducting surfaces such as the surfaces of electrodes which are generally of high purity (Re & Milczarek 2016). Over the years there has been development and study of different polymeric materials, however polyaniline (PANI), polypyrrole (PPy) and poly(3,4-ethylenedioxythiophene) (PEDOT) constitute an important class. PEDOT shows outstanding stability, produces homogenous films and can be produced electrochemically from aqueous and non-aqueous media, for these reasons it has received significant interest in its application as an electrode material for a many of applications. In phosphate buffer PEDOT shows exceptional stability than other conducting polymers, suggesting that PEDOT may be a potential candidate for sensor applications and hence it is chosen for sensing NaClO (T. H. Tsai *et al.* 2011). Electrochemical polymerization of the

EDOT monomer results in the formation of a highly transmissive blue, doped PEDOT film on the surface of electrodes. Electronic conductivity and surface morphology of the conducting polymers can be tuned by the application of various electrosynthesis conditions. Electrolytic medium including solvent and salt has a significant influence on the morphological properties of polymer films. The electropolymerization conditions which play a vital role on the electronic conductivity has been also been reported. Electropolymerization conditions have an effect on the conductivity of conducting polymers in their doped state. The supporting electrolyte has also a strong effect on the conductivity of the polymer material. In contrast, no significant effect of the solvent has been clearly identified (Louet *et al.* 2015). There are various electrochemical techniques that can be used for the preparation of conducting polymers. These techniques are classified as: potentiostatic, galvanostatic and potentiodynamic. Potentiostatic refers to the application of a positive potential (for oxidative polymerization) (Si *et al.* 2014a; He *et al.* 2014; Pineda *et al.* 2018). It is of importance to choose a potential that will be high enough to ensure that the polymerization reaction proceeds but also low enough to avoid over oxidation of the polymer and to prevent side reactions from taking place. Galvanostatic technique refers to the formation of the polymer shown in fig 2.2 at a constant current density (Harraz *et al.* 2008; Patra *et al.* 2008; Mo *et al.* 2014). This technique allows control of the polymer thickness by adjusting the duration of the polymerization and yields a polymer in its doped form (Harraz *et al.* 2008).

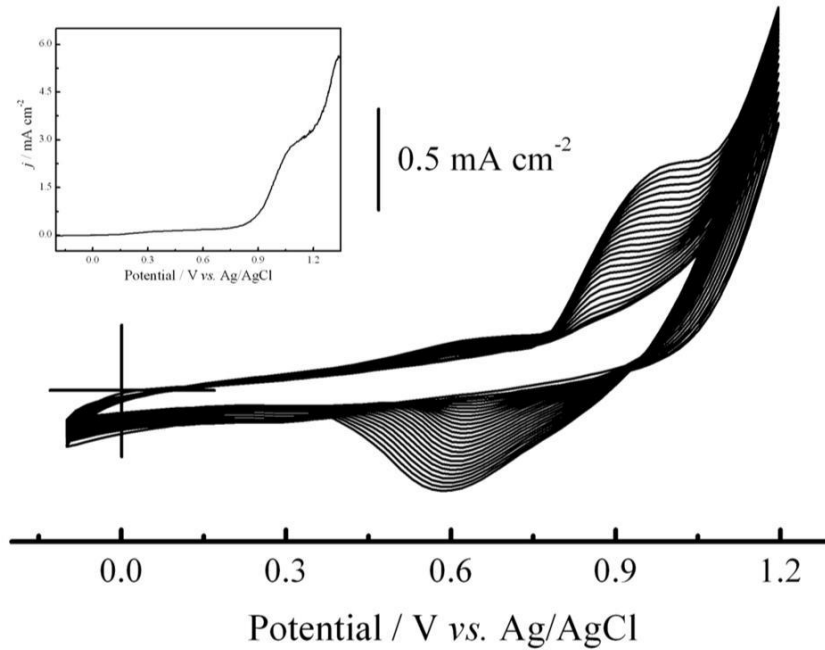


Figure 2. 2: Galvanostatic polymerization of EDOT at 1 mA/cm². The EDOT monomer dissolved in acetonitrile together with a supporting salt (lithium perchlorate) was polymerised until a significant increase of potential indicating the end of polymerization was observed (Scrosati 1989).

In the potentiodynamic approach, cyclic voltammetry (CV) was used for the polymerization, where the electrode was subjected to cyclic regular change of the potential which resulted in the polymer changing between dedoped and doped forms (Su *et al.* 2013; Shanmugham & Rajendran 2015). Potentiodynamic method provides information on the rate of the growth of the polymer as depicted in fig 2.3. There is direct proportionality between the number of cycles of a multisweep cyclic voltammogram and the current generated which is attributed to the increase in the surface and the rechargeable redox sites (Obaid *et al.* 2014; Sandoval *et al.* 2015).

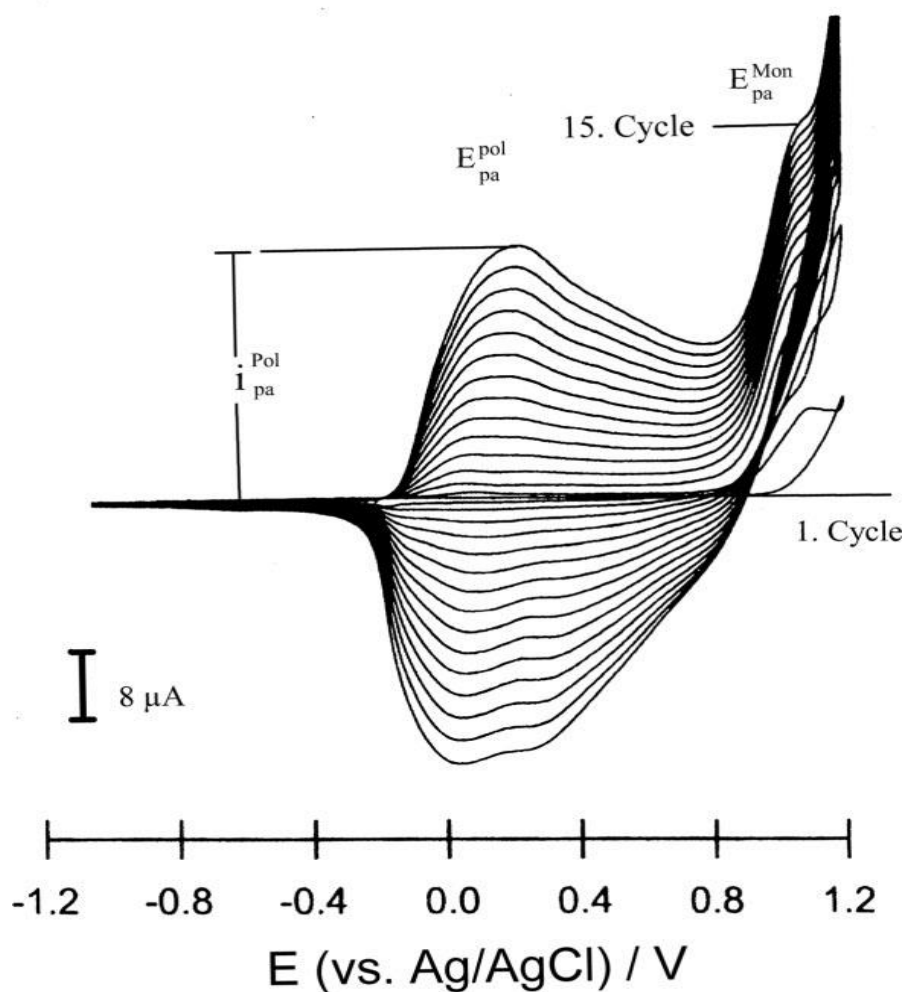
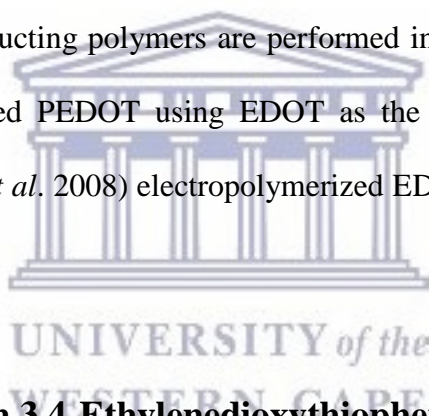


Figure 2. 3: Typical potentiodynamic experiment of conducting polymer growth. Potentiodynamic growth of a polypyrrole film in acetonitrile (+1% H₂O)/0.1 M TBAPF₆, V) 100 mV s⁻¹, T 298 K (Road *et al.* 1979).

(Gonalves *et al.* 2011) synthesized PEDOT films on carbon-film electrodes (CFE) in aqueous solution using electropolymerisation by potential cycling, potentiostatically and galvanostatically. Electrochemical characterization of the film by cyclic voltammetry and electrochemical impedance spectroscopy (EIS) is used to investigate the method appropriate for the formation of a polymer with suitable properties for sensor applications. G.M. Abou-Elenien, 2004 investigated the electro-synthesis of polythiophene films using different

electrochemical techniques and studied the stability and electrical conductivity of the polymer films and found that the most stable with a low relaxation time was the one obtained using a galvanostatic technique. The electrochemical synthesis is usually performed in a three-electrode set up in an electrochemical cell. The three electrode system consists of a working electrode which acts as an anode where the electrochemical deposition of the polymer material will occur. In the counter electrode reduction of compounds found in the electrolyte takes place while the reference electrode serves as the potential control. An electrolyte is required in an electrochemical cell which contains the monomer of choice, a solvent and acid which serves as the source of dopant ions (Gurunathan *et al.* 1999). The solvent should not only be capable of dissolving the monomer but also be stable at the potentials being used for the polymerization. Most electrosynthesis of conducting polymers are performed in aqueous electrolytes (Cui & Martin 2003) electrosynthesized PEDOT using EDOT as the EDOT monomer and PSSN aqueous solution. (Vasantha *et al.* 2008) electropolymerized EDOT in an aqueous solution of EDOT and LiClO₄.



2.3 Copolymers Based on 3,4-Ethylenedioxythiophene

Almost after five decades since the development of the first copolymer, there is still an increased interest in the field (Azzahari *et al.* 2013; Mangold *et al.* 2010). They represent a subject on various current research within macromolecular chemistry and physics, stretching from the development of new synthetic strategies and molecular structures to applications of theoretical and computational methods (Seung *et al.* 2004). Block copolymers are made up of two or more polymer chains (Deniz *et al.* 2004; Kataoka *et al.* 2001), each chemically different from the other, these chains are linked together at one or more junction points via either covalent or noncovalent bonds. According to the theory of Erukhimovich, 1) when comparing graft copolymers to triblock copolymers, the former shows better phase separation than the

latter. Graft copolymers are prepared using copolymerization of macromonomers (MM) with low molecular weight monomers. 2) the structure of the polymers is determined by three parameters: (i) side chain lengths, which can be achieved through synthesis of the macromonomer using living polymerization; (ii) the length of the chain of the polymer backbone, given by living copolymerization, lastly (iii) the by the spaces that are present on the side chains, which is controlled by the molar ratio of the comonomers and the reactivity ratio of the low-molecular weight monomer, r_1) k_{11}/k_{12} . However, the scattering of spacing may not be a very easy parameter to control since there is inconsistency in the polymer backbone and the macromonomers.

2.4 Applications of conducting polymers

2.4.1 Sensors

A sensor can be defined as an analytical device that can be used to detect and respond to electrical or optical signals. It converts the physical parameter into a signal which is measured electrically (Trifigny et al. 2013; Si et al. 2014b). During the last two decades, interest in research based on sensors has seen a significant increase. Sensors have the ability to give information about the physical, biological and chemical changes in the environment (Chen *et al.* 2018; Nezhadali & Mojarrab 2014). Polymers have been applied in the fabrication of sensors since they are material whose properties can be tuned to meet their needs. Interest has increased on a particular class of polymers known as conducting polymers which they have been applied in electrochemical sensors as electrode material. On the surfaces of electrodes, they can enhance the surface of the electrode by improving the conductivity and electron transfer between electrolyte and electrode surface (X. Liu *et al.* 2015; Liu *et al.* 2010). These properties of conductive polymers have made them interesting material for the modification of

electrode surfaces, these properties include good and high conductivity, low cost fabrication processes, easy tailoring to achieve required performance, CPs are generally light in weight and have good environmental stability. Various conducting polymers, such as polyaniline (PANI), polypyrrole (PPy) and poly (3,4- ethylenedioxythiophene and their composites have been applied to improve the electrochemical performances of electrodes using several electrode modification techniques including dropcoating (Wisitsoraat *et al.* 2013), inkjet-printing (Wu *et al.* 2017; Nguyen *et al.* 2016), electrospinning (Wang *et al.* 2009; Lee & Chen 2016), electrospraying (Borghetti *et al.* 2013; Tirawattanakoson *et al.* 2016) and electrodeposition (Du *et al.* 2008; Jiao *et al.* 2006; Obaid *et al.* 2014). Poly (3,4- ethylenedioxythiophene): poly (styrenesulfonate) (PEDOT:PSS) is one of an interesting conducting polymers for electrode modification owing to its high conductivity, low redox potential and thermal stability (Chou *et al.* 2015). (Borghetti *et al.* 2013) Developed a chronoamperometric sensor using an electrosprayed Graphene/PEDOT: PSS modified SPCE coupled with DPPH assay for free radical scavenger screening of TAC for evaluation of TAC content in Thai herb and beverages. (Mazloun-ardakani *et al.* 2016) prepared a sensitive enzyme-free electrochemical glucose sensor prepared by electrodeposited of nickel nanostructure (NiNS) supported on the surface of poly(3,4-ethylenedioxythiophene) polystyrene sulfonate (PEDOT:PSS), the sensor was characterized by a low detection limit, low glucose oxidation potential and high sensitivity. A highly sensitive disposable biosensor was developed by A. Phongphut based on Au/PEDOT-PSS nanocomposite inkjet-printed on screen-printed carbon electrodes (SPCEs) and co-immobilization of lipase, glycerol kinase and glycerol-3-phosphate oxidase.

2.4.2 Biosensors

Biosensors are chemical sensing devices in which a biological element is coupled to a transducer to allow the development of complex biochemical parameters. They have been applied in different fields such as clinical diagnostics, environmental monitoring. Since

biosensors are based on biological elements, the application of CPs improves the stability of those biomolecules. CPs are important because they provide support and increase the number of biomolecules on the surface of the sensor. Polypyrrole is one of the CPs that have been used for the construction of biosensors due to the solubility of PPy in water and the ease of counterion incorporation (Sadik 1999).

In biosensors, enzymes can be used as the biological components. Enzymes are known as biological catalyst having the ability to promote transformation of chemicals in living organisms (Mäntsälä & Niemi n.d.; Van Dyk & Pletschke 2011; Brena *et al.* 2013). They are able to catalyse a number of different chemical reactions taking place in cells. They have the ability to catalyse reactions as individual molecules in solution, with other entities and attached in surfaces. It is in the attached state that is of particular interest in their applications in biosensors. The attachment of enzymes is known as the immobilization (Putzbach & Ronkainen 2013; Xia *et al.* 2015), which can be defined as the physical localization of enzymes in a defined space while retaining their catalytic activities, this means that they may be used repeatedly and continuously (Bickerstaff *et al.* 1997). Chibata and co-workers were the first to report on the use of immobilized enzymes in 1966, they developed the immobilization of *Aspergillus oryzae* aminoacylase for the resolution of synthetic racemic D-L amino acids (Brena & Batista-viera 2006) the most important step to consider in the fabrication of any electrochemical sensor including biosensors is the immobilization of the biological element onto the surface of the transducer. Several problems have surfaced in the development of biosensors which are related to the activity of the enzyme system such as the loss of enzyme, maintenance of enzyme stability and the shelf-life of the biosensor. In order to overcome these challenges and to ensure the success of immobilization, several immobilization procedures have been developed. To ensure efficient deposition of biomolecule is achieved it must satisfy a few prerequisites; (i) the biological recognition properties and catalytic properties of biomaterial

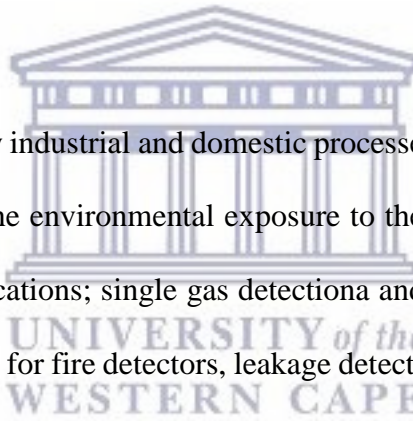
should be intact after immobilization, (ii) the biomolecule should be chemically inert and compatible towards the host molecule, (iii) the biomaterial should be fixed on the substrate to avoid the loss of sensitivity on in the sensor and (iv) it should be accessible after immobilization. CPs can help in solving some of these issues if not all (Oztekin et al. 2011; Ramanavicius *et al.* 2010). There are various procedures used for the immobilization of biomolècules. The immobilization can be carried out via **covalent attachment, physical adsorption or electrostatic entrapment** while maintaining the biorecognition properties of the molecule.

Physical adsorption: The adsorption technique is the oldest and most simple method for the preparation of immobilized enzymes, this method is cheaper and easy to use. Its main drawback is the fact that it has weak binding forces between the carrier and the enzyme. The interaction between the enzyme and surface of the matrix are by weak forces such as salt linkage, hydrogen bonds, hydrophobic bonds, ionic bonds and van der Waals forces. The nature of the weak forces in adsorption immobilization result in a process that can be reversed by the changes in the conditions that influence the strength of the interaction, these conditions include; polarity of solvent, temperature, ionic strength and pH (Brena & Batista-viera 2006). The advantage of this method is that it requires minimum activation step and as a result, minimum number of reagents is required and usually there is preservation of the catalytic activity of the enzyme (Karthick 2012).

Covalent immobilization: Covalent linkage of the transducer and biomolecule is an efficient method of immobilization in order to achieve an increase in the lifetime of the stability of the enzyme electrode (Zucca & Sanjust 2014). It is important to have strong and efficient bonding between the biomolecule and the immobilizing material. The use of this method is advantageous in the sense that it has low diffusional resistance and thus the sensor shows good stability under adverse conditions (Porat *et al.* 1993). The formation of strong and stable bonds

between the enzyme and matrix is what ensures that the enzyme is not released into the solution once immersion occurs. Achieving high levels of binding activity, the amino acid residues responsible for the catalytic activity should not interfere in the covalent linkage to the matrix, in some cases this may prove difficult to fulfill. Covalent methods are mainly employed when the enzyme is not required in the product. Though the covalent method produces a stable enzyme-matrix bond, once the enzyme activity depletes, the enzyme and matrix must be discarded. The disadvantage in the use of this method is that it is costly and results in an irreversible bond.

2.5 Gas sensors



Gases are produced in many industrial and domestic processes. There has been an increased interest in the monitoring of the environmental exposure to these gases (Lakard *et al.* 2015). There are two important applications; single gas detection and the discrimination of odours. Single gas detectors can be used for fire detectors, leakage detectors, controllers of ventilation in vehicles and in aircrafts and alarms that warn when the threshold concentration of gases is passed (Capone *et al.* 2004). In the food industry the detection of volatile compounds or smells that are generated by food or household products are very important (Yamini *et al.* 2017). Multi-sensor systems often referred to as the electronic noses are the modern gas sensing devices designed for the analysis of such environmental mixtures. (Kumar *et al.* 2017) developed a sensor based on a multistep reduced graphene oxide for the detection of sulfur dioxide (SO₂) which is emitted to the environment from the combustion of fossil fuel at power plants, transport services such as automobiles, locomotives, ships, etc., and other industrial facilities. SO₂ has poisonous properties and has been rendered harmful, it equally affects plants, animals and human beings. It is the main cause of acid rain and a wide range of breathing problems in

human beings. An exposure limit of (SO₂) for human respiratory system is 5 ppm, therefore, its regular monitoring using appropriate sensors is critically important. (Kang *et al.* 2017) proposed the selective detection of toluene and formadehyde using a micro gas sensor capable working under low power conditions. Thin films based on SnO were used as sensing materials on MEMS structures to ensure the sensitivity of the sensors is preserved and for enhancing the sensor sensitivity towards CO, toluene and HCHO gases.

Since the early 1980's conducting polymers have been used as active materials in the fabrication of gas sensors. In comparison to commercially available sensors, sensors based on conducting polymers show an improvement on the characteristics. Their necessity for operation at room temperatures motivate the reasearch into alternative materials such as CPs. They have short response times coupled with high sensitivity. Their ease of preparation through electrochemical and chemical polymerization makes them interesting materials (Bai & Shi 2007; Rahman *et al.* 2008). Their molecular structures can be manipulated through modification by functionalizing with other materials such as metals, different monomers and oxides. Their good mechanical properties makes them ideal for the development of sensors. Conducting polymers that have been used in the fabrication of gas sensors include polypyrrole, polyaniline and polythiophene. These polymers have intrinsict conducting properties owing to the presence of alternating single and double bonds in thier main chains. This leads to a broad π -electron conjugation. However in their pure forms, the conductivities of these polymers are quite low. In order to maximize these conductivities doping of these material is an important step. Doping can be achieved by redox reaction or protonation, although protonation is only possible in doping of PANi (Bai & Shi 2007).

2.6 Molecularly imprinted polymers

The chemical sensor and biosensor technology has seen an increase in the interest in the field of modern analytical chemistry. There is a high demand for these technologies due to an increase in the need to develop the tools that are used in clinical diagnostics, environmental analysis, detection of drugs and xenobiotics (Iskierko *et al.* 2016). Chemical sensors and biosensors are based on the recognition element which is in close contact to the transducer. The recognition element is responsible for the specific recognition and binding of the target analyte. The transducer then translates the signal generated once the analyte has been bound and converted to an output signal. Biosensors rely on biological elements such as enzymes, antibodies, receptors and cells as the recognition element. A new type of semisynthetic receptor for biosensors are nucleic acids and peptides, however they are generally have poor chemical and physical stability of biomolecules, this prevents them from being used in harsh environments. However there is an emerging technique that is increasingly being adopted, molecularly imprinted polymers (Tun 2004). In this technique the binding sites are generated through the imprinting process and have the affinity and selectivities similar to those of antibody-antigen systems (Tang *et al.* 2015), for this reason they have been termed “antibody mimics” (Qian *et al.* 2014). These antibody mimics show potential over real antibodies for use in sensor technology (Jenkins *et al.* 2001). Due to their highly crosslinked polymeric nature they have improved stability and robust leading to their use even in harsh conditions such as high temperatures, high pressure and in the presence of acids (Erdőssy *et al.* 2016; Kryscio & Peppas 2012). They are also advantageous in the sense that they are easy and cheap to fabricate and have a long lifespan (Zhang *et al.* 2008).

Molecular imprinting technology (MIT) involves the process where functional monomer and crosslinkers are polymerized in the presence of a target molecule which acts as the molecular template (Huang *et al.* 2015; Ho *et al.* 2005). There is a complex formation between the target molecule and the functional monomer, following polymerization their functional groups are held

in place by the highly cross-linked polymeric structure (Hu *et al.* 2015). The removal of the target molecule leads to the development of binding sites that are complimentary in shape and size of the target molecule (Sharma *et al.* 2012; Granado *et al.* 2012). In that way a molecular memory is introduced into the polymer with high affinity for the imprinted molecule and the target analyte can bind with ease onto the created site (Haupt & Mosbach 2000). Thus their selectivity can be compared to that of biological receptors. (Bitar, Maalouly, Chebib, Lerbret, Cayot, et al. 2015) prepared high specific MIPs that have high performance to iprodion (a fungicide found in wine residue) binding (Du *et al.* 2014).

Composites of molecularly imprinted conducting polymers result in the formation of material with enhanced properties due to the combination of the conducting nature of conducting polymers together with selective molecular selectivity that are offered by the imprinting technology (Öpik 2009; Malhotra *et al.* 2006). This type of material is of special interest for applications in the field of sensor technology (Piletsky *et al.* 2006). Overoxidised polypyrrole is the polymer of choice to use (Rezaei *et al.* 2014). This is attributed to the fact that polypyrrole shows improved selectivity that is brought about by the elimination of positive charges from its film after oxygen functionality such as carbonyl groups are introduced (Malinauskas 2006). The preparation of molecularly imprinted polypyrrole requires polymerization around printed species (Deng *et al.* 2012) reported the successful preparation of a MIP based on the conducting polymer nanocomposite polypyrrole/titanium dioxide using methyl orange as the template molecule.

Molecularly imprinting technology using conducting polymers uses various electrosynthesis approaches which include galvanostatic, potentiostatic and voltammetric methods (Meng & Chen 2005). These techniques are suitable as they provide simplicity and decrease in preparation time (Yuan *et al.* 2015), they also offer control of conducting polymer thickness making them tunable according to the shape and size of the transducer element (Li *et al.* 2009). Conducting

polymers and their applications in sensing devices have been described in literature, they have only been limited in the detection of large biomolecules such as peptides, leaving out the smaller bio molecules since their simple association pendant sensing groups on the CPs is not enough to create the needed change of the electrochemical signature. The most important factor is to build highly specific recognition sites in the CP in order to improve both the selectivity and sensitivity of the recognition process. In order to obtain material with high sensitivity and selectivity it is imperative to pair CPs together with MIT. (Pardieu *et al.* 2009) reported the design of molecularly imprinted conducting polymers (MICPs), used as a transducer for the selective detection of atrazine, a small molecule. Monomers that have been reported and found useful in the design of molecularly imprinted conducting polymers include polypyrrole, aniline, o-phenylenediamine and m-aminophenol. Recently, electropolymerization of o-aminophenol has been reported (Tirawattanakoson *et al.* 2016). (Li *et al.* 2009) proposed a method for the preparation of a dopamine selective sensor based on molecularly imprinted electropolymer of o-aminophenol. They determined that the sensor had good selectivity towards dopamine even in the presence of high concentrations of ascorbic acid. This was determined using cyclic and differential pulse voltammetry by monitoring the changes in the oxidative currents of ferricyanides. The sensor showed good sensitivity, selectivity and reproducibility.

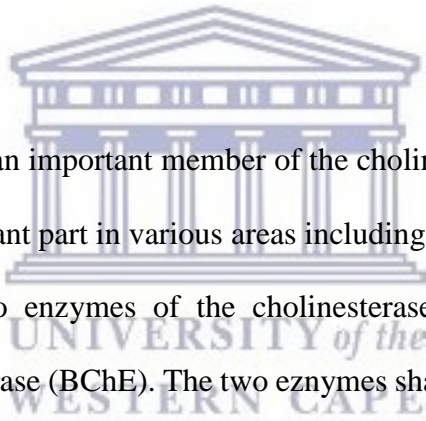
2.7 Estrogens

Estrogen is a steroid hormone (Nieto *et al.* 2008) that is known to play an important role in a normal physiology of various tissues including the mammary glands, reproductive tract, central nervous system and the skeletal systems (Guo *et al.* 2014; Gong *et al.* 2016), they are also known to be responsible for the development of secondary sexual features, and is also influential in bone growth, the cardiovascular and immune systems. In women it is known for the regulation of homeostasis and the menstrual cycle. Estrogens are produced in the ovaries,

adrenal glands and placenta during pregnancy (Bronowicka-Kłys *et al.* 2016; Sukocheva *et al.* 2015; Botelho *et al.* 2015). In the cardiovascular system they have protective effects through either their interaction with blood vessels or indirectly through plasma lipoprotein metabolism. In the skeletal system they regulate mineralisation, controlling and maintaining the balance between bone formation and bone resorption, while in the central nervous system various neuroendocrine functions are attributed to estrogens such as neuroprotection against Alzheimer's disease and schizophrenia however prolonged exposure to estrogens can be detrimental (Neves *et al.* 2008). Their biosynthesis is catalysed by aromatase (CYP19A1) a member of the cytochrome superfamily the only enzyme capable of catalysing the formation of estrogens by making use of androgens such as testosterone and androstenedione as substrates. At cellular levels, the enzyme aromatase is found in the endoplasmic reticulum where as at the tissue levels estrogen biosynthesis site varies with menopausal and postmenopausal women. In premenopausal women estrogens are mostly produced in the granulosa cells of the ovaries with every menstrual cycle, while lower levels of estrogen production occurs in other organs including bones, adipose tissue, the vascular endothelium, aortic smooth muscles and the brain. Menopause is characterized by lack of functioning of the ovaries and extra-gonadal sites then become the main source of estrogens (Gérard & Brown 2017). The hypothalamus secretes gonadotropin-releasing hormone (GnRH) which stimulates the anterior pituitary to release follicle-stimulating hormone (FSH) and luteinizing hormone (LH). Both these hormones induce the production of estrogen in the form of estradiol and estrone by the ovaries. These hormones bind to ER in target tissues of the breasts, uterus, brain, bone, liver and heart. Once binding occurs there are changes in the conformation of the estrogen receptor (ER) permitting its interaction with a specific regulatory sequence of the ER gene inducing transcription of the target coding sequence. The resulting protein promotes changes in the cell according to tissue type and underlying conditions. The cycle is completed when

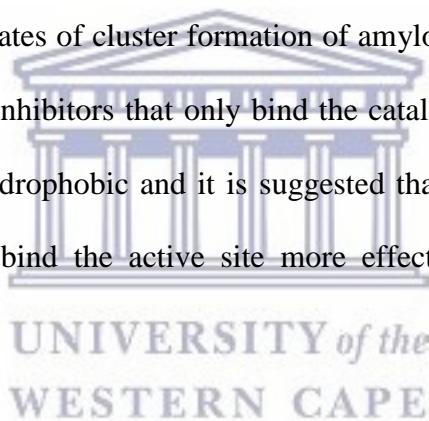
high levels of estrogen in the blood stream sends negative feedback to the hypothalamus to hinder the release of GnRH (Botelho et al. 2015). Estrogens are classified into natural and man-made estrogens, the most potent natural estrogen being 17 β -estradiol (E2) (Tran *et al.* 2016a). The other natural estrogens are estrone (E1) and estriol (E3) (Lin & Li 2006; Pérez & Escandar 2014) however they are the metabolites of E2 with limited estrogenic activity (Luo et al. 2013). 17 α -ethynylestradiol is a synthetic estrogen, a key ingredient in oral contraceptives (Shi et al. 2004; Shyu et al. 2011). The main route of excretion of estrogens are through feces and urine where they tend to end up in waste waters (Li *et al.* 2008; Nie *et al.* 2015; Huang *et al.* 2013). While most natural estrogens are excreted in urine as estrogen conjugates, some are assumed to be changed to their corresponding free estrogens (Z. hua Liu *et al.* 2015).

2.8 Acetylcholinesterase



Acetylcholinesterase (AChE) an important member of the cholinesterase enzymes family (Gu *et al.* 2017), it plays an important part in various areas including neurobiology, toxicology and pharmacology. There are two enzymes of the cholinesterase family acetylcholinesterase (AChE) and butyrylcholinesterase (BChE). The two enzymes share 65 % amino acid sequence homology and have similar molecular and active center structures even though they are products of different genes, AChE on human chromosome 7 (7q22) and BChE on chromosome 3 (3q26) (Ciepluch *et al.* 2013). Cholinesterase (specifically AChE) are responsible for playing a vital role in catalyzing the hydrolysis of the neurotransmitter acetylcholine into choline thus maintaining the levels of acetylcholine in the central nervous system in the normal range (Wiemann *et al.* 2017; Čolović *et al.* 2017; Lee *et al.* 2015) and is mainly found in neuromuscular junctions and cholinergic brain synapses (Xia *et al.* 2015; Sosnowska et al. 2013; Akincioğlu *et al.* 2017). Consequently butyrylcholinesterase (BChE) is not limited to one function but has a multitude of hydrolyzing activities. This is not confined to nonspecific cholinesterase activity but also includes acylamidase and peptidase activities (Liu *et al.* 2017).

The maintenance of AChE in the body is important because at elevated levels it can accelerate the assembly of amyloid peptides into amyloid fibrils thus leading to the development of Alzheimer's disease (Xu *et al.* 2018; Topczewski *et al.* 2013). AChE is characterized by 2 active centers connected by an aromatic gorge (Menéndez *et al.* 2017). The active site of AChE is found at the bottom of a 20 Å long, narrow gorge divided into five regions: the catalytic triad (composed of Glu327, His440 and Ser200), the oxyanion hole (Gly121, Gly122 and Ala201), the choline binding site (Trp84 and Phe330), the acyl binding pocket (Phe288 and Phe290), and the peripheral anionic site (PAS) (Trp279, Phe330 and Tyr70) (Basiri *et al.* 2017). The peripheral anionic site (PAS) of AChE catalyzes a series of reactions on the A β fibrils that lead to the formation of β -sheets with high aggregating potential. AChE inhibitors that bind to the PAS of the enzyme decrease rates of cluster formation of amyloid peptides and monitor their clearance when compared to inhibitors that only bind the catalytic triad of the enzyme. The AChE active site is highly hydrophobic and it is suggested that those molecules possessing multiple aromatic cores can bind the active site more effectively owing to hydrophobic interactions.



2.9 Organophosphate pesticides

Pesticides are a group of different chemical compounds, they are used to mitigate and alleviate the problems that are brought about by pests on crops and crop production in both industry and in households. They ensure that the quantity and quality of crops/produce is controlled (Fenik *et al.* 2011; Wise n.d.). Organophosphorus compounds are constituents of many pesticides with multiple functions in both agricultural and domestic situations (de Blaquièrre *et al.* 2000). Organophosphates (OPs) are phosphoric acid esters or thiophosphoric acid esters. They were developed in the 1930s and 1940s. When they were developed their original compounds were

highly toxic to mammals (Gupta *et al.* 2011). Since pesticides based on organochlorine were banned, alternative pesticides used were OPs, these pesticides are commonly used in the agricultural sector, they are alternative pesticides of organochlorine, widely used in agriculture to prevent the multiplication of pests that are rendered harmful to crop production. Their effectiveness arises from the fact that they have high efficacy, wide range of control, low cost, high selection and are not as harmful as most pesticides (Zhou *et al.* 2017). OPs and their metabolites have inhibitory effect and can deactivate both true and pseudo cholinesterases, acetylcholinesterase (AChE) and plasma or butylcholinesterase (BuChE) respectively by nucleophilic attack to the hydroxyl group of serine in their active sites thus resulting in phosphorylated enzymes (Vahid Shetab-Boushehri *et al.* 2012). They are an alternative use to organochlorine. Their level of toxicity is dependant on the inhibitory effects on the activity of AChE enzyme. AChE is an enzyme responsible for controlling functions of the nervous system (Corral *et al.* 2017). Blocking or inhibiting this enzyme results in an increase in acetylcholine at the synapses leading to hyperarousal and paralysis of the muscles and the main respiratory center (Fenik *et al.* 2011; Akinbo & Pharm n.d.). Important organophosphorus pesticides include TEPP, disulfoton, azinphosmethyl, parathion, methyl parathion, chlorfenvinphos, dichlorvos, diazinon, dimethoate, trichlofon, and malathion (Naidoo & Buckley 2003).

2.10 Conclusion

This review has discussed the history and origin of conducting polymers. The excellent properties that these polymers have rendering them more suitable for application in various fields such as sensors, biosensors, molecularly imprinted polymer sensors. Through electro deposition films of various thickness can be obtained thus making them suitable for applications in the modification of electrode surfaces. Once they are on electrode surfaces they

enhance the electro properties and are best for use to achieve good electron transfer between electrode surface and the electrolyte.

2.11 References

Akinbo, T. & Pharm, D., Organophosphates Poisoning.

Akincioğlu, A. et al., 2017. The synthesis of novel sulfamides derived from β -benzylphenethylamines as acetylcholinesterase, butyrylcholinesterase and carbonic anhydrase enzymes inhibitors. *Bioorganic Chemistry*, 74, pp.238–250.

Alemayehu, T. & Himariam, B., 2014. Synthesis and Characterization of Conducting Polymers : a Review Paper. *International Journal of Recent Research in Physics and Chemical Sciences (IJRRPCS)*, 1(1), pp.24–28.

Anon, 2004. Electrochemical relaxation study of polythiophene as conducting polymer (I). , 146, pp.109–119.

Ateh, D.D., Navsaria, H.A. & Vadgama, P., 2006. Polypyrrole-based conducting polymers and interactions with biological tissues. , (June), pp.741–752.

Azzahari, A.D., Yahya, R. & Hassan, A., 2013. Reactivity ratio determination of newly synthesized copolymers from glycidyl methacrylate and tetrahydrofurfuryl acrylate. *Sains Malaysiana*, 42(4), pp.509–514.

Bai, H. & Shi, G., 2007. Gas Sensors Based on Conducting Polymers. *Sensors*, 7, pp.267–307.

Basiri, A. et al., 2017. Design and synthesis of new piperidone grafted acetylcholinesterase inhibitors. *Bioorganic and Medicinal Chemistry Letters*, 27(2), pp.228–231.

Bickerstaff, G.F. et al., 1997. Immobilization of Enzymes and cells. *Methods in Biotechnology*, 1(May), pp.1–11.

Bitar, M., Maalouly, J., Chebib, H., Lerbret, A., Cayot, P., et al., 2015. Experimental design approach in the synthesis of molecularly imprinted polymers specific for iprodione fungicide. *REACT*, 94, pp.17–24.

Bitar, M., Maalouly, J., Chebib, H., Lerbret, A., Cayot, P., et al., 2015. Initiator-free synthesis of molecularly imprinted polymers by polymerization of self-initiated monomers. *Talanta*, 220(1), pp.558–567.

de Blaquièrre, G.E. et al., 2000. Electrophysiological and biochemical effects of single and multiple doses of the organophosphate diazinon in the mouse. *Toxicology and applied pharmacology*, 166(2), pp.81–91.

Borghetti, M. et al., 2013. Immobilization of Enzymes and cells. *Methods in molecular biology (Clifton, N.J.)*, 1051(May), pp.15–31.

Botelho, M.C. et al., 2015. The role of estrogens and estrogen receptor signaling pathways in cancer and infertility: The case of schistosomes. *Trends in Parasitology*, 31(6), pp.246–250.

Brena, B., González-Pombo, P. & Batista-Viera, F., 2013. Immobilization of enzymes: a literature survey. *Methods in molecular biology (Clifton, N.J.)*, 1051, pp.15–31.

Brena, B.M. & Batista-viera, F., 2006. Immobilization of Enzymes A Literature Survey. *Methods in Biotechnology: Immobilization of Enzyme and Cells, 2nd Edition*, pp.15–30.

Bronowicka-Kłys, D.E., Lianeri, M. & Jagodziński, P.P., 2016. The role and impact of estrogens and xenoestrogen on the development of cervical cancer. *Biomedicine and Pharmacotherapy*, 84, pp.1945–1953.

Capone, S. et al., 2004. Solid State Gas Sensors: State of the Art and Future Activities. *ChemInform*, 35(29), p.no-no.

Chen, P. et al., 2018. Sensors and Actuators B : Chemical In-situ monitoring reversible redox reaction and circulating detection of nitrite via an ultrasensitive magnetic Au @ Ag SERS substrate. *Sensors & Actuators: B. Chemical*, 256, pp.107–116.

Cheng, Y., Yang, S. & Hsu, C., 2009. Synthesis of Conjugated Polymers for Organic Solar Cell Applications. , pp.5868–5923.

Chou, T.-R. et al., 2015. Highly conductive PEDOT:PSS films by post-treatment with dimethyl sulfoxide for ITO-free liquid crystal display. *J. Mater. Chem. C*, 3(15), pp.3760–3766.

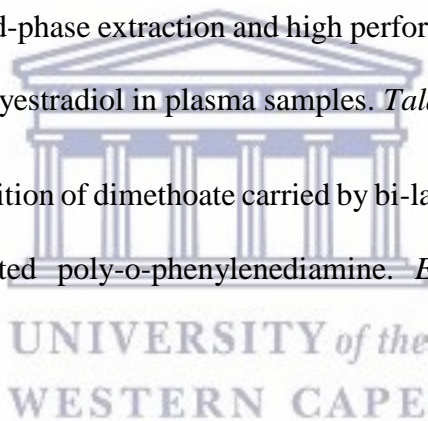
Ciepluch, K. et al., 2013. Effect of viologen-phosphorus dendrimers on acetylcholinesterase and butyrylcholinesterase activities. *International Journal of Biological Macromolecules*, 54(1), pp.119–124.

Čolović, M.B. et al., 2017. Toxicity evaluation of two polyoxotungstates with anti-acetylcholinesterase activity. *Toxicology and Applied Pharmacology*, 333(August), pp.68–75.

Corral, S.A. et al., 2017. Cognitive impairment in agricultural workers and nearby residents exposed to pesticides in the Coquimbo Region of Chile. *Neurotoxicology and Teratology*, 62(June), pp.13–19.

Cui, X. & Martin, D.C., 2003. Electrochemical deposition and characterization of poly(3,4-ethylenedioxythiophene) on neural microelectrode arrays. *Sensors and Actuators, B: Chemical*, 89(1–2), pp.92–102.

- Deng, F. et al., 2012. Colloids and Surfaces A : Physicochemical and Engineering Aspects Preparation of conductive polypyrrole / TiO₂ nanocomposite via surface molecular imprinting technique and its photocatalytic activity under simulated solar light irradiation. *Colloids and Surfaces A: Physicochemical and Engineering Aspects*, 395, pp.183–189.
- Deniz, S. et al., 2004. Synthesis and characterization of block copolymers using polysiloxane based macroazoinitiator. *Turkish Journal of Chemistry*, 28(5), pp.645–657.
- Dhawan, S.K. et al., 1997. Application of conducting polyaniline as sensor material for ammonia. *Sensors and Actuators B: Chemical*, 40(2–3), pp.99–103..
- Du, B. et al., 2014. A novel restricted access material combined to molecularly imprinted polymers for selective solid-phase extraction and high performance liquid chromatography determination of 2-methoxyestradiol in plasma samples. *Talanta*, 129, pp.465–472..
- Du, D. et al., 2008. Recognition of dimethoate carried by bi-layer electrodeposition of silver nanoparticles and imprinted poly-o-phenylenediamine. *Electrochimica Acta*, 53(22), pp.6589–6595.
- Van Dyk, J.S. & Pletschke, B., 2011. Review on the use of enzymes for the detection of organochlorine, organophosphate and carbamate pesticides in the environment. *Chemosphere*, 82(3), pp.291–307.
- Elahi, A. et al., 2015. Effect of loading titanium dioxide on structural, electrical and mechanical properties of polyaniline nanocomposites. *Journal of Alloys and Compounds*, 651, pp.328–332. Available at: <http://dx.doi.org/10.1016/j.jallcom.2015.08.108>.
- Erdössy, J. et al., 2016. Electrosynthesized molecularly imprinted polymers for protein recognition. *TrAC Trends in Analytical Chemistry*, 79, pp.179–190..



Fall, M. et al., 2006. Electrochemical properties and electrochemical impedance spectroscopy of polypyrrole-coated platinum electrodes. *Bulletin of the Chemical Society of Ethiopia*, 20(2), pp.279–293.

Fenik, J., Tankiewicz, M. & Biziuk, M., 2011. Properties and determination of pesticides in fruits and vegetables. *TrAC - Trends in Analytical Chemistry*, 30(6), pp.814–826.

Florea, A. et al., 2015. Electrochemistry Communications Electrochemical sensor for the detection of estradiol based on electropolymerized molecularly imprinted polythioaniline film with signal amplification using gold nanoparticles. , 59, pp.36–39.

Gérard, C. & Brown, K.A., 2017. Obesity and breast cancer - Role of estrogens and the molecular underpinnings of aromatase regulation in breast adipose tissue. *Molecular and Cellular Endocrinology*.

Gonalves, A.R., Ghica, M.E. & Brett, C.M.A., 2011. Preparation and characterisation of poly(3,4-ethylenedioxythiophene) and poly(3,4-ethylenedioxythiophene)/poly(neutral red) modified carbon film electrodes, and application as sensors for hydrogen peroxide. *Electrochimica Acta*, 56(10), pp.3685–3692.

Gong, P. et al., 2016. Estrogen receptor- α and aryl hydrocarbon receptor involvement in the actions of botanical estrogens in target cells. *Molecular and Cellular Endocrinology*, 437, pp.190–200.

Granado, V.L. V et al., 2012. Design of molecularly imprinted polymers for diphenylamine sensing. *Talanta*, 94, pp.133–139.

Gu, W. et al., 2017. Fluorescent black phosphorus quantum dots as label-free sensing probes for evaluation of acetylcholinesterase activity. *Sensors and Actuators, B: Chemical*, 250, pp.601–607.

Guo, J. et al., 2014. Two natural products, trans-phytol and (22E)-ergosta-6,9,22-triene-3 β ,5 α ,8 α -triol, inhibit the biosynthesis of estrogen in human ovarian granulosa cells by aromatase (CYP19). *Toxicology and Applied Pharmacology*, 279(1), pp.23–32.

Gupta, R.C., Malik, J.K. & Milatovic, D., 2011. Organophosphate and Carbamate Pesticides. *Reproductive and Developmental Toxicology*, pp.471–486.

Gurunathan, K. et al., 1999. Electrochemically synthesised conducting polymeric materials for applications towards technology in electronics, optoelectronics and energy storage devices. *Materials Chemistry and Physics*, 61(3), pp.173–191.

Harraz, F.A. et al., 2008. Hybrid nanostructure of polypyrrole and porous silicon prepared by galvanostatic technique. , 53, pp.3734–3740.

Haupt, K. & Mosbach, K., 2000. Molecularly Imprinted Polymers and Their Use in Biomimetic Sensors. , pp.2495–2504.

He, K. et al., 2014. Amperometric determination of hydroquinone and catechol on gold electrode modified by direct electrodeposition of poly(3,4-ethylenedioxythiophene). *Sensors and Actuators B: Chemical*, 193, pp.212–219.

Hernández, L.A. et al., 2017. Enhanced morphology, crystallinity and conductivity of poly(3,4-ethyldioxythiophene)/ErGO composite films by in situ reduction of TrGO partially reduced on PEDOT modified electrode. *Electrochimica Acta*, 240, pp.155–162.

Ho, K.C. et al., 2005. Amperometric detection of morphine based on poly(3,4-ethylenedioxythiophene) immobilized molecularly imprinted polymer particles prepared by precipitation polymerization. *Analytica Chimica Acta*, 542(1 SPEC. ISS.), pp.90–96.

Hu, Y. et al., 2015. Detection of melamine in milk using molecularly imprinted polymers – surface enhanced Raman spectroscopy. *FOOD CHEMISTRY*, 176, pp.123–129.

Hu, Y. et al., 2017. Free-standing oligo(oxyethylene)-functionalized polythiophene with the 3,4-ethylenedioxythiophene building block: electrosynthesis, electrochromic and thermoelectric properties. *Electrochimica Acta*, 228, pp.361–370.

Huang, B. et al., 2013. Occurrence, removal and bioaccumulation of steroid estrogens in Dianchi Lake catchment, China. *Environment International*, 59, pp.262–273.

Huang, B. et al., 2015. Talanta Determination of malachite green in fish based on magnetic molecularly imprinted polymer extraction followed by electrochemiluminescence. *Talanta*, 142, pp.228–234.

Iskierko, Z. et al., 2016. Molecularly imprinted polymers for separating and sensing of macromolecular compounds and microorganisms. *Biotechnology Advances*, 34(1), pp.30–46.

Jenkins, A.L., Yin, R. & Jensen, J.L., 2001. Molecularly imprinted polymer sensors for pesticide and insecticide detection in water. *Analyst*, 126(6), pp.798–802.

Jiao, L.S. et al., 2006. In situ electrochemical SERS studies on electrodeposition of aniline on 4-ATP/Au surface. *Journal of Solid State Electrochemistry*, 10(11), pp.886–893.

Kang, J., Park, J.-S. & Lee, H.-J., 2017. Pt-doped SnO₂ thin film based micro gas sensors with high selectivity to toluene and HCHO. *Sensors and Actuators B: Chemical*, pp.2–7.

Karthick, A.S., 2012. A Review on Methods, Application and Properties of Immobilized Enzyme. *Che Sci Rev Lett*, 1(3), pp.148–155.

Kataoka, K., Harada, A. & Nagasaki, Y., 2001. Block copolymer micelles for drug delivery: Design, characterization and biological significance. *Advanced Drug Delivery Reviews*, 47(1), pp.113–131.

Kryscio, D.R. & Peppas, N.A., 2012. Surface imprinted thin polymer film systems with selective recognition for bovine serum albumin. *Analytica Chimica Acta*, 718, pp.109–115.

Kudoh, Y., Akami, K. & Matsuya, Y., 1998. Chemical polymerization of 3,4-ethylenedioxythiophene using an aqueous medium containing an anionic surfactant. , pp.65–70.

Kumar, R., Avasthi, D.K. & Kaur, A., 2017. Fabrication of chemiresistive gas sensors based on multistep reduced graphene oxide for low parts per million monitoring of sulfur dioxide at room temperature. *Sensors and Actuators, B: Chemical*, 242, pp.461–468.

Lakard, B. et al., 2015. Gas Sensors Based on Electrodeposited Polymers. *Metals*, 5(3), pp.1371–1386.

Lakouraj, M.M., Zare, E.N. & Moghadam, P.N., 2014. Synthesis of novel conductive poly(p-phenylenediamine)/ Fe₃O₄ nanocomposite via emulsion polymerization and investigation of antioxidant activity. *Advances in Polymer Technology*, 33(1), pp.1–7.

Lakshmi, D. et al., 2009. Electrochemical sensor for catechol and dopamine based on a catalytic molecularly imprinted polymer-conducting polymer hybrid recognition element. *Analytical Chemistry*, 81(9), pp.3576–3584.

Lee, C.R. & Chen, L.J., 2016. Polyvinylbutyral assisted synthesis and characterization of kesterite quaternary semiconductor Cu₂ZnSnSe₄nanofibers by electrospinning route. *Solar Energy Materials and Solar Cells*, 151, pp.24–29.

Lee, S.H. et al., 2015. Mutation and duplication of arthropod acetylcholinesterase: Implications for pesticide resistance and tolerance. *Pesticide Biochemistry and Physiology*, 120, pp.118–124.

Li, F. et al., 2008. Behavior of natural estrogens in semicontinuous activated sludge biodegradation reactors. *Bioresource Technology*, 99(8), pp.2964–2971.

Li, J., Zhao, J. & Wei, X., 2009. Sensors and Actuators B: Chemical A sensitive and selective sensor for dopamine determination based on a molecularly imprinted electropolymer of o -aminophenol. , 140, pp.663–669.

Li, Y., 2015. Conducting Polymers.

Lin, X. & Li, Y., 2006. A sensitive determination of estrogens with a Pt nano-clusters/multi-walled carbon nanotubes modified glassy carbon electrode. *Biosensors and Bioelectronics*, 22(2), pp.253–259.

Linko, K. et al., 1999. ELECTRONIC STRUCTURE OF CONJUGATED POLYMERS : CONSEQUENCES OF ELECTRON } LATTICE COUPLING Electronic structure of conjugated polymers : consequences of electron } lattice coupling. , 319, pp.231–251.

Liu, X., Duckworth, P.A. & Wong, D.K.Y., 2010. Square wave voltammetry versus electrochemical impedance spectroscopy as a rapid detection technique at electrochemical immunosensors. *Biosensors and Bioelectronics*, 25(6), pp.1467–1473.

Liu, X., Wu, W. & Gu, Z., 2015. Poly (3,4-ethylenedioxythiophene) promotes direct electron transfer at the interface between *Shewanella loihica* and the anode in a microbial fuel cell. *Journal of Power Sources*, 277, pp.110–115.

Liu, Y.M. et al., 2017. Isosteroidal alkaloids as potent dual-binding site inhibitors of both acetylcholinesterase and butyrylcholinesterase from the bulbs of *Fritillaria walujewii*. *European Journal of Medicinal Chemistry*, 137, pp.280–291.

Liu, Z. hua et al., 2015. Sample-preparation methods for direct and indirect analysis of natural estrogens. *TrAC - Trends in Analytical Chemistry*, 64, pp.149–164.

Louet, C. et al., 2015. Solar Energy Materials & Solar Cells A comprehensive study of infrared reflectivity of poly (3 , 4-ethylene- dioxithiophene) model layers with different morphologies and conductivities. , 143, pp.141–151.

Luo, L. et al., 2013. Electrochemical sensing platform of natural estrogens based on the poly(l-proline)-ordered mesoporous carbon composite modified glassy carbon electrode. *Sensors and Actuators, B: Chemical*, 187, pp.78–83.

Malhotra, B.D., Chaubey, A. & Singh, S.P., 2006. Prospects of conducting polymers in biosensors. *Analytica Chimica Acta*, 578(1), pp.59–74.

Malinauskas, A., 2006. Electrochemical sensors based on conducting polymer — polypyrrole. , 51, pp.6025–6037.

Mangold, C. et al., 2010. Hetero-multifunctional poly(ethylene glycol) copolymers with multiple hydroxyl groups and a single terminal functionality. *Macromolecular Rapid Communications*, 31(3), pp.258–264.

Manisankar, P., Vedhi, C. & Selvanathan, G., 2007. Synthesis of a nanosize copolymer of 3,4-ethylenedioxythiophene with diclofenac and characterization. *Journal of Polymer Science, Part A: Polymer Chemistry*, 45(13), pp.2787–2796.

Mäntsälä, P. & Niemi, J., *Enzymes: the Biological Catalysts of Life*. , II.

Mazloum-ardakani, M., Amin-sadrabadi, E. & Khoshroo, A., 2016. Enhanced activity for non-enzymatic glucose oxidation on nickel nanostructure supported on PEDOT:PSS.

Menéndez, C.A. et al., 2017. Design, synthesis and biological evaluation of 1,3-dihydroxyxanthone derivatives: Effective agents against acetylcholinesterase. *Bioorganic Chemistry*, 75, pp.201–209.

Meng, Z. & Chen, W., 2005. Removal of Estrogenic Pollutants from Contaminated Water Using Molecularly Imprinted Polymers. *Environmental Science & Technology*, 39(22), pp.8958–8962.

Mo, D. et al., 2014. Electrochemical synthesis and capacitance properties of a novel poly(3,4-ethylenedioxythiophene bis-substituted bithiophene) electrode material. *Electrochimica Acta*, 132, pp.67–74.

Mousavi, Z. et al., 2008. (PEDOT) doped with sulfonated thiophenes. , 53, pp.3755–3762.

Naidoo, V. & Buckley, C., 2003. Survey of Pesticide Wastes in South Africa and Review of Treatment Options. , (1128), pp.1–82.

Neves, M.A.C. et al., 2008. Biochemical and computational insights into the anti-aromatase activity of natural catechol estrogens. *Journal of Steroid Biochemistry and Molecular Biology*, 110(1–2), pp.10–17.

Nezhadali, A. & Mojarrab, M., 2014. Sensors and Actuators B : Chemical Computational study and multivariate optimization of hydrochlorothiazide analysis using molecularly imprinted polymer electrochemical sensor based on carbon nanotube / polypyrrole film. *Sensors & Actuators: B. Chemical*, 190, pp.829–837.

Nguyen, T.-T.-N., Chan, C.-Y. & He, J.-L., 2016. One-step inkjet printing of tungsten oxide-poly(3,4-ethylenedioxythiophene):polystyrene sulphonate hybrid film and its applications in electrochromic devices. *Thin Solid Films*, 603, pp.276–282.

Nie, M. et al., 2015. Occurrence, distribution and risk assessment of estrogens in surface water, suspended particulate matter, and sediments of the Yangtze Estuary. *Chemosphere*, 127, pp.109–116.

Nieto, A. et al., 2008. Determination of natural and synthetic estrogens and their conjugates in sewage sludge by pressurized liquid extraction and liquid chromatography-tandem mass spectrometry. *Journal of Chromatography A*, 1213(2), pp.224–230.

Obaid, A.Y. et al., 2014. Electrodeposition and characterization of polyaniline on stainless steel surface via cyclic, convolutive voltammetry and SEM in aqueous acidic solutions. *International Journal of Electrochemical Science*, 9(2).

Öpik, A., 2009. Molecularly imprinted polymers : A new approach to the preparation of Functional materials. , (October 2016).

Ouyang, J. et al., 2004. On the mechanism of conductivity enhancement in poly(3,4-ethylenedioxythiophene):poly(styrene sulfonate) film through solvent treatment. *Polymer*, 45(25), pp.8443–8450.

Ozcan, L., 2007. Determination of paracetamol based on electropolymerized-molecularly imprinted polypyrrole modified pencil graphite electrode. , 127, pp.362–369.

Oztekin, Y., Ramanaviciene, A. & Ramanavicius, A., 2011. Electrochemical determination of cu(ii) ions by 4-formylphenylboronic acid modified gold electrode. *Electroanalysis*, 23(7), pp.1645–1653.

Paradee, N. & Sirivat, A., 2013. nanoparticles via chemical oxidation polymerization. , (January).

Pardieu, E. et al., 2009. Analytica Chimica Acta Molecularly imprinted conducting polymer based electrochemical sensor for detection of atrazine. , 649, pp.236–245.

Patra, S., Barai, K. & Munichandraiah, N., 2008. Scanning electron microscopy studies of PEDOT prepared by various electrochemical routes. *Synthetic Metals*, 158(10), pp.430–435.

Pérez, R.L. & Escandar, G.M., 2014. Liquid chromatography with diode array detection and multivariate curve resolution for the selective and sensitive quantification of estrogens in natural waters. *Analytica Chimica Acta*, 835, pp.19–28.

Piletsky, S.A., Turner, N.W. & Laitenberger, P., 2006. Molecularly imprinted polymers in clinical diagnostics-Future potential and existing problems. *Medical Engineering and Physics*, 28(10), pp.971–977.

Pineda, E.G. et al., 2018. Tubular-structured polypyrrole electrodes decorated with gold nanoparticles for electrochemical sensing. *Journal of Electroanalytical Chemistry*, 812(January), pp.28–36.

Porat, Z., Rubinstein, I. & Zinger, B., 1993. The Effect of Composition of Nafion Deposition Solutions on the Diffusional Properties of the Films. *Journal of the Electrochemical Society*, 140(9), pp.2501–2507.

Putzbach, W. & Ronkainen, N.J., 2013. Immobilization techniques in the fabrication of nanomaterial-based electrochemical biosensors: a review. *Sensors (Basel, Switzerland)*, 13(4), pp.4811–4840.

Pyshkina, O., 2010. Poly(3,4-ethylenedioxythiophene):Synthesis and Properties. *Scientific Journal of Riga Technical University Material Science and Applied Chemistry*, 21, pp.51–54.

Pyshkina, O. & Kubarkov, A., 2010. Poly (3 , 4-ethylenedioxythiophene): Synthesis and Properties. , 21, pp.51–54.

Qian, T. et al., 2014. Ultrasensitive dopamine sensor based on novel molecularly imprinted polypyrrole coated carbon nanotubes. *Biosensors and Bioelectronics*, 58, pp.237–241. Available at: <http://dx.doi.org/10.1016/j.bios.2014.02.081>.

Rahman, M.A. et al., 2008. Electrochemical Sensors Based on Organic Conjugated Polymers. *Sensors*, 8(1), pp.118–141.

Ramanavicius, A. et al., 2010. Electrochemical impedance spectroscopy of polypyrrole based electrochemical immunosensor. *Bioelectrochemistry*, 79(1), pp.11–16.

Re, T. & Milczarek, G., 2016. Electrochimica Acta A comparative study on the preparation of redox active bioorganic thin films based on lignosulfonate and conducting polymers. , 204, pp.108–117.

Rezaei, B., Khalili Boroujeni, M. & Ensafi, A.A., 2014. Caffeine electrochemical sensor using imprinted film as recognition element based on polypyrrole, sol-gel, and gold nanoparticles hybrid nanocomposite modified pencil graphite electrode. *Biosensors and Bioelectronics*, 60, pp.77–83.

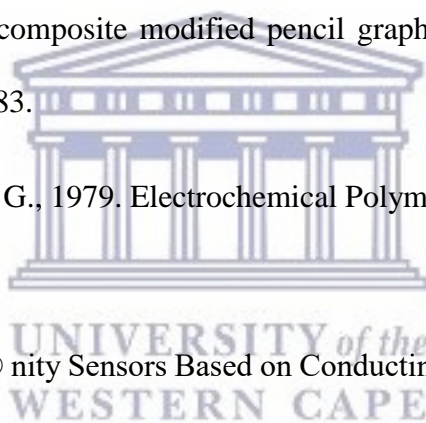
Road, C., Jose, S. & Piero, G., 1979. Electrochemical Polymerization of Pyrrole. , pp.635–636.

Sadik, O.A., 1999. Bioaf® nity Sensors Based on Conducting Polymers : A Short Review. , pp.839–844.

Sandoval, A.P., Suárez-Herrera, M.F. & Feliu, J.M., 2015. IR and electrochemical synthesis and characterization of thin films of PEDOT grown on platinum single crystal electrodes in [EMMIM]Tf₂N ionic liquid. *Beilstein J. Org. Chem*, 11, pp.348–357.

Scrosati, B., 1989. Conducting Polymers and Their Applications. *Materials Science Forum*, 42(December), pp.207–220.

Selvaganesh, S.V. et al., 2007. Chemical synthesis of PEDOT-Au nanocomposite. *Nanoscale Research Letters*, 2(11), pp.546–549.



Sen, T., Mishra, S. & Shimpi, N.G., 2016. Synthesis and sensing applications of polyaniline nanocomposites: a review. *RSC Adv.*, 6(48).

Seung, B. et al., 2004. Highly Oriented and Ordered Arrays from Block Copolymers via Solvent Evaporation **. , (3), pp.226–231.

Shanmugham, C. & Rajendran, N., 2015. Corrosion resistance of poly p-phenylenediamine conducting polymer coated 316L SS bipolar plates for Proton Exchange Membrane Fuel Cells. *Progress in Organic Coatings*, 89, pp.42–49.

Sharma, P.S. et al., 2012. Electrochemically synthesized polymers in molecular imprinting for chemical sensing. *Analytical and Bioanalytical Chemistry*, 402(10), pp.3177–3204.

Shi, J. et al., 2004. Biodegradation of natural and synthetic estrogens by nitrifying activated sludge and ammonia-oxidizing bacterium *Nitrosomonas europaea*. *Water Research*, 38(9), pp.2322–2329.

Shyu, C. et al., 2011. Computational estimation of rainbow trout estrogen receptor binding affinities for environmental estrogens. *Toxicology and Applied Pharmacology*, 250(3), pp.322–326.

Si, W. et al., 2014a. Electrochemical sensing of acetaminophen based on poly(3,4-ethylenedioxythiophene)/graphene oxide composites. *Sensors and Actuators B: Chemical*, 193, pp.823–829.

Si, W. et al., 2014b. Sensors and Actuators B: Chemical Electrochemical sensing of acetaminophen based on poly (3 , 4-ethylenedioxythiophene)/ graphene oxide composites. *Sensors & Actuators: B. Chemical*, 193, pp.823–829.

Sosnowska, B. et al., 2013. The effect of bromfenvinphos, its impurities and chlorfenvinphos on acetylcholinesterase activity. *International Journal of Biological Macromolecules*, 57, pp.38–44.

Su, Y. et al., 2013. Use of Electrochemical Impedance Spectroscopy (EIS) for the Evaluation of Electrocoatings Performances. *Journal of Colloid and Interface Science*, 399(1), pp.1–27.

Sukocheva, O. et al., 2015. Sphingosine-1-phosphate receptor 1 transmits estrogens' effects in endothelial cells. *Steroids*, 104, pp.237–245.

Tang, Y. et al., 2015. Biosensors and Bioelectronics Upconversion particles coated with molecularly imprinted polymers as fluorescence probe for detection of clenbuterol. *Biosensors and Bioelectronics*, 71, pp.44–50.

Tirawattanakoson, R., Rattanarat, P. & Ngamrojanavanich, N., 2016. Free radical scavenger screening of total antioxidant capacity in herb and beverage using graphene / PEDOT : PSS-modified electrochemical sensor. , 767, pp.68–75.

Topczewski, J.J. et al., 2013. Reversible inhibition of human acetylcholinesterase by methoxypyridinium species. *Bioorganic and Medicinal Chemistry Letters*, 23(21), pp.5786–5789..

Toshima, N. & Hara, S., 1995. Contents 1. , 20(94), pp.155–183.

Tovide, O. et al., 2014. Graphenated polyaniline-doped tungsten oxide nanocomposite sensor for real time determination of phenanthrene. *Electrochimica Acta*, 128, pp.138–148.

Tran, T.K.A. et al., 2016. Mechanistic insights into induction of vitellogenin gene expression by estrogens in Sydney rock oysters, *Saccostrea glomerata*. *Aquatic Toxicology*, 174, pp.146–158.

Trifigny, N. et al., 2013. PEDOT:PSS-Based Piezo-Resistive Sensors Applied to Reinforcement Glass Fibres for in Situ Measurement. , pp.10749–10764.

Tsai, T.H., Lin, K.C. & Chen, S.M., 2011. Electrochemical synthesis of poly(3,4-ethylenedioxythiophene) and gold nanocomposite and its application for hypochlorite sensor. *International Journal of Electrochemical Science*, 6(7), pp.2672–2687.

Tun, P., 2004. Electrochemical sensors based on molecularly imprinted polymers. , 23(1).

Vahid Shetab-Boushehri, S., Farid Shetab-Boushehri, S. & Abdollahi, M., 2012. Author's personal copy Possible role of Mg²⁺ ion in the reaction of organophosphate (dichlorvos) with serine. *Journal of Medical Hypotheses and Ideas*, 6(1), pp.53–57.

Vasanth, V.S., Thangamuthu, R. & Chen, S., 2008. Electrochemical Polymerization of 3,4-Ethylenedioxythiophene from Aqueous Solution Containing Hydroxypropyl- β -cyclodextrin and the Electrocatalytic Behavior of Modified Electrode Towards Oxidation of Sulfur Oxoanions and Nitrite. , pp.1754–1759.

Waenkaew, P., Phanichphant, S. & Advincula, R.C., 2011. Electropolymerization of layer-by-layer precursor polymer films. *Polymers for Advanced Technologies*, 22(5), pp.753–758.

Wang, L., Li, X. & Yang, Y., 2001. Preparation, properties and applications of polypyrroles. , 47, pp.125–139.

Wang, Y. et al., 2009. Preparation, Characterization and Sensitive Gas Sensing of Conductive Core-sheath TiO₂-PEDOT Nanocables. , pp.6752–6763.

Wiemann, J. et al., 2017. Piperlongumine B and analogs are promising and selective inhibitors for acetylcholinesterase. *European Journal of Medicinal Chemistry*, 139, pp.222–231.

Wise, J.C., Introduction to Pesticides : Toxicology 101.

Wisitsoraat, A. et al., 2013. Graphene-PEDOT:PSS on screen printed carbon electrode for enzymatic biosensing. *Journal of Electroanalytical Chemistry*, 704(September), pp.208–213.

Wu, Y. et al., 2017. Sensitive inkjet printing paper-based colorimetric strips for acetylcholinesterase inhibitors with indoxyl acetate substrate. *Talanta*, 162(July 2016), pp.174–179.

Xia, N. et al., 2015. Ferrocene-phenylalanine hydrogels for immobilization of acetylcholinesterase and detection of chlorpyrifos. *Journal of Electroanalytical Chemistry*, 746, pp.68–74.

Xu, J. et al., 2018. Thiol-triggered disaggregation-induced emission controlled by competitive coordination for acetylcholinesterase monitoring and inhibitor screening. *Sensors and Actuators, B: Chemical*, 255, pp.22–28.

Yamini, K. et al., 2017. Optical Fiber Technology Clad modified optical fiber gas sensors based on nanocrystalline nickel oxide embedded coatings. *Optical Fiber Technology*, 36, pp.139–143.

Yao, Y. et al., 2014. Electrochemical recognition and trace-level detection of bactericide carbendazim using carboxylic group functionalized poly(3,4-ethylenedioxythiophene) mimic electrode. *Analytica Chimica Acta*, 831, pp.38–49.

Yuan, Y. et al., 2015. Ionic liquid-molecularly imprinted polymers for pipette tip solid-phase extraction of (Z) -3- (chloromethylene) - 6-flourothiochroman-4-one in urine. *Journal of Chromatography A*, 1408, pp.49–55.

Yurtsever, M. & Yurtsever, E., 2000. Structural Defects in Polythiophenes : Monte Carlo Simulations with Quantum Mechanical Growth Probabilities. , pp.362–369.

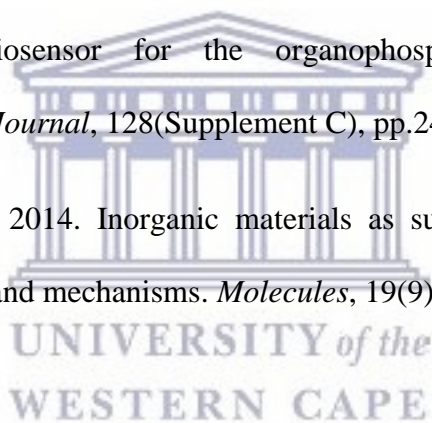
Zanardi, C., Terzi, F. & Seeber, R., 2013. Polythiophenes and polythiophene-based composites in amperometric sensing. *Analytical and Bioanalytical Chemistry*, 405(2–3).

Zhang, H. et al., 2008. Synthesis and characterization of molecularly imprinted polymers for phenoxyacetic acids. *International Journal of Molecular Sciences*, 9(1), pp.98–106.

Zhao, Q. et al., 2014. The structure and properties of PEDOT synthesized by template-free solution method. *Nanoscale research letters*, 9(1), p.557.

Zhou, L. et al., 2017. Acetylcholinesterase/chitosan-transition metal carbides nanocomposites-based biosensor for the organophosphate pesticides detection. *Biochemical Engineering Journal*, 128(Supplement C), pp.243–249.

Zucca, P. & Sanjust, E., 2014. Inorganic materials as supports for covalent enzyme immobilization: Methods and mechanisms. *Molecules*, 19(9), pp.14139–14194.



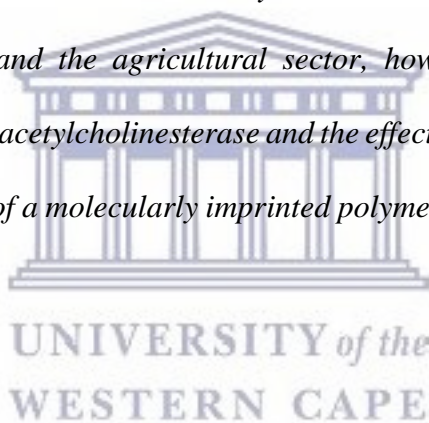
CHAPTER THREE

Electrochemical synthesis of a polypyrrole based molecularly imprinted polymer sensor on surfaces of glassy carbon electrodes sensitive to dimethoate- an acetylcholinesterase inhibitor organophosphate pesticide.

UNIVERSITY *of the*
WESTERN CAPE

Summary

The use of pesticides is important for ensuring that there is high produce in conjunction with high productivity of crops. This can be achieved by means of eliminating those pests that target specific crops leading to a decrease in the amount of high quality crops that can be consumed thus ensuring the quality of life. However they do pose a threat to both human and the environment at large, for once they are consumed they can alter the functioning of the endocrine system and thus lead to deformities. This has led to an increase in the concern on the use of certain pesticides such as organophosphates including dimethoate which is one of the most popular organophosphates. The detection methods that are currently in use for the determination of these compounds lack reliability. In this chapter the background on the pesticide use in households and the agricultural sector, how it affects the human body, specifically the human enzyme acetylcholinesterase and the effect of its disruption. This chapter also includes the preparation of a molecularly imprinted polymer sensor and its application in the detection of dimethoate.



Electrochemical synthesis of polypyrrole based molecularly imprinted polymer sensor on surfaces of glassy carbon electrodes sensitive to dimethoate- an acetylcholinesterase inhibitor organophosphate pesticide.

Abstract

Dimethoate is an organophosphate (OP) pesticide that has inhibitory effects on the enzyme acetylcholinesterase an enzyme that hydrolyses the neurotransmitter acetylcholine which is responsible for the transmission signals across a synapse or junction from one neuron to another "target" neuron, muscle cell or gland cell. Like other OPs, dimethoate is an acetylcholinesterase inhibitor which deactivates cholinesterase. Organophosphorus pesticides can enter the body through different routes, including inhalation, ingestion, and dermal absorption. The inhibitory effect they have on the acetylcholinesterase enzyme leads to a pathologic excess of acetylcholine in the body. Their toxicity is not limited to the severe phase, however, and chronic effects have long been noted. Neurotransmitters such as acetylcholine (which is affected by organophosphate pesticides) are extremely important in the development of the brain and a number of organophosphates have neurotoxic effects on developing organisms, even at low levels of exposure. It is therefore imperative to detect the presence of the pesticides immediately, effectively and at low concentrations. In this study a sensor was developed for the detection of dimethoate through the formation of a MIP composed of PPy and dimethoate template on the surface of glassy carbon electrode. The prepared sensor was electrochemically characterised by cyclic voltammetry (CV) and square wave voltammetry (SWV) which was determined to be a suitable material for the mediation of electron transfer from the solution to the electrode and was characterised by a D_0 of $4.1 \times 10^{-5} \text{ m}^2 \cdot \text{s}^{-1}$ showing a relatively fast electron transfer. The developed sensor had a dynamic linear range (DLR) of 0.01 nM – 0.14 nM. The

LOD of the sensor was determined to be 0.035 nM thus showing that the sensor can be able to detect concentrations of ATCl even at as low concentrations as 0.035 nM of dimethoate that may be present and sensitivity of 0.32 $\mu\text{A/nM}$.

3.0 Introduction

Pesticides play an important role in the high production and high quality of crops in the agricultural sector by means of pest control (Van Dyk & Pletschke 2011; Münze *et al.* 2017). However they have proven to be detrimental to animal species and human (Han *et al.* 2017). The first discovery of the properties of organophosphate compounds occurred in the 1930s which led to their use as pesticide material in the 1940s (Toro *et al.* 2015). Their usage increase since the 1970s following the ban of organochlorine pesticides which posed an environmental threat (Piccoli *et al.* 2016). OPs are a class of insecticides, quite a number of them being highly toxic (Du *et al.* 2008; González-Curbelo *et al.* 2017). Insecticides can be described as natural or man-made substances that are formulated to repel, mitigate, harm or kill one or more species of insects (Osorio 2009; EPA n.d.; Nowell *et al.* 2017; Algae *et al.* 2013; Morillo & Villaverde 2017). They are one of the many classes of endocrine disrupting chemicals, as they have the ability to alter and cause distraction to the proper functioning of the endocrine system. Their ability to interact with various receptors has been researched and their long term effect is unknown (Van Dyk & Pletschke 2011). The endocrine system is also known as the hormone system, it is responsible for communicating, coordinating and controlling the activities in the bodies of mammals (Genthe & Steyn n.d.). Together with the nervous system they regulate important bodily functions including but not limited to reproduction, growth and development, energy metabolism and homeostasis. EDCs consists of both natural and man-made organic compounds however the majority of these compounds are man-made, including

polychlorinated bisphenols (PCBs) (ZHANG *et al.* 2017), steroid hormone, phthalates and alkylphenols (Olujimi *et al.* 2010). In the past they were amongst the widely used insecticides available. In the United States they have thirty-six that are registered and can be used in the country, however they all have the potential to cause toxicity. Though they can be used in different aspects including agriculture, homes, in gardens and veterinary practices several of OPs have been banned, some of these banned insecticides include parathion and chlorpyrifos (Products 1989). According to a report compiled by the city of Cape Town; in South Africa cases of OP poisoning tend to be under-diagnosed, primarily due to little training that healthcare providers receive in occupational and environmental health (Razwiedani & Rautenbach 2017). These OPs can enter the body through various exposure routes, including inhalation, ingestion and through skin contact (Beránková *et al.* 2017; Coscollà *et al.* 2017; Carlo *et al.* n.d.). Their absorption is dependent on the exposure route. Poisoning depends on the rate of absorption, once absorption has occurred, the compounds are broken down in the liver through the process known as hydrolysis, and the rate of hydrolysis varies from one compound to another. Some organophosphates are lipid soluble, they can be stored in fats thus delaying toxicity. Many organothiophosphates undergo conversion from thions to oxons, this can be achieved by exposure to an environment that possesses oxygen and light, while in the body is made possible by liver microsomes. Oxons are the most toxic in comparison with thion OPs (T. Zhang *et al.* 2014). However oxons break down very easy than thions, in both hydrolysis occurs at the ester linkage yielding an alkyl phosphate with lower toxicity.

Lack of exposure history means that poisoning through pesticide exposure goes unrecognized in most cases (de Blaquièrre *et al.* 2000). Another factor that brings about difficulty in proper diagnosis of pesticide poisoning is the fact that it presents symptoms that are similar to that of common illnesses, it displays nonspecific symptoms and physical signs. The symptoms that

are brought about by pesticide poisoning are similar to those of influenza, heat prostration, alcohol intoxication, exhaustion, hypoglycemia, asthma, gastroenteritis, pneumonia, and brain haemorrhage and thus can be confused with them (Ye *et al.* 2017). Organophosphates are used in agriculture, homes, gardens and veterinary practices (Van Maele-Fabry *et al.* 2017). In general organophosphorus pesticides have a short life span in the environment (usually lasting only days to months instead of years) and, generally, chemical breakdown is accelerated as temperatures or pH or both increase (Prasad & Jauhari 2015). Organophosphorus pesticides are known to have an inhibitory effect on the function of the enzyme acetylcholinesterase (AChE) (Kiyama & Wada-Kiyama 2015) a hydrolase enzyme that is mainly found in the neuromuscular junctions and cholinergic brain synapses where it hydrolyses the neurotransmitter acetylcholine as depicted by the mechanism in fig 3.1 (Anirudhan & Alexander 2015; Bucur *et al.* 2013), it is important for the control of nerve signals in the body (Santos-Silva *et al.* 2017). Acetylcholine (ACh) is a neurotransmitter with various functions (Pochini *et al.* 2016) in both the peripheral and central nervous systems (Sonięcka *et al.* 2015; Maruyama *et al.* 2016), playing a role in learning and memory processes as well as locomotor control and cerebral blood flow (Obajuluwa *et al.* 2017; Nugroho *et al.* 2017). A result of AChE inhibition is large accumulation of acetylcholine in muscle and muscle tissues (Europe 2009) leading to severe muscular paralysis. This accumulation is due to the fact that the amount of acetylcholine level depends on the availability of active AChE, thus a fewer number of active AChE results in large amounts of acetylcholine (Periasamy *et al.* 2009).

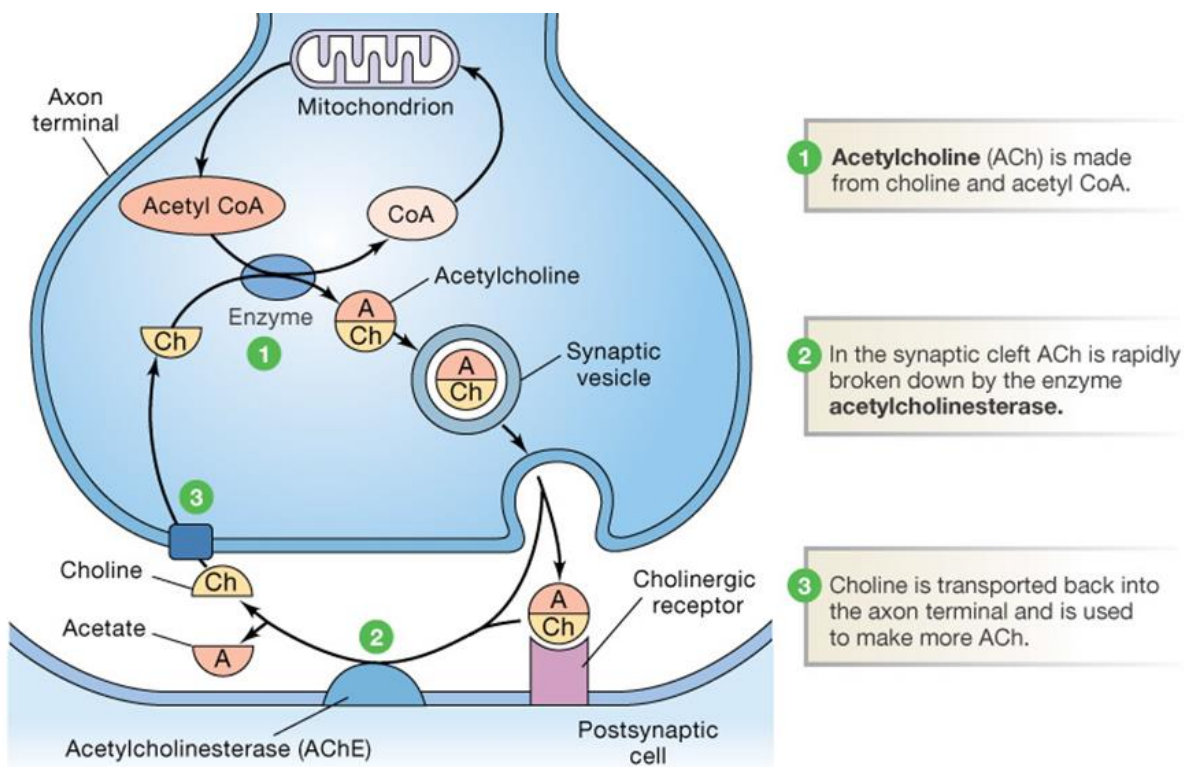


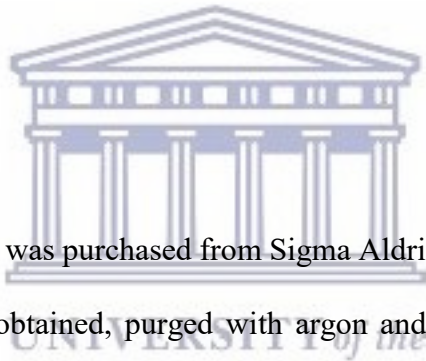
Figure 3.1: Acetylcholine in cholinergic synapses (Pochini *et al.* 2016).

After exposure the alkyl phosphates which are products after OP hydrolysis can be detected in urine during absorption or 48 hours thereafter making the identification and quantification of the type of pesticide absorbed possible. However it is almost impossible to detect intact OPs in the blood except during or soon after absorption of a large amount of pesticide. In general pesticides do not remain unhydrolyzed for more than a few minutes of hours unless in cases where large amounts are absorbed or in cases where the liver enzymes are inhibited. Based on a report by the World Health Organization (WHO 1990) there are about three million pesticide poisoning reported each year, most of them due to organophosphates. They also report that there are some 200 000 death cases related to OP poisoning, some of the death cases due to self-poisoning while others occur as a result of occupational exposure (Gothwal *et al.* 2014). There are a number of methods used for the qualitative determination of organophosphates (Jenkins *et al.* 2001). The most common and widely used being gas chromatography and liquid chromatography coupled with tandem mass spectroscopy, however liquid chromatography-

mass spectrometry was also found applicable for organophosphate determination (Pohanka *et al.* 2008). Even though chromatography and mass spectroscopy are well-developed methods for pesticide detection with a low detection limit, the bulky and expensive apparatus still impede their practical applications. Several studies reported the use of electrochemical and gravimetric methods combining with enzymes, predominantly acetylcholinesterase and organophosphate hydrolase, to detect OP pesticides. However, the major disadvantage is their low selectivity of acetylcholinesterase (AChE) because the degree of inhibition on AChE by OP pesticides is almost the same. This study proposes the use of a highly sensitive and selective molecularly imprinted polymer sensor, polypyrrole selected as the polymer material for the selective detection of dimethoate.

3.1 Experimental section

3.1.1 Chemicals

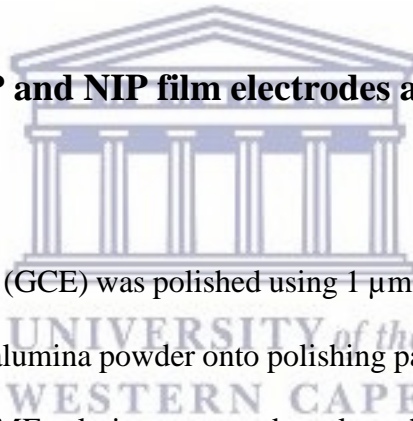


Monomer pyrrole (Py) ($\geq 99\%$) was purchased from Sigma Aldrich and distilled under vacuum until a colourless liquid was obtained, purged with argon and kept in darkness at $-30\text{ }^{\circ}\text{C}$. Acetylthiocholine chloride ($\geq 99\%$), acetylcholinesterase ($\geq 99\%$), dimethoate ($\geq 99\%$), potassium hexacyanoferrate (III) ($\text{K}_3[\text{Fe}(\text{CN})_6]$) (ACS reagent, $\geq 99.0\%$), potassium hexacyanoferrate(II) trihydrate ($\text{K}_4[\text{Fe}(\text{CN})_6]$) (ACS reagent 98.5-102.0%) and potassium chloride (KCl) were purchased from Sigma-Aldrich (Milan, Italy). Disodium hydrogen phosphate (Na_2HPO_4) ($\geq 99.5\%$), sodium dihydrogen phosphate (NaH_2PO_4) ($\geq 99\%$) from Sigma-Aldrich (Milan, Italy) were used for the preparation of 0.1 M phosphate buffer pH 7. Alumina micro polishing pads were obtained from Buehler LL, USA. Deionized ultra-purified water used throughout these experiments was prepared with a Milli-Q water purification system.

3.1.2 Instrumentation and procedure

A three electrode configuration was used for all electrochemical experiments. A glassy carbon electrode with diameter 3 mm from Bio Analytical Systems (BAS) was used as the working electrode. An Ag/AgCl/KCl (3 M) as the reference electrode from BAS, and a platinum wire as the counter electrode. All the measurements were carried out at room temperature. All electrochemical measurements (CV and SWV) were performed on a computer-controlled Autolab potentiostat-galvanostat controlled by a GPES 4.9.007 software. Alumina micro polishing pads were obtained from Buehler LL and used to polish the surface of the glassy carbon working electrode before modification.

3.1.3 Preparation of MIP and NIP film electrodes and electrochemical measurements



A bare glassy carbon electrode (GCE) was polished using 1 μm alumina slurry prepared by the addition of a small amount of alumina powder onto polishing pad surface, 3 drops of trimethyl pentane and distilled water. DMF solution was used to clean the surface of the electrode and the electrode was rinsed with distilled water. The electrode was then sonicated in a mixture of ethanol and water ratio (1:1) for 6 min and rinsed thoroughly with distilled water until a mirror-like surface was obtained. Finally the electrode was washed with distilled water and allowed to dry at room temperature before use. For the modification of the working electrode, the polished GCE was immersed in 0.1 M phosphate buffer solution pH 6.8 containing 30 mM pyrrole and 10 mM dimethoate, electrochemical polymerization was performed using cyclic voltammetry at 0.05 V/s for 10 cycles in the potential window -0.4 V to +1.5 V. The electrode was denoted dim-PPy electrode and used for the preparation of the MIP electrode. The dim-PPy electrode was immersed in an HCl pH 2 solution under stirring for the removal of

dimethoate for 30 min at room temperature as demonstrated in fig 3.3. The electrode was denoted as the MIP electrode and used for the determination of dimethoate. For the rebinding step of dimethoate, the MIP electrode was incubated into dimethoate solutions with various concentrations (0.01 nM to 5 nM) for 15 min in the refrigerator at 4° C. The non-imprinted polymer (NIP) electrode was prepared using the same conditions but without dimethoate in the electrochemical polymerization step the electrode was denoted NIP electrode and used as the control electrode as demonstrated in figure 3.2.

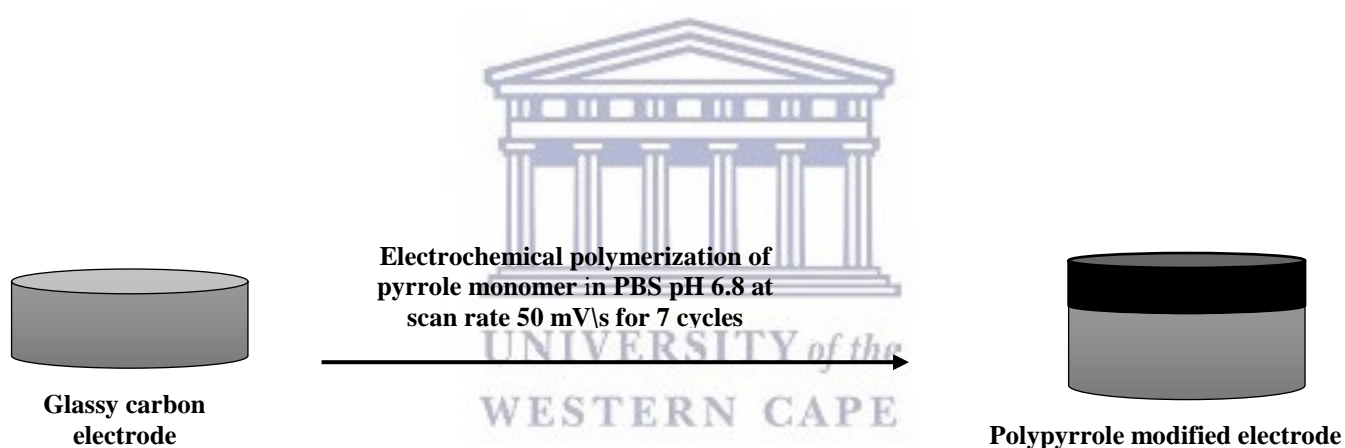


Figure 3.2: Preparation of PPy modified electrode

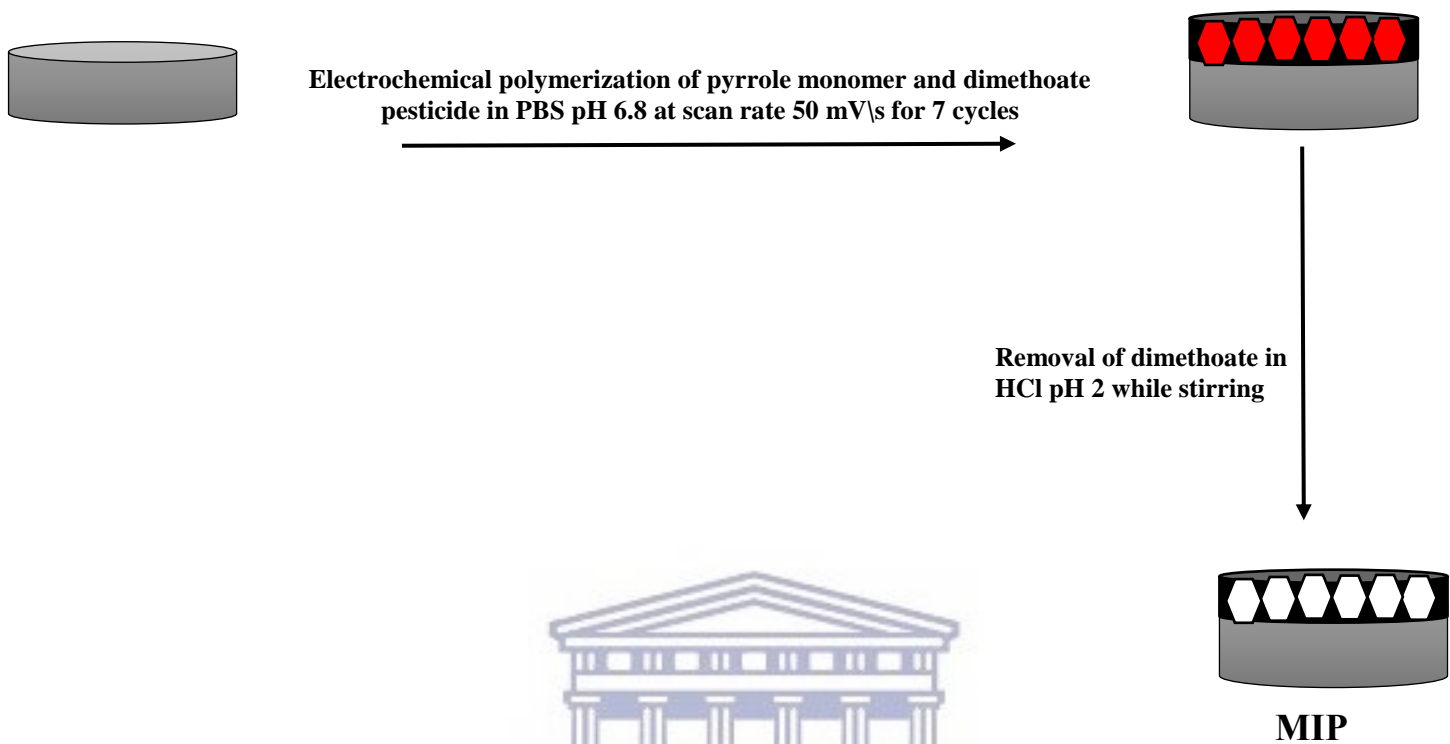


Figure 3.3: preparation of MIP electrode



3.2 Results and discussion

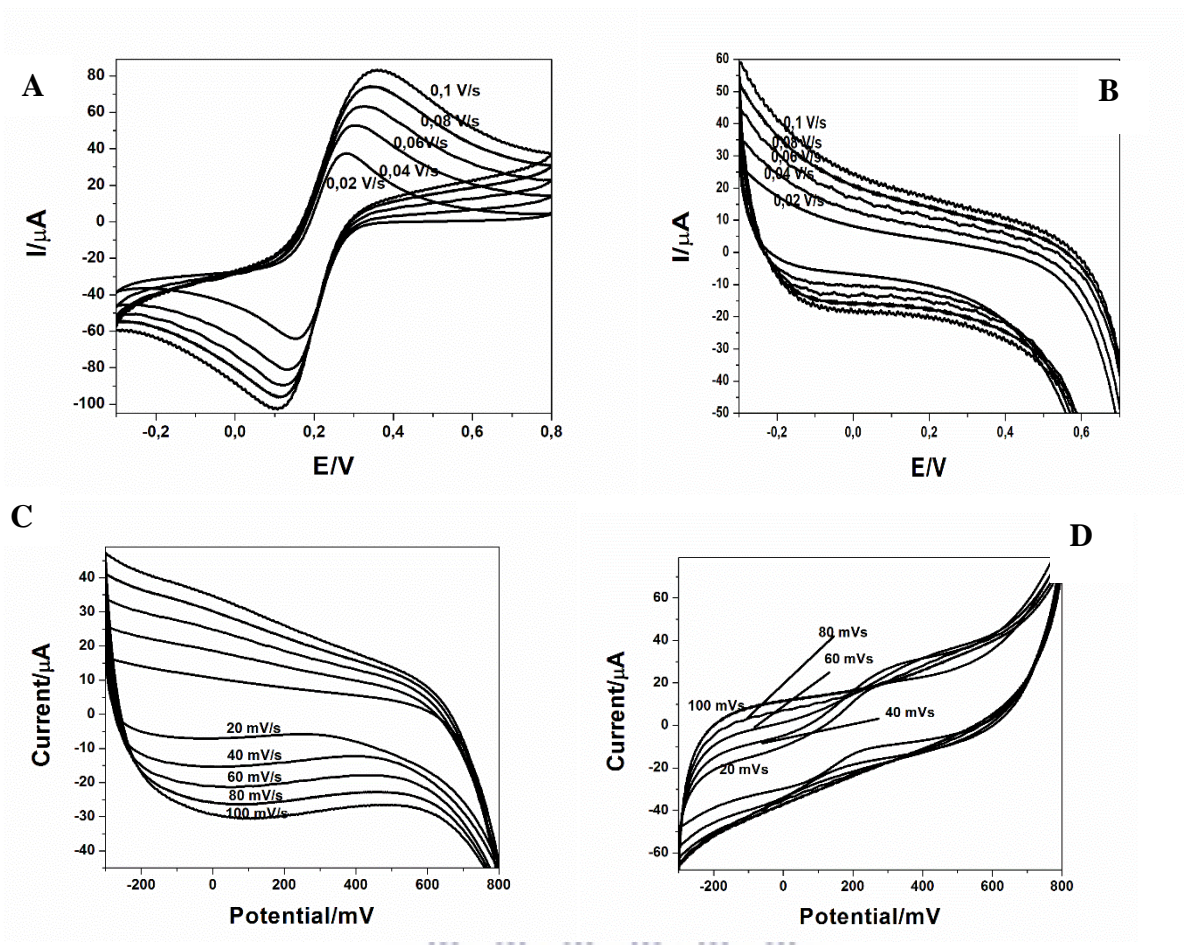


Figure 3.4: Cyclic voltammograms of (A) GCE, (B) polypyrrole (PPy), (C) PPy and dimethoate and (D) MIP in 0.1 M PBS pH 7, 0.1 M KCl and 1 mM $K_3Fe(CN)_6$.

Table 3.1: Cyclic voltammetric parameters for GCE, PPY, dim-MIP and MIP

	ΔE_p (V)	I_{pc}/I_{pc}	D_0 ($m^2 \cdot s^{-1}$)
GCE	0.104	1.66	5.4×10^{-5}
PPy	0.150	1.29	3.5×10^{-5}
Dim-MIP	0.060	1.81	8.64×10^{-5}
MIP	0.187	1.90	4.1×10^{-5}

Figure 3.4 shows the cyclic voltammograms of GCE, PPy, dim-MIP and MIP where they show an increase in current response with an increase in scan rate. CV of bare GCE shows higher I_{pa} than the modified electrodes. ΔE_p and I_{pc}/I_{pa} indicate quasi-reversibility of the systems. The MIP has a higher ΔE_p , this is indicative of the fact that $Fe(CN)_6$ which diffused from the bulk solution to the imprinted polymer on the surface of the electrode characteristic of a surface-bound species. PPy is characterized by a low diffusion coefficient than bare GCE as denoted in table 3.1 thus showing that PPy can be used in the fabrication of MIP. The MIP modified electrode also showed good diffusion coefficient than dim-PPy meaning it was a better electron mediator material due to the cavities that it has over dim-PPy.

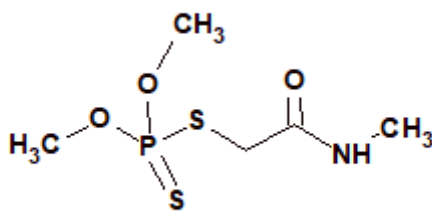


Figure 3.5: Structure of dimethoate

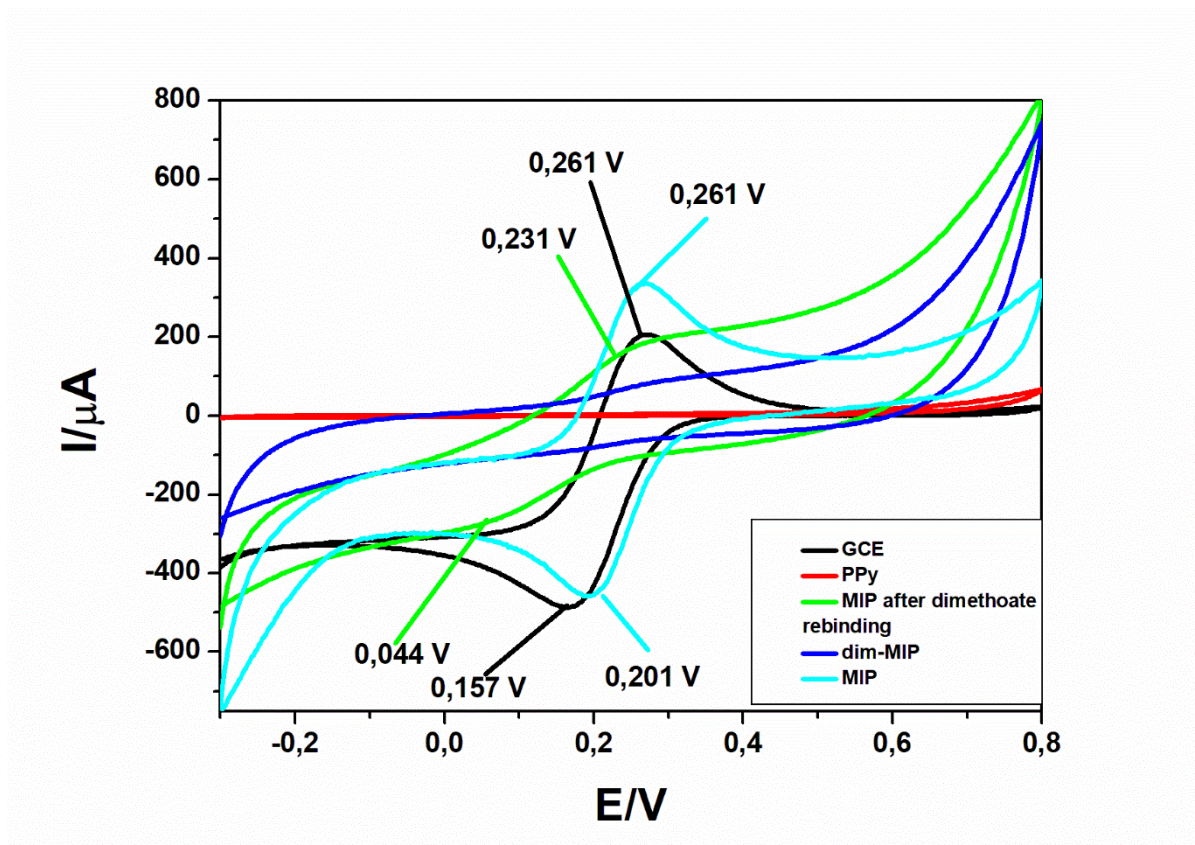


Figure 3.6: Cyclic voltammograms of 1 mM $K_3[Fe(CN)_6]$ at 10 mV/s in 0.1 M PBS solutions containing 0.1 M KCl at bare GCE, PPy, dim-PPy film, MIP and Dimethoate rebinding MIP film.

Cyclic voltammetry was performed for the characterisation of the imprinted sensor in the presence of the redox probe $Fe(CN)_6^{3-}$ the obtained voltammograms are denoted in figure 3.6. Clear redox peaks are observed for the bare glassy carbon electrode at +0.261 V for the oxidation scan and +0.157 V for the reductive scan. These peaks can be attributed to the oxidation of the Fe ion under the equation $Fe^{2+} \longrightarrow Fe^{3+} + e^-$ and cathodic peaks are due to $Fe^{3+} + e^- \longrightarrow Fe^{2+}$. There is a slight shift in the anodic and cathodic potentials which can be attributed to the interaction of the polymer film that is deposited on the surface of the glassy carbon electrode. There are no redox peaks observable for polypyrrole and for the electrode modified and denoted dim-MIP which can be due to the fact that there was presence of a dense film on the surface of the electrode which resulted in the hindrance of the transfer

of the electrolyte from the solution to the surface of the electrode. From the voltammogram of MIP which is obtained by washing the electrode surface with acid repeatedly thus removing the dimethoate thus forming cavities that are complementary in shape and size to the dimethoate analyte, the peaks that are observed for the MIP are found at potentials of +0.226 V and +0.201 V for anodic and cathodic scans respectively. The voltammogram obtained after the introduction of the analyte molecule whose shape and size compliment those of the cavities showed a decrease in the current and a shift in both the anodic and cathodic potentials which can be attributed to the attachment of the analyte on the sensor and filling the cavities.



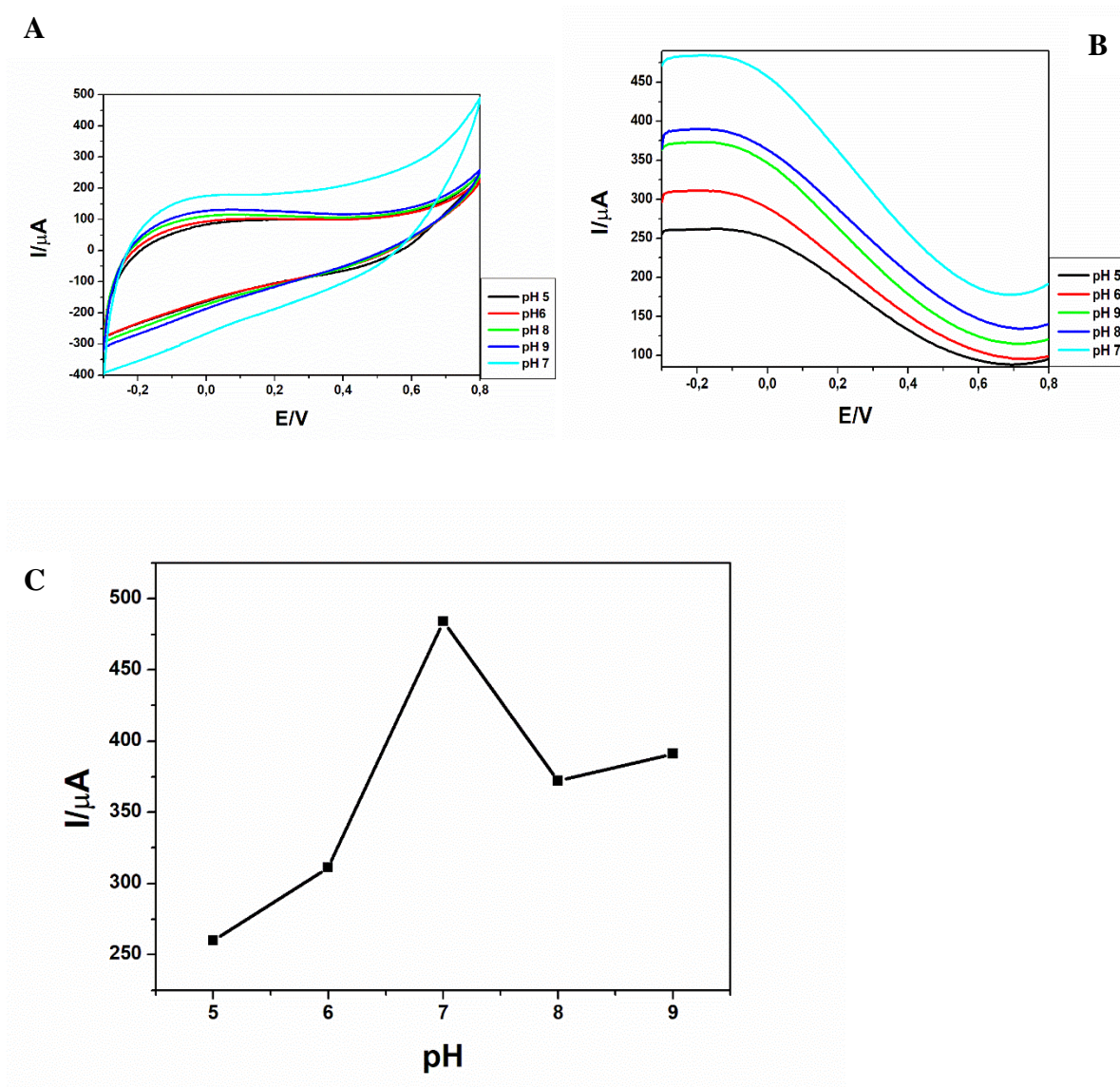


Figure 3.7: (A) Cyclic voltammogram, (B) Square wave voltammogram of 1 mM $K_3[Fe(CN)_6]$ at 10 mV/s in 0.1 M PBS solutions containing 0.1 M KCl, (C) shows plot of I_{pa} Vs pH to 0.1 nM substrate effect of pH at MIP electrode.

The pH of the solutions containing substrates play a significant role on the enzyme activity, it can affect the transfer of electrons. At extreme pH values enzymes such as AChE can denature due to conformational changes observed in a native tertiary structure of AChE enzyme. A series of test solutions of $Fe(CN)_6^{3-}$ PBS containing KCl were evaluated at pH values ranging from 5-9 and the responses of the sensor system were recorded using Cyclic voltammetry and square wave voltammetry at scan rate 0.01 V/s which is shown in figure 3.7 A), B) and C) where it is

observed that the highest current response was reached at pH 7 (fig 3.7 (C)) which is the optimum pH for AchE, which thus lead to the conclusion that pH 7 was the most suitable pH to use in the test solution similar results were obtained by (Zhang *et al.* 2012).

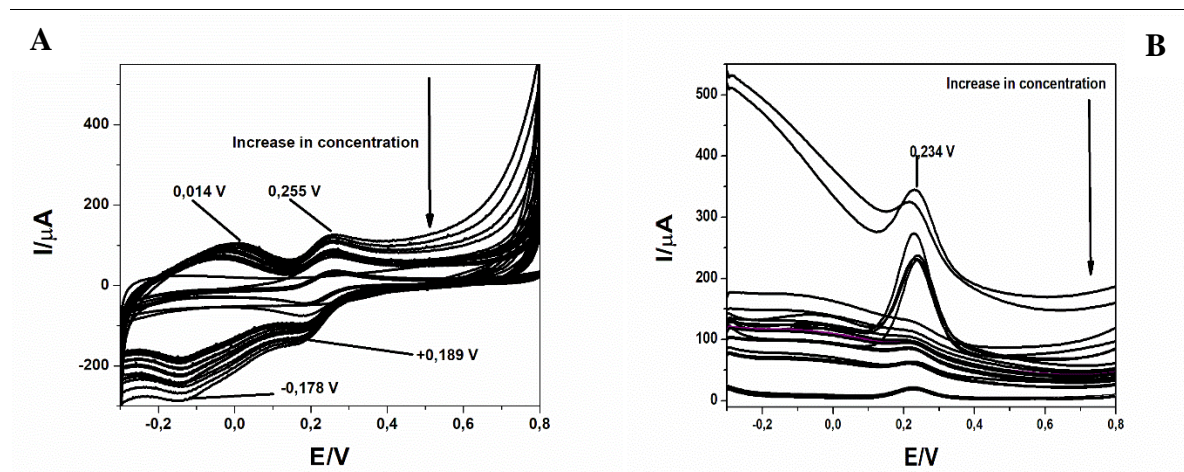


Figure 3.8: Cyclic voltammograms (A), Square wave voltammogram (B) of MIP after rebinding of dimethoate at different concentrations (0.01, 0.02, 0.03, 0.04, 0.06, 0.08, 0.1, 0.12, 0.14, 0.16, 0.18, 0.2, 0.3, 0.4, 0.5, 0.6, 0.7, 0.8, 0.9 and 1 nM) in 0.1 M PBS pH 7, 0.1 M KCl, and 1 mM $K_3[Fe(CN)_6]$.

For the determination of the response of the MIP electrode in the detection of dimethoate, the electrode containing the MIP system was incubated in different concentrations of dimethoate solutions for a duration of 15 min at 4°C. The results obtained in figure 3.8 shows that there was a decrease in the current after each consecutive concentration followed by a constant current response which can be attributed to the saturation of the MIP electrode after rebinding of the pesticide. The MIP system shows good response towards the detection of the probe which shows four distinct peaks at +0.189 V, -0.176 V, +0.255 V and +0.014 V. There is a redox couple +0.255 and +0.189 V which is due to the change in the ferrate state of the probe solution after gaining and loss of an electron, the peaks at +0.014 and -0.176 V may be due to

the interaction between the bound dimethoate and the analytical probe. The decrease in current response can be attributed to the rebinding of the template molecule onto the imprinted cavities, thus slowing down electron exchange between the electrode surface and the electrolyte.



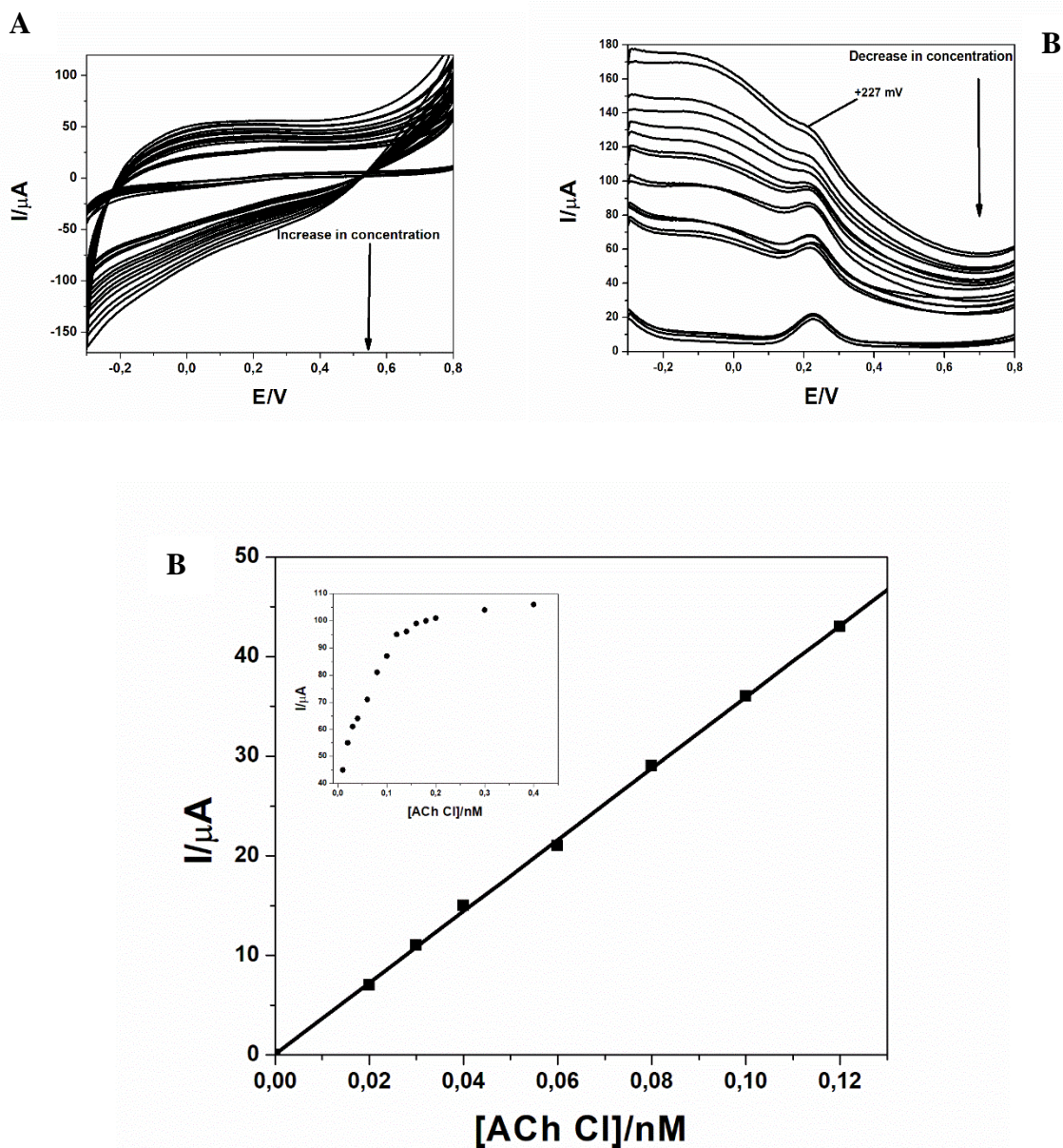


Figure 3.9: (A) CV, (B) SWV of acetylthiocholine at MIP at different concentrations (0.01, 0.02, 0.03, 0.04, 0.06, 0.08, 0.1, 0.12, 0.14, 0.16, 0.18, 0.2, 0.3, 0.4, 0.5, 0.6, 0.7, 0.8, 0.9 and 1 nM) in the presence of AchE, 0.1 M PBS pH 7, 0.1 M KCl, and 1 mM $\text{K}_3[\text{Fe}(\text{CN})_6]$. (D) Linear range of the calibration curve for the response of the MIP electrode to hydrolysis of ATCl by AchE.

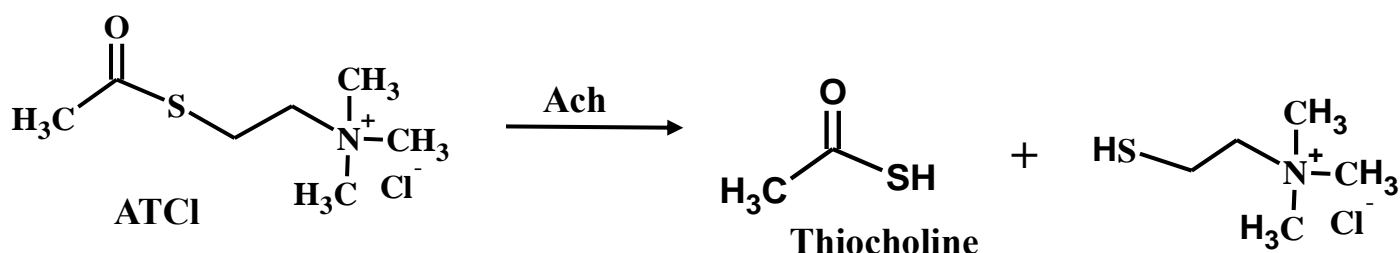


Figure 3.10: Mechanism of ATCI hydrolysis catalyzed by AChE

Measurements were performed by incubation of MIP electrodes in ATChCl solutions of variable concentrations of substrates. In both the cyclic voltammogram and square wave voltammograms represented in fig 3.9 (A) and (B) there is an observed a decrease in current with an increase in concentration of substrate added. Even though on the cyclic voltammogram there were no clearly visible peaks in SWV there was a clearly visible oxidation peak at +0.227 V which can be attributed to the oxidation of thiocholine, which was the hydrolysis product of ATCI and catalysed by the enzyme AChE by the mechanism represented in fig 3.10. Thiocholine is produced during enzymatic reactions and anodically oxidised on electrodes (Nunes *et al.* 1998). From the linear range of the calibration curve represented in fig 3.9 (C) it was determined that the dynamic linear range (DLR) was 0.01 nM – 0.12 nM thus signifying that the sensor can be able to detect concentrations of ATCI even at as low concentrations as 0.01 nM. The LOD of the sensor was determined to be 0.023 nM and sensitivity of 0.42 $\mu\text{A}/\text{nM}$.

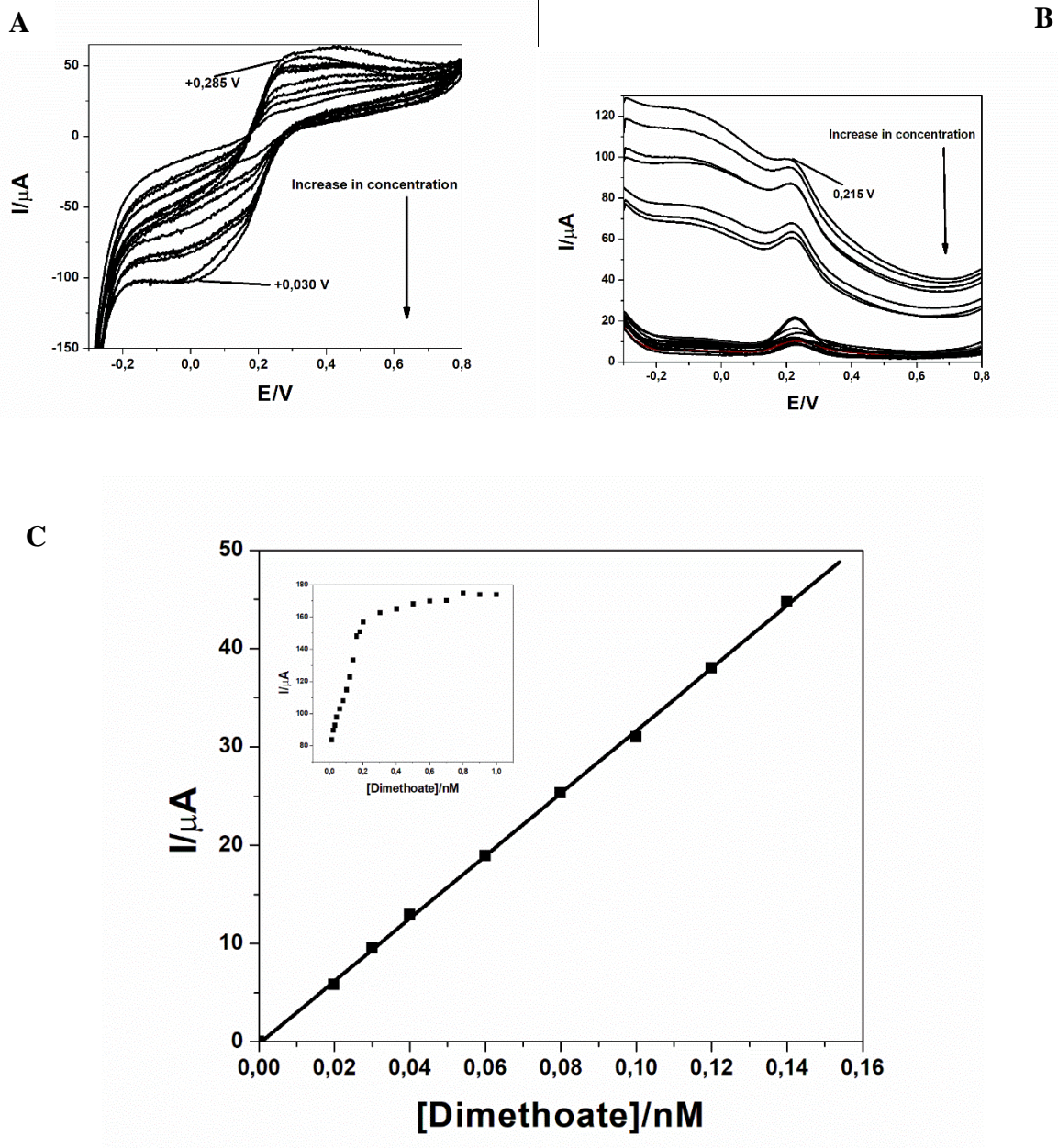


Figure 3.11: (A) CV, (B) SWV of inhibition of AchE in the presence of dimethoate at MIP electrode at different concentrations (0.01, 0.02, 0.03, 0.04, 0.06, 0.08, 0.1, 0.12, 0.14, 0.16, 0.18, 0.2, 0.3, 0.4, 0.5, 0.6, 0.7, 0.8, 0.9 and 1 nM) in the presence of 0.1nM acetylthiocholine, 0.1 M PBS pH 7, 0.1 M KCl, and 1 mM $\text{K}_3\text{Fe}(\text{CN})_6$. (C) Linear range of the calibration curve for the response of the MIP electrode to inhibition of ATCl by dimethoate.

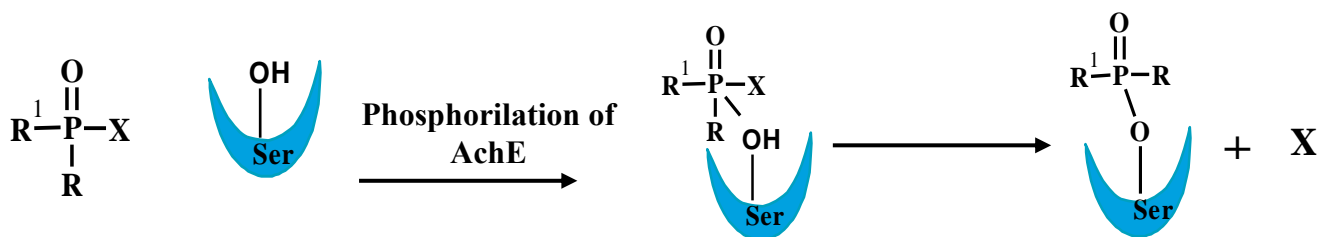


Figure 3.12: Phosphorilation of AchE by dimethoate

Fig 3.11 A) and B) show the cyclic and square wave voltammograms respectively of the inhibition of AchE by dimethoate, an organophosphoric pesticide, both voltammograms showing the decrease in the analytical signal with an increase in the concentration of the analyte of interest; dimethoate. In fig 3.11 (A) there is a shift in the anodic peak potentials with the increase in concentration to more negative potentials, this is indicative of OPs are substrate analogues to ATCl, and thus just like the natural substrate have the ability to bind to the active site and covalently binding to serine –OH group. The OP is split and the enzyme is phosphorylated as denoted in fig 3.12. While the acyl enzyme is quickly hydrolysed to regenerate the free enzyme, dephosphorylation is very slow and takes days to occur, and once the enzyme is phosphorylated the function of the enzyme which is to hydrolyse the neurotransmitter ATCl is hindered. The inhibition of the enzyme leads to accumulation of ATCl in the synaptic cleft causing over-stimulation of nicotinic and muscarinic Ach receptors and impedes neurotransmission, resulting in symptoms of acute poisoning (Krsti et al. 2013). From the linear range of the calibration curve presented in fig 3.11 (C) it was determined that the dynamic linear range (DLR) was 0.01 nM – 0.14 nM. The LOD of the sensor was determined to be 0.035 nM thus showing that the sensor can be able to detect concentrations of ATCl even at as low concentrations as 0.035 nM of dimethoate that may be present and sensitivity of 0.32 $\mu\text{A}/\text{nM}$.

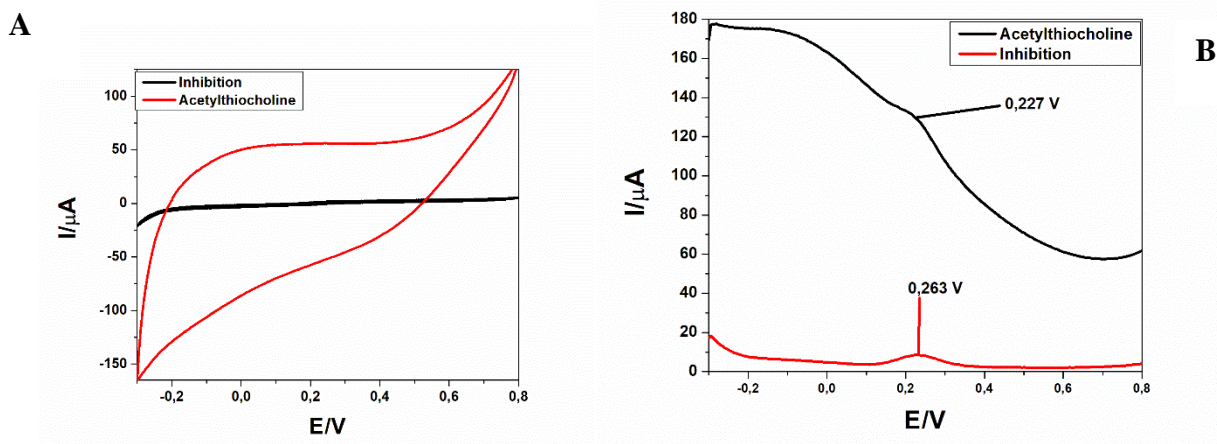


Figure 3.13: (A) CV, (B) anodic SWV of inhibition of AchE in the presence and absence of dimethoate at MIP electrode at different in the presence of 0.1nM acetylthiocholine, 0.1 M PBS pH 7, 0.1 M KCl, and 1 mM $\text{K}_3\text{Fe}(\text{CN})_6$].

The inhibition efficiency (I %) was calculated as follows:

$$I\% = \frac{i_{p,\text{con}} - i_{p,\text{exp}}}{i_{p,\text{con}}} \times 100 \quad (1)$$

Where $i_{p,\text{con}}$ and $i_{p,\text{exp}}$ were the peak current of ATChCl on AChE MIP/GCE before and after dimethoate inhibition, respectively. Dimethoate, one of the organophosphorus pesticides, was chosen as the analyte of interest to study the inhibitory effect dimethoate has on the enzyme AChE. Following incubation of MIP/GCE in 0.1 nM dimethoate for 15 min CV and SWV shown in fig 3.13 (A) and (B) respectively were performed to determine the inhibitory effect of dimethoate on the activity of AChE, the signal was lesser than that from uninhibited (where there was no dimethoate) present by AChE, similar results were obtained by (Du *et al.* 2010). The decrease in peak current increased with increasing concentration of dimethoate. However, the maximum inhibition value of the enzyme AChE by dimethoate was obtained using equation

1, the value was not 100%, which was possibly due to the binding equilibrium between the pesticide and binding sites in the enzyme.

Table 3.2: comparison of detection methods, their DLR and LOD in nM to the present study

REFERENCES	METHOD	DLR (nM)	LOD (nM)
(Du et al. 2008)	o-phenylenediamine-AgNPs MIP	0.084 – 8.4	2.18
(Li et al. 2016)	Biosensor	1-0.37	0.37
This study	MIP	0.01 – 0.14	0.035

3.3 Conclusion

The MIP film based on polypyrrole was successfully prepared electrochemically. The resulting imprinted polymer sensor comprising the high conductive nature of polypyrrole which is a useful material that can function as a good electric conductor and a good electron mediator. Electrochemical preparation of the MIP film is a cost effective, uses less reagents thus ensuring a decrease in by-products and contaminated waste which would likely cause harm to the environment and its preparation is not time consuming and thus it will be suitable for use even in households. MIP is the best choice of technique for the determination of pesticides as it ensures sensitivity and selectivity towards the analyte of interest, this was determined by comparing the results obtained by other methods shown in table 3.2. This is due to the fact that during preparation of MIPs the analyte to be detected is used and imprinted on the polymer matrix, thus resulting in cavities that are complimentary in shape and size to that of the analyte

to be detected. This makes the MIP susceptible to binding only the analyte of interest even when there is presence of other analytes since the other analytes are very much less likely to have the affinity to bind on the imprinted sites. The binding of the analyte to the imprinted cavities resulted in a decrease in analytical signal after successive incubation of MIP electrode in various increasing concentration of dimethoate, this was visible in both cyclic and square wave voltammetry. The low LOD shows that it can be used to detect even the lowest concentrations of dimethoate.

3.4 References

Algae, A. et al., 2013. Aromatic amino acids and their derivatives as ligands for the isolation of aspartic proteinases. *The Communication of Ideas*, 3(2), pp.285–290.

Anirudhan, T.S. & Alexander, S., 2015. Design and fabrication of molecularly imprinted polymer-based potentiometric sensor from the surface modified multiwalled carbon nanotube for the determination of lindane (γ -hexachlorocyclohexane), an organochlorine pesticide. *Biosensors and Bioelectronics*, 64, pp.586–593.

Beránková, M., Hojerová, J. & Melegová, L., 2017. Exposure of amateur gardeners to pesticides via the non-gloved skin per day. *Food and Chemical Toxicology*, 108, pp.224–235.

de Blaquièrre, G.E. et al., 2000. Electrophysiological and biochemical effects of single and multiple doses of the organophosphate diazinon in the mouse. *Toxicology and applied pharmacology*, 166(2), pp.81–91.

Bucur, M.P., Bucur, B. & Radu, G.L., 2013. Critical evaluation of acetylthiocholine iodide and acetylthiocholine chloride as substrates for amperometric biosensors based on acetylcholinesterase. *Sensors (Switzerland)*, 13(2), pp.1603–1613.

Carlo, M. Del et al., Acetylcholinesterase inhibition assay for the determination of pirymiphos methyl in durum wheat samples.

Coscollà, C. et al., 2017. Human exposure and risk assessment to airborne pesticides in a rural French community. *Science of the Total Environment*, 584–585, pp.856–868.

Du, D. et al., 2010. Acetylcholinesterase biosensor design based on carbon nanotube-encapsulated polypyrrole and polyaniline copolymer for amperometric detection of organophosphates. *Biosensors and Bioelectronics*, 25(11), pp.2503–2508.

Du, D. et al., 2008. Recognition of dimethoate carried by bi-layer electrodeposition of silver nanoparticles and imprinted poly-o-phenylenediamine. *Electrochimica Acta*, 53(22), pp.6589–6595.

Van Dyk, J.S. & Pletschke, B., 2011. Review on the use of enzymes for the detection of organochlorine, organophosphate and carbamate pesticides in the environment. *Chemosphere*, 82(3), pp.291–307.

EPA, What is the Difference Between Pesticides , Insecticides and Herbicides ? Pesticide Effects on Food Production. , pp.1–4.

Europe, P.D.B. in, 2009. Acetylcholinesterase: A gorge-ous enzyme. , pp.1–22.

Genthe, B. & Steyn, M., An Overview of Health Effects of Endocrine Disrupting Chemicals in Water - Where are we in South Africa?

González-Curbelo, M.Á. et al., 2017. Dissipation kinetics of organophosphorus pesticides in milled toasted maize and wheat flour (gofio) during storage. *Food Chemistry*, 229, pp.854–859.

Gothwal, A. et al., 2014. Preparation of electrochemical biosensor for detection of organophosphorus pesticides. *International Journal of Analytical Chemistry*, 2014.

Han, Y. et al., 2017. Pesticide residues in nut-planted soils of China and their relationship between nut/soil. *Chemosphere*, 180, pp.42–47.

Jenkins, A.L., Yin, R. & Jensen, J.L., 2001. Molecularly imprinted polymer sensors for pesticide and insecticide detection in water. *Analyst*, 126(6), pp.798–802.

Kiyama, R. & Wada-Kiyama, Y., 2015. Estrogenic endocrine disruptors: Molecular mechanisms of action. *Environment International*, 83, pp.11–40.

Krsti, D.Z. et al., 2013. Acetylcholinesterase Inhibitors : Pharmacology and Toxicology. , pp.315–335.

Li, J. et al., 2016. Sensing Estrogen with Electrochemical Impedance Spectroscopy. *Journal of Analytical Methods in Chemistry*, 2016, pp.1–6.

Van Maele-Fabry, G., Gamet-Payraastre, L. & Lison, D., 2017. Residential exposure to pesticides as risk factor for childhood and young adult brain tumors: A systematic review and meta-analysis. *Environment International*, 106(June), pp.69–90.

Maruyama, T. et al., 2016. Intracoronary acetylcholine application as a possible probe inducing J waves in patients with early repolarization syndrome. *Journal of Arrhythmia*, 33(5), pp.424–429.

Morillo, E. & Villaverde, J., 2017. Advanced technologies for the remediation of pesticide-contaminated soils. *Science of the Total Environment*, 586, pp.576–597.

Münze, R. et al., 2017. Pesticides from wastewater treatment plant effluents affect invertebrate communities. *Science of the Total Environment*, 599–600, pp.387–399.

Nowell, L.H. et al., 2017. Complex mixtures of dissolved pesticides show potential aquatic toxicity in a synoptic study of Midwestern U.S. streams. *Science of the Total Environment*.

Nugroho, A. et al., 2017. Anti-acetylcholinesterase activity of the aglycones of phenolic glycosides isolated from *Leonurus japonicus*. *Asian Pacific Journal of Tropical Biomedicine*, 7(10), pp.849–854.

Nunes, G.S. et al., 1998. Determination of carbamate residues in crop samples by cholinesterase- based biosensors and chromatographic techniques. *Analytica Chimica Acta*, 362(1), pp.59–68.

Obajuluwa, A.O. et al., 2017. Exposure to radio-frequency electromagnetic waves alters acetylcholinesterase gene expression, exploratory and motor coordination-linked behaviour in male rats. *Toxicology Reports*, 4(October), pp.530–534.

Olujimi, O.O. et al., 2010. Endocrine disrupting chemicals (phenol and phthalates) in the South African environment: A need for more monitoring. *Water SA*, 36(5), pp.671–682.

Osorio, A., 2009. PESTICIDES : Insecticides , Rodenticides &.

Periasamy, A.P., Umasankar, Y. & Chen, S.M., 2009. Nanomaterials - Acetylcholinesterase enzyme matrices for organophosphorus pesticides electrochemical sensors: A review. *Sensors*, 9(6), pp.4034–4055.

Piccoli, C. et al., 2016. Pesticide exposure and thyroid function in an agricultural population in Brazil. *Environmental Research*, 151, pp.389–398.

Pochini, L. et al., 2016. Acetylcholine and acetylcarnitine transport in peritoneum: Role of the SLC22A4 (OCTN1) transporter. *Biochimica et Biophysica Acta - Biomembranes*, 1858(4), pp.653–660.

Pohanka, M., Jun, D. & Kuca, K., 2008. Improvement of acetylcholinesterase-based assay for organophosphates in way of identification by reactivators. *Talanta*, 77(1), pp.451–454.

Prasad, B.B. & Jauhari, D., 2015. A dual-template biomimetic molecularly imprinted dendrimer-based piezoelectric sensor for ultratrace analysis of organochlorine pesticides. *Sensors and Actuators, B: Chemical*, 207(PartA), pp.542–551.

Products, C., 1989. Organophosphate Insecticides 1. , 37(March), pp.1–7.

Razwiedani, L.L. & Rautenbach, P., 2017. Epidemiology of Organophosphate Poisoning in the Tshwane District of South Africa. *Environmental health insights*, 11(0), p.1178630217694149.

S??oniecka, M., Backman, L.J. & Danielson, P., 2015. Acetylcholine enhances keratocyte proliferation through muscarinic receptor activation. *International Immunopharmacology*, 29(1), pp.57–62.

Santos-Silva, A.P. et al., 2017. Frontiers in endocrine disruption: Impacts of organotin on the hypothalamus-pituitary-thyroid axis. *Molecular and Cellular Endocrinology*.

Toro, M.J.U., Marestoni, L.D. & Del Pilar Taboada Sotomayor, M., 2015. A new biomimetic sensor based on molecularly imprinted polymers for highly sensitive and selective determination of hexazinone herbicide. *Sensors and Actuators, B: Chemical*, 208, pp.299–306.

Ye, M. et al., 2017. Pesticide exposures and respiratory health in general populations. *Journal of Environmental Sciences (China)*, 51, pp.361–370.

ZHANG, C. et al., 2017. Uptake and translocation of organic pollutants in plants: A review. *Journal of Integrative Agriculture*, 16(8), pp.1659–1668.

Zhang, L. et al., 2012. Electrochemical behaviors of roxithromycin at poly(3,4-ethylenedioxythiophene) modified gold electrode and its electrochemical determination. *Electrochimica Acta*, 72, pp.179–185.

Zhang, T. et al., 2014. Ultrasensitive electrochemical sensor for p-nitrophenyl organophosphates based on ordered mesoporous carbons at low potential without deoxygenization. *Analytica Chimica Acta*, 822, pp.23–29.



CHAPTER FOUR

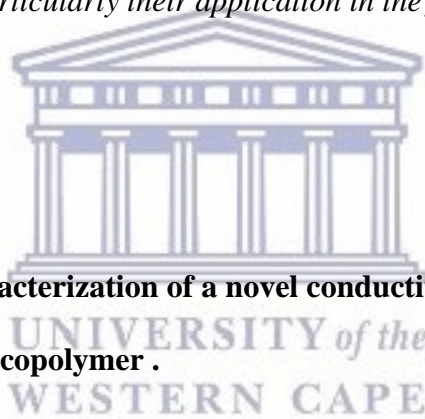
Chemical synthesis and characterization of a novel conductive poly(methacrylic acid-co-3,4-ethylenedioxythiophene) copolymer.



UNIVERSITY *of the*
WESTERN CAPE

Summary

Conducting polymers (CPs) have been materials of interest for decades, due to the intrinsic properties that they have. There is combination of properties of conventional plastics i.e mechanical properties and metal-like properties i.e electric conductivity. It is these properties that make them suitable for various applications such as sensors, light-emitting diodes (LEDs), photovoltaic cells and electric circuits. Composites of CPs have seen an increase in interest, they can be used in the preparation of copolymers, both homopolymers and heteropolymers. In this chapter the background on conducting polymers, their properties and applications are discussed. Particularly their application in the fabrication of copolymers.



Chemical synthesis and characterization of a novel conductive poly(methacrylic acid-co-3,4-ethylenedioxythiophene) copolymer .

Abstract

For more than three decades conducting polymers (CPs) have drawn significant interest of researchers due to their economical importance, excellent superior stability, light weight, improved workability, resistance to corrosion and satisfactory electrical conductivity. Due to these properties, interest in their application in various fields has seen an increase, including the applications in rechargeable batteries, electrochromic display devices, light reflecting or light transmitting appliances for optical information, sensors, smart windows in automobiles and buildings, light emitting diodes (LEDs), photovoltaic cells, transistors and electronic

circuits. There has been a noticeable increase in the application of CPs in sensor technology, attributed to the fact that during polymerization the film thickness can be controlled and they offer electrical properties. Moreover, CP based biosensors are likely to accommodate to the demanding necessities such as biocompatibility, possibility of in vivo sensing, constant monitoring of drugs or metabolites, multi-parametric assays, miniaturization and high information density. These conducting polymers can be synthesized using two methods; electrochemical and chemical polymerization. A conductive P(MAA-co-EDOT) was synthesised. HRSEM was used for the determination of the surface morphologies. The polymers were found to be packed coral in and irregular coral-like structures were observed in P(MAA-co-EDOT) while the surface of PMAA was rough which can be attributed to the hard gel-like material obtained after the drying in the oven. Optical properties investigated using UV-Vis spectroscopy showed maximum absorption peak at approximately 280 nm which can be attributed to the π - π^* transition of the thiophene ring for PEDOT. Maximum absorption peak for PMAA at 250 which can be attributed to the π - π^* transition that is due to the C=O. While the peak at 218 nm may be due to the transitions n - σ^* which is attributed to the interaction between carbon and oxygen (C-O) characteristic peaks where the peak at 227 nm can be attributed to n - σ^* whilst that at 252 nm can be assigned to the n - π^* transitions. The wavelengths were used to determine the energy band gaps of PMAA, PEDOT and P(MAA-co-EDOT) and were found to be 4.96, 4.32 and 4.92 eV respectively.

4.0 Introduction

The exploration of the electrical conductivity of polymers dates back to the 1960's. Traditional polymers commonly known as plastics have been used because of the attractive chemical, electrically insulating and mechanical properties (Malhotra *et al.* 2006; Xia *et al.* 2010; Shanmugham & Rajendran 2015). The use of conducting polymers as electronic material is fairly new. While behaving as insulators or semiconductors in the pristine form, conjugated

polymers can reach metallic-like electrical conductivity when doped (Linko *et al.* 1999; Janáky & Visy 2013; Molapo *et al.* 2012). Since 1977, the dream of combining the processing and mechanical properties of polymers with the electrical and optical properties of metals has driven the technology of *conducting polymers*. In 1977 it was found by Shirakawa, Heeger and McDiarmid discovered that films of polyacetylene (PAC) increase their conductivity tremendously when they are exposed to iodine vapour, from a basic value at the lower end of the semiconducting range up to values comparable to metals (Shirakawa 2001; Ates 2013). In the year 2000 they jointly received a Nobel Prize in chemistry for their discovery and development of conducting polymers. Soon after this discovery, a series of stable conducting polymers, including **polypyrrole (PPy)** (Du *et al.* 2010; Deng *et al.* 2012), **polyphenylene** (Neagu *et al.* 2015), **polyaniline (PAn)** (Elahi *et al.* 2015; Molapo *et al.* 2012; Tovide, Jahed, *et al.* 2014), and **polythiophene (PTh)** (McCullough 1998; Zanardi *et al.* 2013; Huynh *et al.* 2015) were reported since the 1970s, which greatly promoted the research on conducting polymers. They are applied in the development of batteries (Wei *et al.* 2016; Seo *et al.* 2015), electronic displays (C. Pinto *et al.* 2014), sensors (Pardieu *et al.* 2009), functional electrodes (K. Zhang *et al.* 2014) to name a few. The conductivity of almost all conjugated polymers can reach the order of 10^{-3} – 10^3 S/cm after doping (Li 2015a). Currently there are 25 conducting polymers that have been reported (Ateh *et al.* 2006). All these polymers share a similar structural feature, a conjugation of double bonds (Tovide, Jahed, *et al.* 2014). This structural feature is what brings about the properties, notably, low-energy optical transitions (Wong & Ho 2006) and ionization potentials (Krivorotova *et al.* 2015) as well as high-electron affinities. In addition, there is special electrochemical redox activity with conducting polymers (Agarwal & Sharma 2017; Garcimartín *et al.* 2017). Obviously, conducting polymers, including doped conducting polymers (Leeuw *et al.* 1997; Nie *et al.* 2014; Boskovic *et al.* 2017) and intrinsic semiconducting conjugated polymers (Hu *et al.* 2017), will play a key role in the future

development of optoelectronic (Li 2015b) and electrochemical devices. Conducting polymers can be classified into two major group based on the synthetic method: chemically polymerized materials and electropolymerized (Lu *et al.* 2014; Bougrini *et al.* 2016). Chemical polymerization brings about a lot of advantages including the ability of mass production and low costs, this is almost difficult to achieve using the electrochemical polymerization synthetic methods (Toshima & Hara 1995). Copolymers based on methacrylic acid are relatively important in their applications on various industries. Copolymerization technique is one of the most important techniques that are efficient in initiating systematic changes in properties of polymers (Kumar *et al.* 2011). Copolymerization improves the ability of scientists in tailor-making polymer products with specific desired properties. Polymers based on single monomers present a limitation in the number of possible products. Homopolymerization (Pei *et al.* 2016) is a term that is used to distinguish the polymerization of a single monomer. Copolymerization allows synthesis of an almost unlimited number of different products by the simple variation in the nature and amounts of the two monomer units in the copolymer unit (O dian 2004; Thakur & Thakur 2014; Nikovia *et al.* 2015). This study presents the synthesis and characterization of a copolymer based on the conductive poly(3,4-ethylenedioxythiophene) and poly(methacrylic acid) and its potential in applications in sensors.

4.1 Experimental

4.1.1 Chemicals

3,4-ethylenedioxythiophene (EDOT) 97% and Methacrylic acid (MAA) 99% monomers, polyvinyl chloride (PVC), tetrahydrofuran (THF), 17 β -estradiol (E2) \geq 98%, estrone \geq 99% were purchased from Sigma Aldrich. Disodium hydrogen phosphate (Na₂HPO₄), sodium

dihydrogen phosphate (NaH_2PO_4) were used for the preparation of pH 7 phosphate buffer. Ammonium persulfate ($(\text{NH}_4)_2\text{S}_2\text{O}_8$ (APS) was purchased from BIO-RAD laboratories, acetic acid (CH_3COOH), methanol (CH_3OH) and acetonitrile ($\text{C}_2\text{H}_3\text{N}$) were purchased from Sigma-Aldrich.

4.1.2 Instrumentation and procedure

A three electrode configuration was used for all electrochemical experiments. A gold electrode with a surface area of 0.0201 cm^2 from Bio Analytical Systems (BAS) was used as the working electrode. A saturated calomel electrode (SCE) as the reference electrode from BAS, and a platinum wire as the counter electrode. All the measurements were carried out at room temperature. All electrochemical measurements were performed on a computer-controlled potentiostat/ galvanostat (CH instruments electrochemical workstation) coupled with Model 270/250 Research Electrochemistry Software 4.30. Alumina micro polishing pads were obtained from BAS and used to polish the surface of the gold working electrode before modification. HRSEM images were taken with a Hitachi S3000N scanning electron microscope at an acceleration voltage of 20 kV at various magnifications. All FTIR spectra were recorded on Spectrum 100 FTIR spectrometer (PerkinElmer, USA) at a region of $400\text{-}4000 \text{ cm}^{-1}$. X-ray diffraction (XRD) patterns of the prepared polymers were performed on (XRD, Model No D/MAXPC 2500 X-ray, made in UK) operating in the scanning mode ($12.082^\circ\text{-}90.061^\circ$) and using $\text{CuK}\alpha$ radiation ($\lambda = 1.5418 \text{ \AA}$) generated at 40 kV and at a current of 30 mA. Raman analysis was done with an XPlora Horiba Jobin-Yvon spectrometer equipped with high stability OLYMPUS BX41TF optical microscope and an Ivac CCD detector. Ultraviolet–visible (UV–Vis) absorption measurements for all the prepared polymers were

obtained using 1 cm quartz cuvette on a Nicolet Evolution 100 UV-Visible spectrophotometer (Thermo Electron, UK) over a wavelength range of 200 to 350 nm.

4.1.3 Cleaning of electrodes

Prior to the electrodes being used, they were polished on 1 μm and 0.05 μm alumina slurries and sonicated in mili Q water for 10 min to remove any adsorbed material on the surface of the electrode. A very mild version of a piranha clean was prepared from 50 mM H_2SO_4 and 25% hydrogen peroxide. Gold samples spent 10 min in this treatment before being rinsed with Milli-Q. Lastly the electrodes were cleaned by cycling the electrode potential in a weak sulfuric acid solution 0.5 M until a stable CV scan was achieved. Sample potential was cycled from -400 to 1400 mV (vs. Ag/AgCl) at a rate of 100 mV/s in 50 mM sulfuric acid until a stable CV was achieved (approximately 12 cycles).

4.1.4 Preparation of polymer materials

4.1.4.1 Preparation of PMAA

1.6 mL MAA monomer and 100 mL ammonium persulfate (APS) solution were added in a 250 mL round bottom flask under stirring. The pre-solution was purged with nitrogen for 15 min to drive out oxygen, and then was sealed rapidly. Afterwards, the reaction flask was put in a pre-heated oil bath at 60 °C for polymerization for 24 h under moderate stirring. A white gel was formed and collected using vacuum filtration, washed with methanol and dried in a vacuum oven for 24 h. The obtained precipitate was mixed with polyvinyl chloride (PVC) and dissolved in tetrahydrofuran (THF). 20 μL of the solution was then drop-coated onto the surface of a gold working electrode and dried for 24 h.

4.1.4.2 Preparation of PEDOT

1.6 mL of EDOT and 100 mL ammonium persulfate (APS) solution were added in a 250 mL round bottom flask under stirring. The pre-solution was purged with nitrogen for 15 min to drive out oxygen, and then was sealed rapidly. Afterwards, the reaction flask was put in a pre-heated oil bath at 60 °C for polymerization for 24 h under moderate stirring. A black precipitate was formed and collected using vacuum filtration, washed with methanol and dried in a vacuum oven for 24 h. The obtained precipitate was mixed with polyvinyl chloride (PVC) and dissolved in tetrahydrofuran (THF). 20 µL of the solution was then drop-coated onto the surface of a gold working electrode and dried for 24 h.

4.1.4.3 Preparation of P(MAA-co-EDOT)

1.6 mL MAA monomer, 1.6 mL of EDOT monomer and 100 mL ammonium persulfate (APS) solution were added in a 250 mL round bottom flask under stirring. The pre-solution was purged with nitrogen for 15 min to drive out oxygen, and then was sealed rapidly. Afterwards, the reaction flask was put in a pre-heated oil bath at 60 °C for polymerization for 24 h under moderate stirring. A black precipitate was formed and collected using vacuum filtration, washed with methanol and dried in a vacuum oven for 24 h. The obtained precipitate was mixed with polyvinyl chloride (PVC) and dissolved in tetrahydrofuran (THF). 20 µL of the solution was then drop-coated onto the surface of a gold working electrode and dried for 24 h.

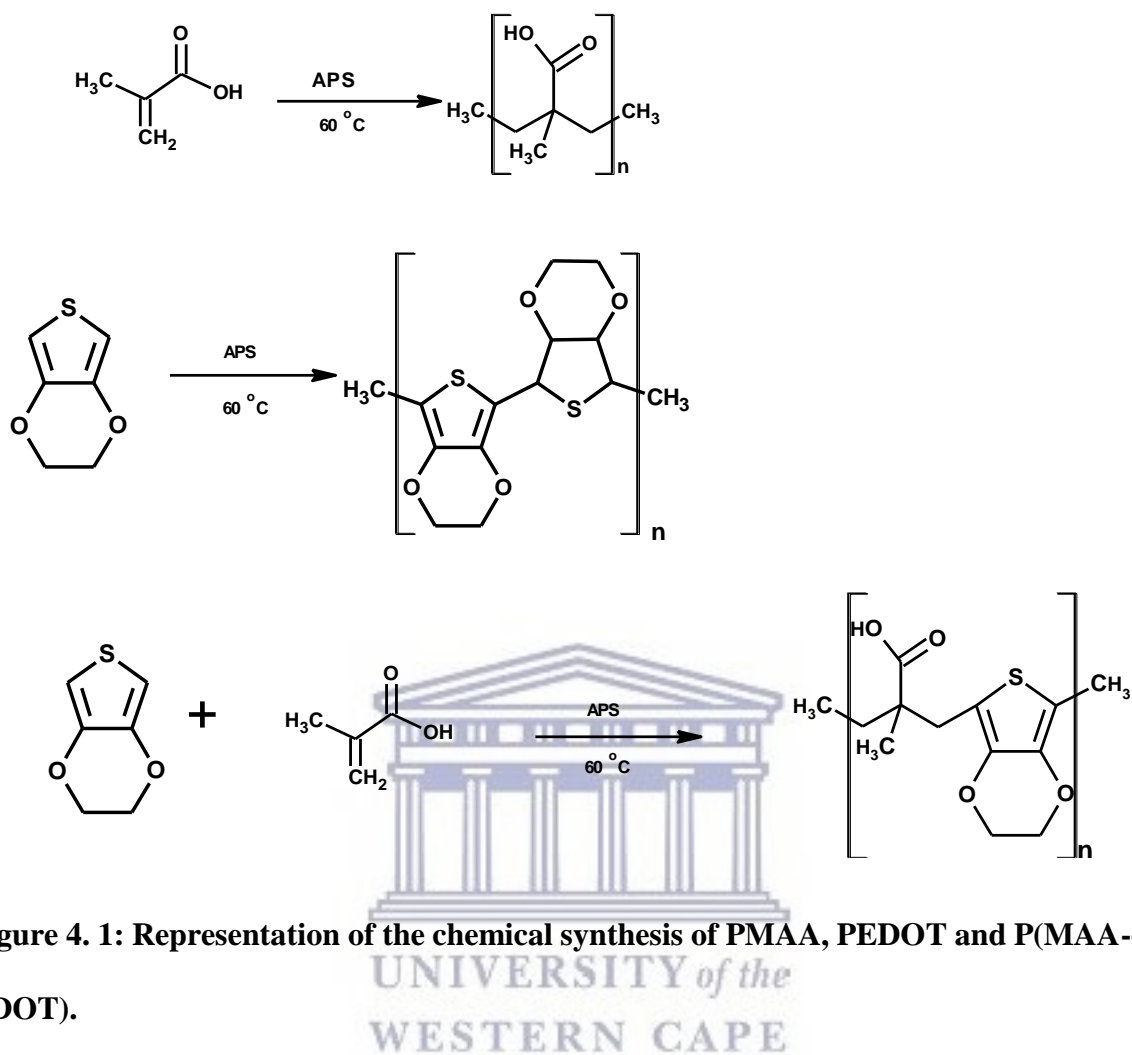
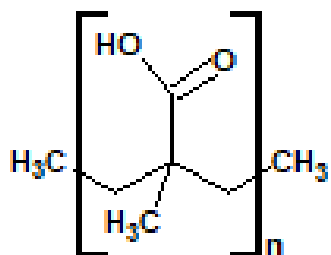


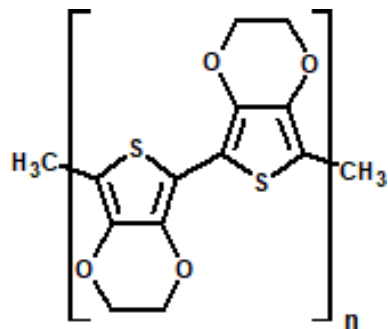
Figure 4. 1: Representation of the chemical synthesis of PMAA, PEDOT and P(MAA-co-EDOT).

4.2 Results and discussion

A



B



C

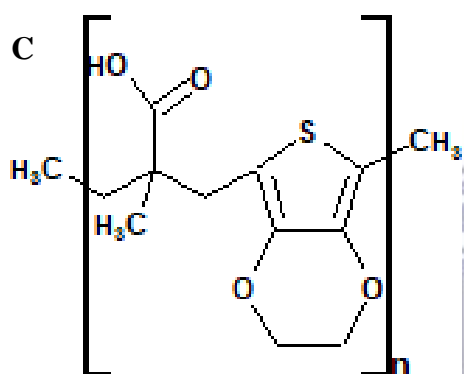
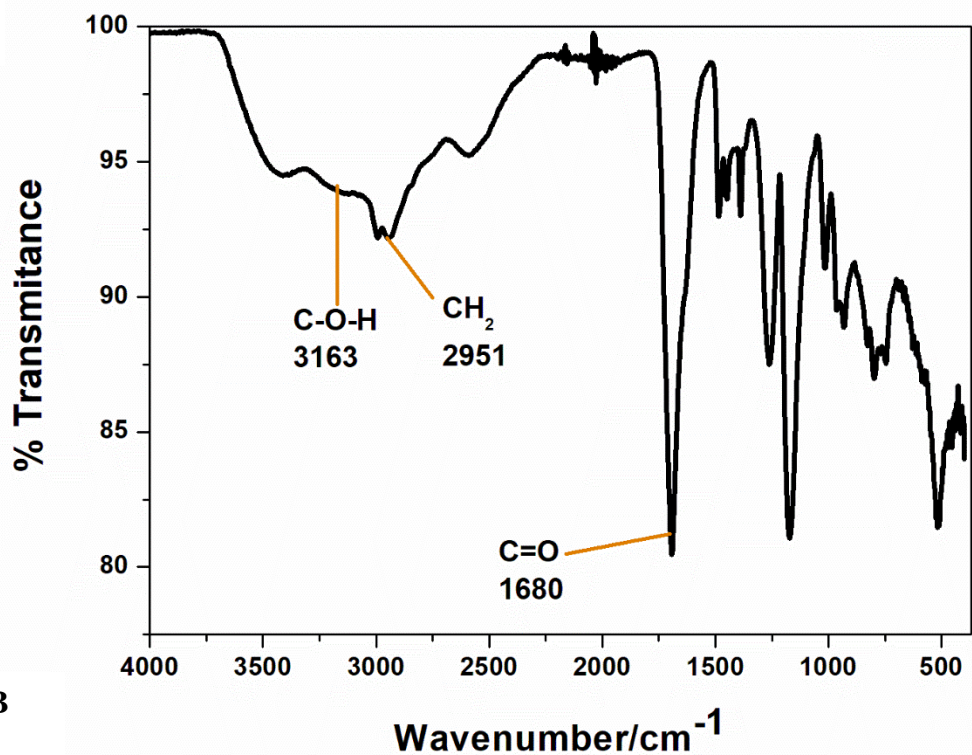


Figure 4. 2: Structure of (A) PMAA, (B) PEDOT and (C) P(MAA-co-EDOT)

UNIVERSITY OF
WESTERN CAPE

A



B

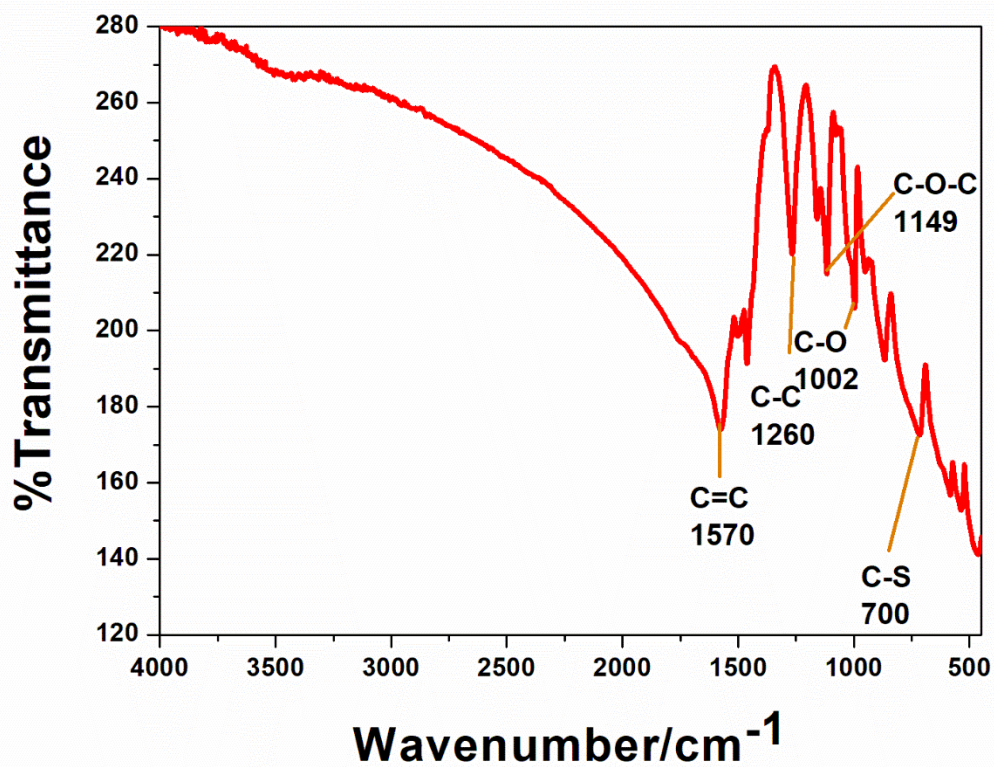


Figure 4. 3: FTIR of (A) PMAA and (B) PEDOT.

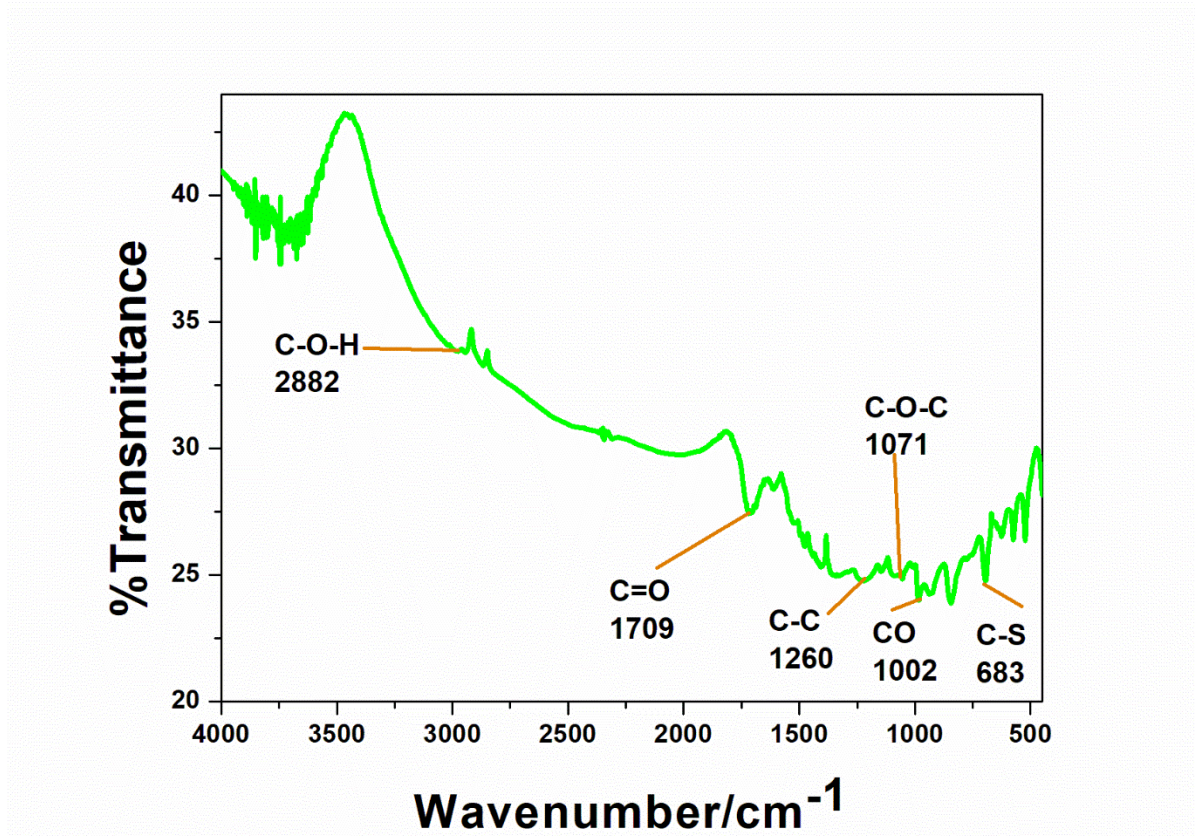
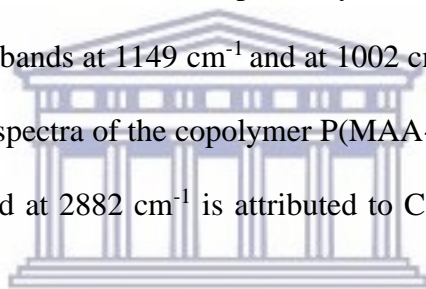


Figure 4. 4: FTIR spectra of P(MAA-co-EDOT).

Table 4. 1: Bonds and their respective frequencies in the structure of the PMAA, PEDOT and P(MAA-co-EDOT) copolymer.

Bond Type	Frequency, [cm ⁻¹]
C-H-O	3400-3250
-C=O	1680-1640
C=C Stretch aromatic	1335-1250
C-O Stretch	1600–1585
C-S Stretch aliphatic	1250-1220
C-C Stretch	2800-3000

The FTIR spectra shown in (Fig 4.3 A) was attributed to the successful synthesis shown in fig 4.1 of poly(methacrylic acid) PMAA from its monomer methacrylic acid in the presence of an oxidizing agent ammonium persulfate. This is confirmed by appearance of the C-O-H broad band stretch which is normally found at approximately 3163 cm^{-1} (Nobile *et al.* 2014). The band at 1680 cm^{-1} can be assigned to the carboxyl group of PMAA (Ye *et al.* 2006) while the band at 2951 cm^{-1} (Minhas *et al.* 2013) structure fig 4.2 (A). Fig 4.3 (B) shows the spectra of PEDOT, showing the presence of a band at 1149 cm^{-1} is attributed to C-O-C band of the ethylenedioxy ring of PEDOT (Hernández *et al.* 2017) as shown in fig 4.2 (B) . While the band at 700 cm^{-1} and at 1570 are associated with C-S and C=C respectively from the thiophene ring of PEDOT (Alvi *et al.* 2011). The stretch bands at 1149 cm^{-1} and at 1002 cm^{-1} are assigned to C-O-C and C-O respectively. In fig 4.4 a spectra of the copolymer P(MAA-co-EDOT) whose structure is shown if fig 4.2 (C). The band at 2882 cm^{-1} is attributed to C-O-H from PMAA which has shifted from 3163 cm^{-1} .



UNIVERSITY of the
WESTERN CAPE

Depicted in fig 4.5 are the SEM micrographs of PMAA, PEDOT and P(MAA-co-EDOT) polymers. The images highlight the extraordinary differences in the morphology of the polymer materials. The SEM image of PMAA (A) shows a very rigid surface of the polymer which is tightly bound together being attributed to the gel-like/rubbery nature/texture of PMAA which after its drying in the oven became very hard and rigid (Nobile *et al.* 2014). Its corresponding elemental analysis 4.5 (A') showed the presence of carbon and oxygen which are the primary functionalities present in the polymer backbone (Wang *et al.* 2010). The surface of PEDOT shows tightly packed coral-like structures, its corresponding elemental analysis fig 4.5 (B') shows carbon, oxygen present in the dioxy ring and sulphur groups from the thiophene ring from the chemical structure of PEDOT. The SEM image of PMAA-co-PEDOT fig 4.5 (C) shows that the surface of the polymer is made up of irregular coral-like particles, while the

elemental analysis shown in fig 4.5 (C') of P(MAA-co-EDOT) showed functionalities of oxygen, carbon and sulphur thus signifying the success synthesis of a P(MAA-co-EDOT) copolymer.

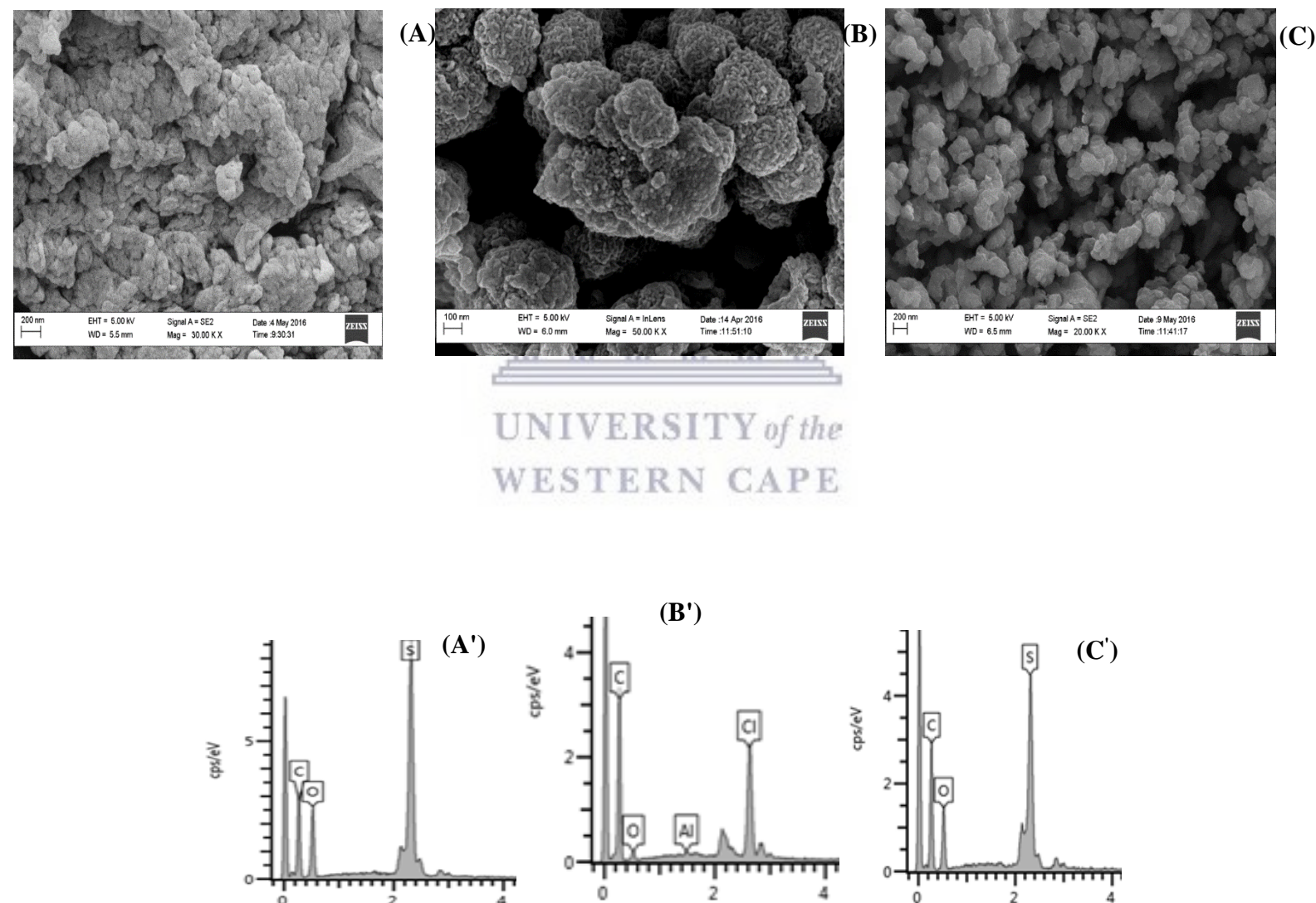


Figure 4. 5: HRSEM images and elemental analysis of PMAA, PEDOT and P(MAA-co-EDOT).

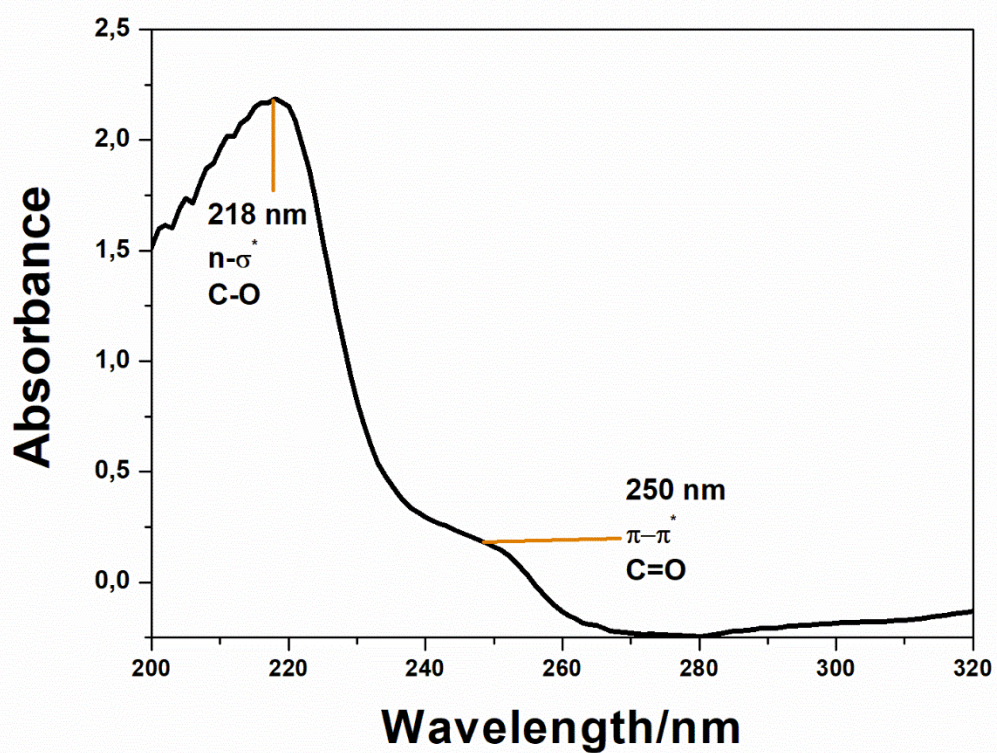
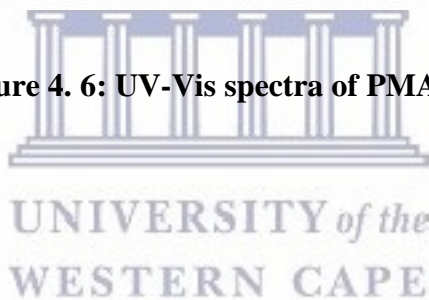


Figure 4. 6: UV-Vis spectra of PMAA.



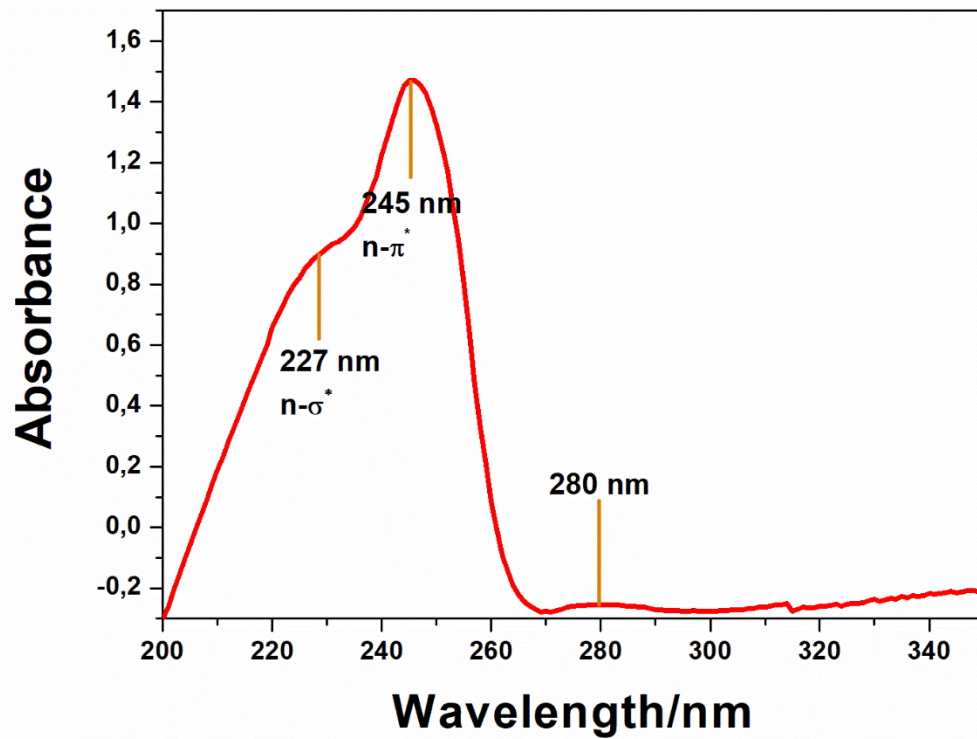
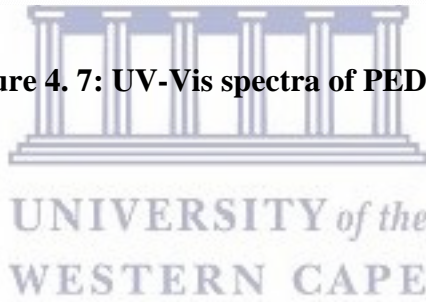


Figure 4. 7: UV-Vis spectra of PEDOT



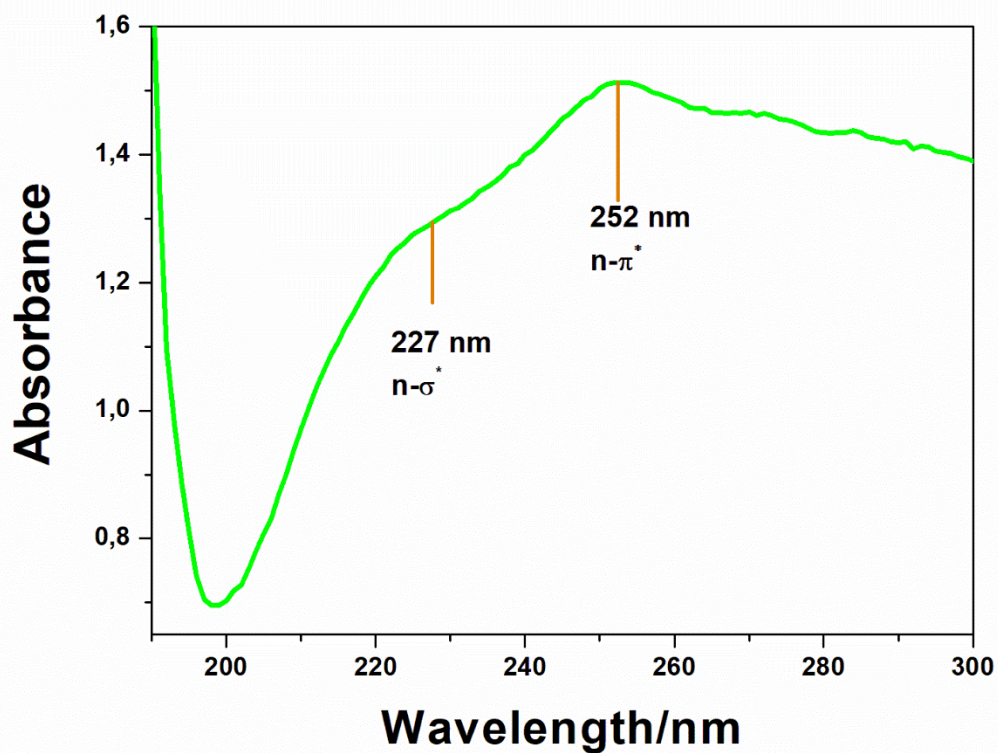


Figure 4. 8: UV-Vis of P(MAA-co-EDOT).

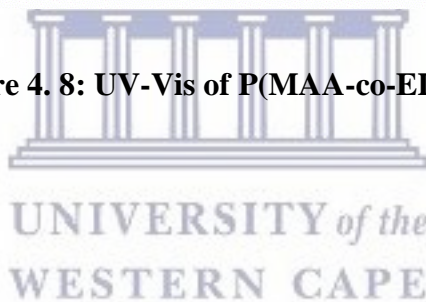


Table 4. 2: Table of energy band gaps of polymers

POLYMER	BAND GAP, [eV]
PMAA	5.14
PEDOT	4.50
P(MAA-co-EDOT)	3.85

Fig 4.6 shows the UV-Vis spectra of P(MAA) with maximum absorption band at 250 nm which can be attributed to the $\pi\text{-}\pi^*$ transition that is due to the C=O present on the structure of methacrylic acid. While the peak at 218 nm may be due to the transitions $n\text{-}\sigma^*$ which is attributed to the interaction between carbon and oxygen (C-O). The UV-vis absorption spectrum of PEDOT shown in fig 4.7 shows maximum absorption band at approximately 280 nm which can be attributed to the $\pi\text{-}\pi^*$ transition of the thiophene ring (Boskovic *et al.* 2017). The peak at is due to polaron and bipolaron bands characteristic of an oxidised PEDOT with a high conjugation length (Zhao *et al.* 2014). The spectrum of showed a band at 245 nm which can be attributed to the $\pi\text{-}\pi^*$ transition. The spectrum of (P(MAA-co-EDOT) depicted in fig 4.8 showed two characteristic bands where the band at 227 nm can be attributed to $n\text{-}\sigma^*$ whilst that at 252 nm can be assigned to the $n\text{-}\pi^*$ transitions. The nature of interaction between the valence band and conduction band as well as the band gap size determines the optical properties of semiconducting materials. The energy band gaps of PMAA, PEDOT and P(MAA-co-PEDOT) were determined to be 5.14, 4.50 and 3.85 respectively as shown in Table 4.2 signifying that the copolymer is characteristic of a biocompatible platform for applications in biosensors (Molapo *et al.* 2012).

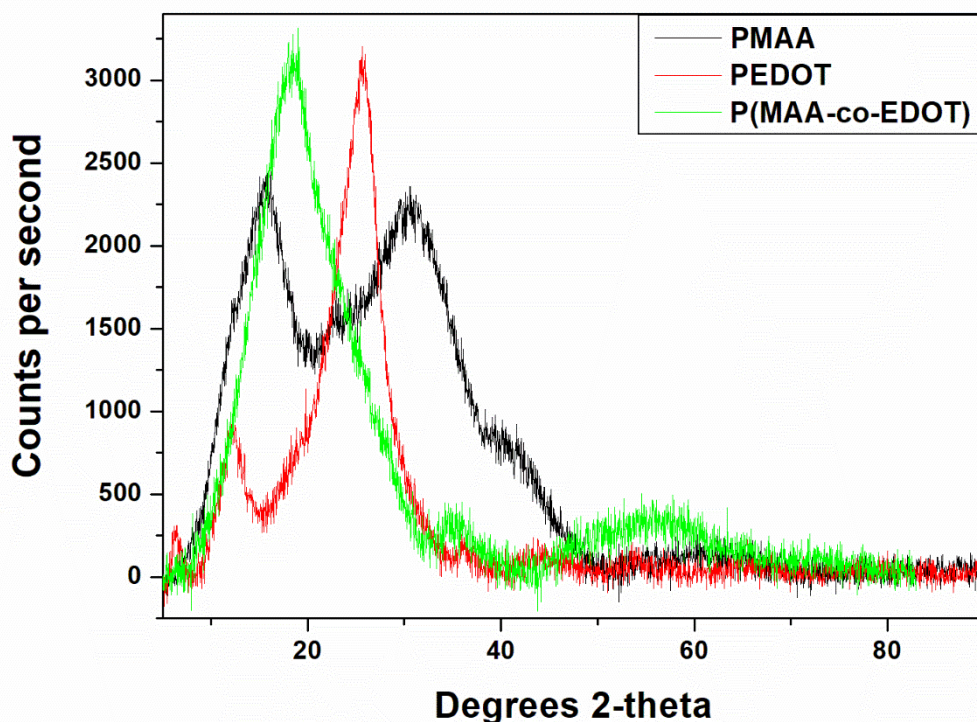


Figure 4. 9: XRD spectra of PMAA, PEDOT and P(MAA-co-EDOT).

Some information about the structure of PEDOTs has been achieved by the analysis of Raman spectra ($\lambda_{\text{exc}} = 1,064 \text{ nm}$). As seen from fig 4.10 and 4.11, the bands at 438, 700, 991, and 1,256 cm^{-1} are assigned to the C-O-C deformation, symmetric C-S-C deformation, oxyethylene ring deformation, and $C\alpha-C\alpha$ inter-ring stretching, respectively. Especially, the characteristic band at 1,425 cm^{-1} due to symmetric $C\alpha=C\beta$ (-O) stretching is indicative of a high level of conjugation in the structure of PEDOT. The second band between 1400 and 1500 cm^{-1} , which corresponds to the stretching vibration of $C\alpha=C\beta$ on the five-member ring of PEDOT. (Lee *et al.* 2015) have already found that a characteristic band corresponding to the stretching vibration of C=C becomes narrow, which could prove a change of resonance structure of the PEDOT chain from a benzoid to a quinoid (Ouyang *et al.* 2004) and a longer degree of conjugate length.

Shown in fig 4.9 are XRD patterns of polymers. All the polymers show characteristic peak at nearly $2\theta \sim 26^\circ$, which can be attributed to the interchain planar ring stacking. Furthermore, the diffraction peaks with low intensity at $2\theta \sim 13^\circ$ and $2\theta \sim 12.4^\circ$ occur in the case of PEDOT. Generally, the peak at $2\theta \sim 13^\circ$ is known as the distance between two stacks in the two-dimensional stacking arrangement of polymer chains and intervening dopant ions (Zhao *et al.* 2014).



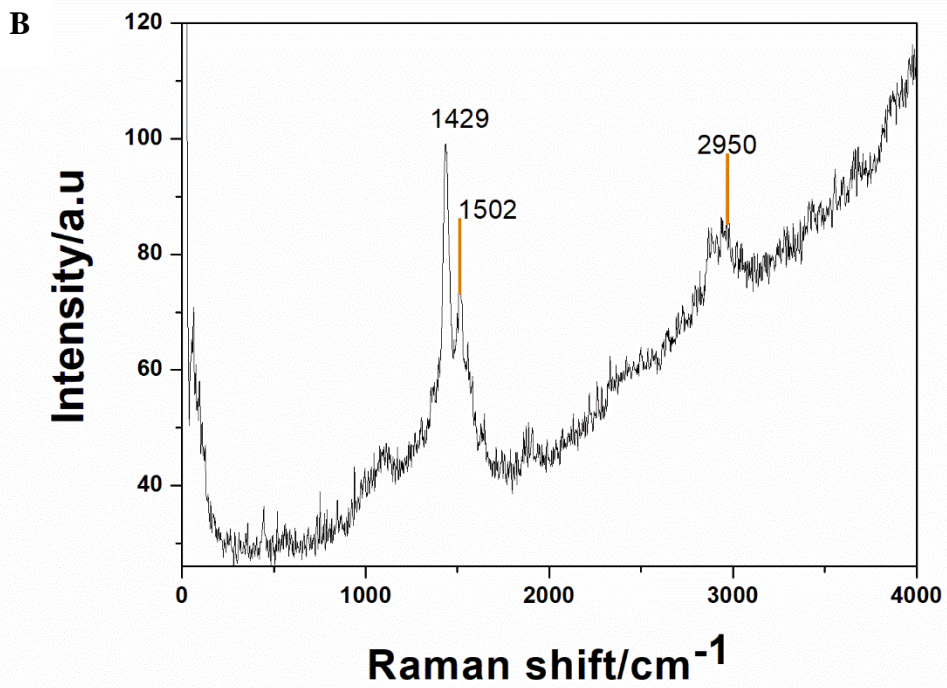
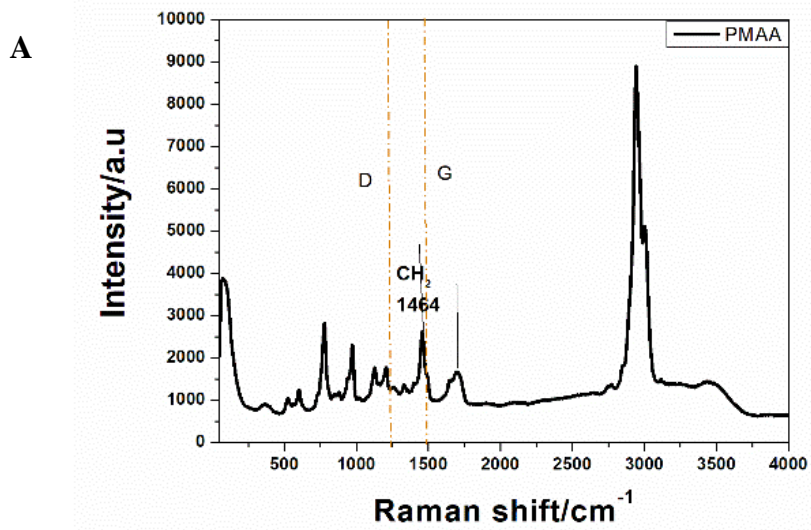


Figure 4. 10: Raman spectra of A) PMAA, B) PEDOT.

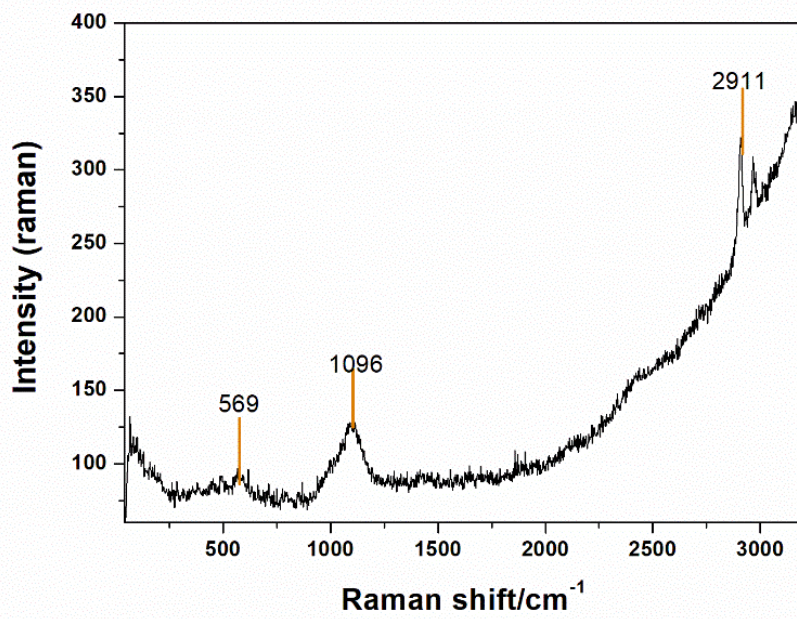


Figure 4. 11: P(MAA-co-EDOT).



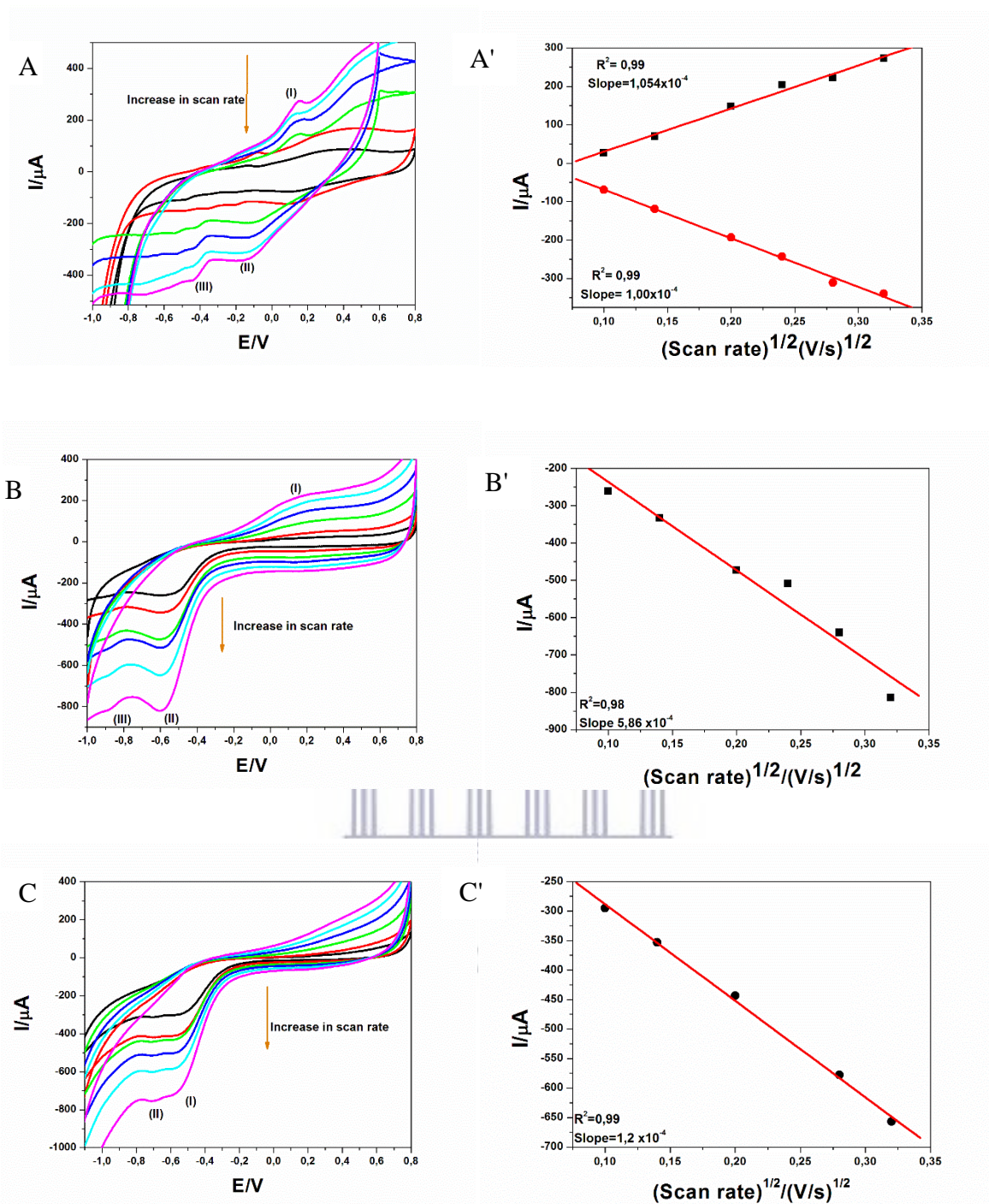


Figure 4. 12: CV of A) PMAA, B) PEDOT, P(MAA-co-PEDOT) in 0.1 M pH 7 phosphate buffer at scan rates (0.01 V/s – 0.1 V/s). (A', B', and C') Randle Sevčik plots of PMAA, PEDOT and P(MAA-co-PEDOT) respectively in 0.1M phosphate buffer at (0.01 V/s – 0.1 V/s) for the determination of the diffusion co-efficient.

Fig 4.12 (A) is a plot of the cyclic voltammograms of PMAA/Au in 0.1 M pH phosphate buffer at the potential window of (-0.1V to 0.8 V). There are three observable peaks in the voltammograms where the anodic peak (I) at +0.15 V mV is due to the oxidation of PMAA while the cathodic peak at -0.15 V (II) is due to the deposited pyrrole onto the electrode surface. The peak at -0.44 V (III) is attributed to. There is a shift of the anodic potential (I) towards more positive potentials with an increase in scan rate from -0.13 V to +0.15 V showing a more readily oxidised species. There is a shift in cathodic potentials towards more negative potentials indicative of more readily reduced species. There is an observable linear increase in the anodic and cathodic peak currents with an increase in scan rate which indicates the occurrence of the electrochemistry of surface confined species. $\Delta E_p [E_{pa} - E_{pc}]$ was calculated for the polymer at different scan rates resulted in a value of ΔE_p greater than 0.065 V. Fig. 4.12 (A') indicates an oxidation reaction that was occurring at E_{pa} which was seen to be diffusion controlled with a correlation coefficient of $R^2 = 0.99$ and a diffusion coefficient of $D_o = 3.55 \times 10^{-5} \text{ cm}^2/\text{s}$; indicating a faster electron transfer kinetics within the diffusion layer. The reduction current peak (E_{pc}) had a correlation coefficient of $R^2 = 0.99$ linearity in the Randle Sevčik plots obvious case was that this reductive reaction that was occurring at that potential was diffusion controlled, and a diffusion coefficient of $3.528 \times 10^{-5} \text{ cm}^2/\text{s}$ indicating a slower electron transfer compared to the anodic electron transfer. Fig. 4.12 (B) Is a plot of the cyclic voltammograms of PEDOT/Au in 0.1 M pH 7 phosphate buffer at the potential window of (-0.1V to 0.8 V). There are three observable peaks in the voltammograms where the anodic peak (I) at +0.2 V is due to the oxidation of the PEDOT, the peak starts to evolve at scan rates 0.06 V/s to 0.1 V, at lower scan rates the peak is not clearly visible. While the cathodic peak at -0.56 V (II) is due to the deposited pyrrole onto the electrode surface. The peak at -0.88 V (III) is attributed to. There is a shift of the anodic potential (I) towards more positive potentials with an increase in scan rate from -0.13 V to +0.15 V showing a more readily oxidised species.

There is a shift in cathodic potentials towards more negative potentials indicative of more readily reduced species. There is an observable linear increase in the anodic and cathodic peak currents with an increase in scan rate which indicates the occurrence of the electrochemistry of surface confined species. $\Delta E_p [E_{pa} - E_{pc}]$ was calculated for the polymer at different scan rates resulted in a value of ΔE_p greater than 0.065 V. Fig. 4.12 (A') indicates an oxidation reaction that was occurring at E_{pa} which was seen to be diffusion controlled with a correlation coefficient of $R^2 = 0.99$ and a diffusion co-efficient of $D_o = 1.243 \times 10^{-5} \text{ cm}^2/\text{s}$; indicating a faster electron transfer kinetics within the diffusion layer. The reduction current peak (E_{pc}) had a correlation coefficient of $R^2 = 0.99$ linearity in the Randle Sevčik plots obvious case was that this reductive reaction that was occurring at that potential was diffusion controlled, and a diffusion co-efficient of $5.528 \times 10^{-5} \text{ cm}^2/\text{s}$ indicating a slower electron transfer compared to the anodic electron transfer. Fig. 4.12 (C) is a plot of the cyclic voltammograms of P(MAA-co-EDOT)/Au in 0.1 M pH 7 phosphate buffer at the potential window of (-0.1V to 0.8 V). There are three observable peaks in the voltammograms where the anodic peak (I) at +0.15 V mV is due to the oxidation of the pyrrole while the cathodic peak at -0.15 V (II) is due to the coated polymer onto the electrode surface. The peak at -0.44 V (III) is attributed to. There is a shift of the anodic potential (I) towards more positive potentials with an increase in scan rate from -0.13 V to +0.15 V showing a more readily oxidised species. There is a shift in cathodic potentials towards more negative potentials indicative of more readily reduced species. There is an observable linear increase in the anodic and cathodic peak currents with an increase in scan rate which indicates the occurrence of the electrochemistry of surface confined species. $\Delta E_p [E_{p,a} - E_{p,c}]$ was calculated for the polymer at different scan rates resulted in a value of ΔE_p greater than 0.065 V. Fig. 4.12 (C') indicates the reduction current peak (E_{pc}) with a correlation coefficient of $R^2 = 0.99$ linearity in the Randle Sevčik plots obvious case was that this reductive reaction that was occurring at that potential was diffusion controlled, and a diffusion co-

efficient of $3.24 \times 10^{-5} \text{ cm}^2/\text{s}$ indicating a slower electron transfer compared to the anodic electron transfer.

Table 4. 3: Electrochemical data of P(MAA), P(EDOT) and P(MAA-co-EDOT)

Polymer	D_o (cm^2/s)	E_{pa} (V)	E_{pc} (V)	E^0 (V)	$\Delta E_p = E_{pa} - E_{pc}$ (V)
PMAA	3.55×10^{-5}	0,14	-0,17	0,015	0,31
PEDOT	$3,7 \times 10^{-5}$	0,16	-0,6	0,22	0,76
P(MAA-co-EDOT)	3.24×10^{-5}	-0,39	-0,57	0,09	0,18

4.3 Conclusion

Over the last decade, conducting polymers have appeared as one of the most promising transducers for chemical sensors. Conducting polymers, such as polythiophene, polyparaphenylene vinylene, polycarbazole, polyaniline and polypyrrole, represent new advanced materials as a key issue for the development of new devices and structures offering the association of the various properties required in advanced applications. Conducting polymers have been considered for important materials in microelectronics applications, electrocatalysis, fuel cell electrodes, light emitting diodes, biosensor microelectrodes, reinforced composites, biomedical applications. In this study a conducting copolymer (P(MAA-co-EDOT)) was prepared chemically. The properties of P(MAA-co-EDOT) were investigated using various techniques. FTIR and Raman were used to determine the structural properties of the copolymer and that of the individual polymers from which it was prepared.

The differences in the surface morphologies and EDS of PMAA, PEDOT and P(MAA-co-EDOT) showed the successful synthesis of the copolymer material. It was found that the prepared P(MAA-co-EDOT) copolymer was conductive by comparing the energy band gaps determined from UV-Vis and from the electrochemical properties. Making it suitable for various applications such as in sensors, batteries and supercapacitors.

4.4 References

Agarwal, R. & Sharma, M.K., 2017. Poly(3,4-ethylenedioxythiophene) poly(styrenesulfonate) modified glassy carbon electrode for electrocatalysis of Pu(IV)/Pu(III) redox couple in 1M H₂SO₄ medium. *Electrochimica Acta*, 224, pp.496–502.

Alvi, F. et al., 2011. Electrochimica Acta Graphene – polyethylenedioxythiophene conducting polymer nanocomposite based supercapacitor. *Electrochimica Acta*, 56(25), pp.9406–9412.

Ateh, D.D., Navsaria, H.A. & Vadgama, P., 2006. Polypyrrole-based conducting polymers and interactions with biological tissues. , (June), pp.741–752.

Ates, M., 2013. A review study of (bio)sensor systems based on conducting polymers. *Materials Science and Engineering C*, 33(4), pp.1853–1859.

Boskovic, D. et al., 2017. Demetallation of electrochemically polymerised Mn porphyrin anion / PEDOT composites under light-illumination. *Synthetic Metals*, 228(April), pp.58–63.

Bougrini, M. et al., 2016. Development of a novel sensitive molecularly imprinted polymer sensor based on electropolymerization of a microporous-metal-organic framework for tetracycline detection in honey. *Food Control*, 59.

Deng, F. et al., 2012. Colloids and Surfaces A : Physicochemical and Engineering Aspects Preparation of conductive polypyrrole / TiO₂ nanocomposite via surface molecular imprinting

technique and its photocatalytic activity under simulated solar light irradiation. *Colloids and Surfaces A: Physicochemical and Engineering Aspects*, 395, pp.183–189.

Du, D. et al., 2010. Acetylcholinesterase biosensor design based on carbon nanotube-encapsulated polypyrrole and polyaniline copolymer for amperometric detection of organophosphates. *Biosensors and Bioelectronics*, 25(11), pp.2503–2508. Available at: <http://dx.doi.org/10.1016/j.bios.2010.04.018>.

Elahi, A. et al., 2015. Effect of loading titanium dioxide on structural, electrical and mechanical properties of polyaniline nanocomposites. *Journal of Alloys and Compounds*, 651, pp.328–332.

Garcimartín, A. et al., 2017. Hydrogen peroxide modifies both activity and isoforms of acetylcholinesterase in human neuroblastoma SH-SY5Y cells. *Redox Biology*, 12(March), pp.719–726.

Hernández, L.A. et al., 2017. Enhanced morphology, crystallinity and conductivity of poly(3,4-ethyldioxythiophene)/ErGO composite films by in situ reduction of TrGO partially reduced on PEDOT modified electrode. *Electrochimica Acta*, 240, pp.155–162.

Hu, Y. et al., 2017. Free-standing oligo(oxyethylene)-functionalized polythiophene with the 3,4-ethylenedioxythiophene building block: electrosynthesis, electrochromic and thermoelectric properties. *Electrochimica Acta*, 228, pp.361–370.

Huynh, T.P. et al., 2015. Functionalized polythiophenes: Recognition materials for chemosensors and biosensors of superior sensitivity, selectivity, and detectability. *Progress in Polymer Science*, 47.

Janáky, C. & Visy, C., 2013. Conducting polymer-based hybrid assemblies for electrochemical sensing: A materials science perspective. *Analytical and Bioanalytical Chemistry*, 405(11).

Krivorotova, T., Radzevicius, P. & Makuska, R., 2015. Synthesis and characterization of anionic pentablock brush copolymers bearing poly(acrylic acid) side chains on the brush blocks separated by linear poly(butyl methacrylate) blocks. *European Polymer Journal*, 66, pp.543–557.

Kumar, G. et al., 2011. Synthesis, characterization of poly (4-benzyloxyphenylmethacrylate) and its copolymer with butyl methacrylate and determination of monomer reactivity ratios. *Journal of Polymer Research*, 18(2), pp.241–250.

Leeuw, D.M. De et al., 1997. Stability of n-type doped conducting polymers and consequences for polymeric microelectronic devices. , 87, pp.53–59.

Li, Y., 2015a. Conducting Polymers.

Li, Y., 2015b. Organic Optoelectronic Materials. , pp.27–33.

Linko, K. et al., 1999. ELECTRONIC STRUCTURE OF CONJUGATED POLYMERS : CONSEQUENCES OF ELECTRON } LATTICE COUPLING Electronic structure of conjugated polymers : consequences of electron } lattice coupling. , 319, pp.231–251.

Lu, B. et al., 2014. Electropolymerization of 3 , 4-Ethylenedithiathophene in the Green Binary Solvent System of Water and Ethanol. , 9, pp.4535–4547.

Malhotra, B.D., Chaubey, A. & Singh, S.P., 2006. Prospects of conducting polymers in biosensors. *Analytica Chimica Acta*, 578(1), pp.59–74.

McCullough, R.D., 1998. The Chemistry of Conducting Polythiophenes. *Advanced Materials*, 10(2), pp.93–116.

Minhas, M.U. et al., 2013. Synthesis of chemically cross-linked polyvinyl alcohol-co-poly (methacrylic acid) hydrogels by copolymerization; a potential graft-polymeric carrier for oral

delivery of 5-fluorouracil. *Daru : journal of Faculty of Pharmacy, Tehran University of Medical Sciences*, 21(1), p.44.

Molapo, K.M. et al., 2012. Electronics of Conjugated Polymers (I): Polyaniline. , 7, pp.11859–11875.

Neagu, E. et al., 2015. Antioxidant activity, acetylcholinesterase and tyrosinase inhibitory potential of *Pulmonaria officinalis* and *Centarium umbellatum* extracts. *Saudi Journal of Biological Sciences*.

Nie, T. et al., 2014. Synthesis and characterization of benzenesulfonate derivatives doped poly(3,4-ethylenedioxythiophene) films and their application in electrocatalysis. *Synthetic Metals*, 189, pp.161–172.

Nikovia, C. et al., 2015. Statistical ring opening metathesis copolymerization of norbornene and cyclopentene by grubbs' 1st-generation catalyst. *Molecules*, 20(9), pp.15597–15615.

Nobile, D. et al., 2014. Improved selective cholesterol adsorption by molecularly imprinted poly (methacrylic acid)/ silica (PMAA – SiO₂) hybrid material synthesized with different molar ratios. *Materials Science & Engineering C*, 44, pp.99–108.

Odian, G., 2004. *Chain copolymerization*,

Ouyang, J. et al., 2004. On the mechanism of conductivity enhancement in poly(3,4-ethylenedioxythiophene):poly(styrene sulfonate) film through solvent treatment. *Polymer*, 45(25), pp.8443–8450.

Pardieu, E. et al., 2009. Analytica Chimica Acta Molecularly imprinted conducting polymer based electrochemical sensor for detection of atrazine. , 649, pp.236–245.

Pei, L., Tang, Y. & Gao, H., 2016. Homo- and copolymerization of ethylene and norbornene with anilido-imine chromium catalysts. *Polymers*, 8(3), pp.1–10.

Pinto, C. et al., 2014. Selectivity of natural, synthetic and environmental estrogens for zebrafish estrogen receptors. *Toxicology and Applied Pharmacology*, 280(1), pp.60–69.

Seo, H., Kim, K. & Yi, C.-W., 2015. Physico-Chemical and Electrochemical Properties of Si-Ti-Ni Alloy Modified with poly(3,4-ethylenedioxythiophene). *Electrochimica Acta*, 165, pp.247–254.

Shanmugham, C. & Rajendran, N., 2015. Corrosion resistance of poly p-phenylenediamine conducting polymer coated 316L SS bipolar plates for Proton Exchange Membrane Fuel Cells. *Progress in Organic Coatings*, 89, pp.42–49.

Shirakawa, H., 2001. The discovery of polyacetylene film - The dawning of an era of conducting polymers. *Current Applied Physics*, 1(4–5), pp.281–286.

Thakur, V.K. & Thakur, M.K., 2014. Recent advances in graft copolymerization and applications of chitosan: A review. *ACS Sustainable Chemistry and Engineering*, 2(12), pp.2637–2652.

Toshima, N. & Hara, S., 1995. Contents 1. , 20(94), pp.155–183.

Tovide, O. et al., 2014. Electro-oxidation of anthracene on polyanilino-graphene composite electrode. *Sensors and Actuators, B: Chemical*, 205, pp.184–192.

Wang, K. et al., 2010. Synthesis and characterization of poly(methoxyl ethylene glycol-caprolactone-co-methacrylic acid-co-poly(ethylene glycol) methyl ether methacrylate) pH-sensitive hydrogel for delivery of dexamethasone. *International Journal of Pharmaceutics*, 389(1–2), pp.130–138.

Wei, L. et al., 2016. Poly (acrylic acid sodium) grafted carboxymethyl cellulose as a high performance polymer binder for silicon anode in lithium ion batteries. *Scientific reports*, 6(January), p.19583.

Wong, W.Y. & Ho, C.L., 2006. Di-, oligo- and polymetallaynes: Syntheses, photophysics, structures and applications. *Coordination Chemistry Reviews*, 250(19–20), pp.2627–2690.

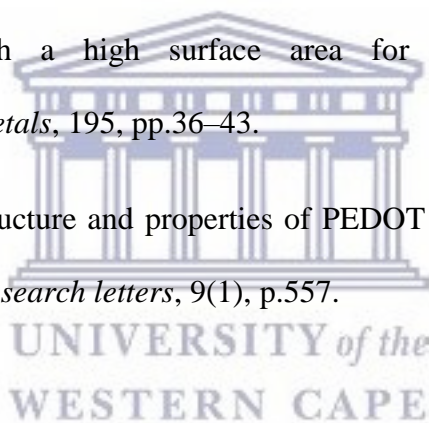
Xia, L., Wei, Z. & Wan, M., 2010. Journal of Colloid and Interface Science Conducting polymer nanostructures and their application in biosensors. , 341, pp.1–11.

Ye, M. et al., 2006. Synthesis, preparation, and conformation of stimulus-responsive end-grafted poly(methacrylic acid-g-ethylene glycol) layers. *Soft Matter*, 2(3), p.243.

Zanardi, C., Terzi, F. & Seeber, R., 2013. Polythiophenes and polythiophene-based composites in amperometric sensing. *Analytical and Bioanalytical Chemistry*, 405(2–3).

Zhang, K. et al., 2014. Nanostructured graphene oxide–MWCNTs incorporated poly(3,4-ethylenedioxythiophene) with a high surface area for sensitive determination of diethylstilbestrol. *Synthetic Metals*, 195, pp.36–43.

Zhao, Q. et al., 2014. The structure and properties of PEDOT synthesized by template-free solution method. *Nanoscale research letters*, 9(1), p.557.



CHAPTER FIVE



Development of a Poly(methacrylic acid)-co-Poly(3,4-ethylenedioxythiophene) molecularly imprinted polymer sensor for the electrochemical detection of 17 β -estradiol-An estrogenic endocrine disrupting compound

Summary

The presence of estrogenic endocrine disrupting compounds in water bodies poses a threat to both the environment and humans. Over the years concern over the presence of endocrine disrupting compounds in the environment has seen a tremendous increase. There are several natural and man-made chemical compounds, they possess the ability to evoke estrogen-like responses. There have been reports of exposure to these endocrine disruptors. The lack of reliable detection methods means that most of exposure to these chemicals will go unnoticed. In this chapter the background on the endocrine system, its disruption and the chemicals that have the effect on the system focusing mainly on estrogenic endocrine disrupting compounds specifically 17- β estradiol. Also a brief description of the detection method used for the detection of 17- β estradiol.



Development of a Poly(methacrylic acid)-co-Poly(3,4-ethylenedioxythiophene) molecularly imprinted polymer sensor for the electrochemical detection of 17 β -estradiol-An estrogenic endocrine disrupting compound

Abstract

The interference of the endocrine system by endocrine disrupting compounds (EDCs) in the daily functions of the endocrine system poses a threat to the proper functions of the processes that are essential for development, reproduction and the immune system in both humans and wildlife. This study reports for the first time the development and characterization of a molecularly imprinted polymer (MIP) sensor based on the copolymer poly (Methacrylic acid)-co-poly (3,4-ethylenedioxythiophene) and 17 β -estradiol an estrogenic endocrine disrupting compound (eEDC) as the template molecule. The sensor was prepared by chemical polymerization of methacrylic and 3,4-ethylenedioxythiophene monomers in the presence of 17 β -estradiol. The removal of the template molecule from the copolymer matrix resulted in the MIP sensor denoted PMAA-co-PEDOT/Au. The structural properties of the MIP were determined by fourier transform infrared spectroscopy (FTIR) which showed the decrease in the intensity of the C-O-H functionality that occurs by the hydrogen bonding between the copolymer and 17 β -estradiol. The high resolution scanning electron microscopy (HRSEM) images of the MIP showed the presence of cavities on its surface which are attributed by the removal of the template from the polymer matrix. The electrochemical behaviour of the MIP sensor was investigated using differential pulse voltammetry (DPV) by comparing the current response between the MIP in the presence of the target analyte, MIP (after removal of nalyte) and MIP after the rebinding of target analyte, where the MIP gave the highest response and rebinding of analyte caused a decrease in current. DPV was employed as the electrochemical

detection technique. The MIP sensor showed a limit of detection (LOD) of 0.006 nM, a dynamic linear range (DLR) of 0.001-0.01 nM and sensitivity of $1,25 \times 10^{-7} \mu\text{A/nM}$ with a good selectivity for 17 β -estradiol detection.

5.0 Introduction

Since the late 1990s the awareness and concern of endocrine disrupting compounds (EDCs) increased. EDCs can be defined as those chemicals or compounds that interfere with the endocrine system (Iwanowicz & Blazer 2009). The endocrine system is one of the body's main communication networks and is responsible for controlling and coordinating numerous body functions (Ohno *et al.* 2002). Hormones are first produced by the endocrine tissues followed by their secretion into the blood to act as the body's chemical messengers where they direct communication and coordination among other tissues throughout the body (Terui *et al.* 2006). The human endocrine system includes the pancreas, pituitary, thyroid, adrenal, and male and female reproductive glands. Endocrine disruptors interfere with the production, release, transport, metabolism, or elimination of the body's natural hormones (Jo *et al.* 2011). This in turn results in the interference on the development, reproduction, neurological and immune system of both human and the wildlife. eEDCs have the ability to mimic naturally occurring hormones, potentially causing overproduction or underproduction of hormones (Florea, Cristea, Vocanson, Săndulescu, et al. 2015). They may also interfere or block the way natural hormones and their receptors are made or controlled through binding with receptors within cells. A number of substances both manmade and natural can be endocrine disrupting (Yildirim *et al.* 2012). These substances include pharmaceuticals, dioxin and dioxin-like compounds, polychlorinated biphenyls (Pinson *et al.* 2017; Singh & Chan 2017), dichlorodiphenyltrichloroethane (DDT) (El-Hefnawy et al. 2017) and other pesticides, phytoestrogens and fungal estrogens and plasticizers (Tahboub *et al.* 2017) such as bisphenol A (BPA) (Esther *et al.* 2014). EDs can be found in products that are frequently used in

households which include plastic bottles (Garfí *et al.* 2016), food cans (Wang *et al.* 2014; Afzal *et al.* 2014), detergents (Gutendorf & Westendorf 2001), pesticides (Migheli 2017; Oliva *et al.* 2017; Lizano-Fallas *et al.* 2017; Corral *et al.* 2017) and cosmetics (Dodson *et al.* 2012; Bronowicka-Kłys *et al.* 2016; Wong & Durrani 2017; Figueiredo *et al.* 2015). There are various exposure routes to EDCs, including food and water ingestion food, through gas and particle inhalation in air, and through skin penetration. Foetus and children can be affected by EDCs through mother to child transfer, occurring during pregnancy or via the placenta or after birth through breast milk. Pregnant mothers and children are the most susceptible to be affected by developmental exposures, and the effect EDCs may have may only become evident at later stages (Kim *et al.* 2007). Research also shows that it may increase the susceptibility to non-communicable diseases. Estrogenic EDCs are compounds that are able to induce estrogen-like responses in organisms. They may vary in structure and come from different sources that have estrogenic and/or anti-estrogenic activities, although they may also affect other endocrine systems (Rgens *et al.* 2002). This category of chemicals includes both natural and synthetic estrogens (e.g., xenoestrogens and pseudoestrogens). Specific examples of e-EDCs include natural hormones and pharmaceutical estrogens (e.g., E2, EE2 and phytoestrogens including isoflavonoides and coumestrol), surfactants (e.g., alkyphenol-ethoxalates), pesticides (e.g., atrazine, dieldrin, and toxaphene), industrial chemicals (e.g., bisphenol A), and heavy metals (e.g., cadmium, nickel, lead) (Roszko *et al.* 2015). These e-EDCs are environmentally significant as many of these have the potential to cause an estrogenic response at very low concentrations (parts per billion to parts per trillion). Sources of estrogenic EDCs include natural estrogens produced by plants (phytoestrogens), fungi (mycoestrogens) and cyanobacteria, synthetic therapeutic drugs (e.g., raloxifene) and numerous synthetic compounds mainly used in industry and agriculture (e.g., polychlorinated biphenyls (PCBs), organochlorine pesticides, phthalate plasticizers or dioxins) (P. I. S. Pinto *et al.* 2014). Estrogen

is one of the two steroids responsible for the regulation of female reproductive functions including sexual behaviour, pregnancy and lactation (Janegitz *et al.* 2014). In males it is present though in minute amounts. This hormone acts primarily by regulating transcription of specific hormone responsive target genes (DeMayo, F.J. *et al.* 2002). The most common EDC determination methods include HPLC, fluorimetry (Uygun *et al.* n.d.), NMR spectroscopy (Kim *et al.* 2009), chromatography (Socas-Rodríguez *et al.* 2017), enzyme linked receptor assay, and linear sweep voltammetry (Li *et al.* 2016).

The technology of MIPs is becoming one of the interesting and important analytical tools. It provides a possibility for a tailor –made highly selective artificial receptor at low costs with improved mechanical, thermal and chemical properties making them ideal chemoreceptors (Tun 2004). MIPs are defined as synthetic polymer material with high affinity and selectivity towards a predefined target molecule (Rachkov *et al.* 2000). They were developed based on the lock and key fit principle (Panagiotopoulou *et al.* 2015). The principle can be observed on many biological processes including signalling between nerve and muscle cells and enzyme/substrate recognition. In MIPs there is creation of polymeric matrices containing cavities which are complimentary in size, shape and chemical interactions with the target molecule which acts as the “key” (Koç *et al.* 2011). The imprinting technology involves the chemical or electrochemical polymerization of functional monomers in the presence of a target/template molecule (Öpik 2009). Following polymerization removal of the target analyte from the polymeric matrix takes place creating some cavities which are the recognition sites. This technique presents some advantages such as low costs from preparation, long term stability, robustness and high affinity to the template (Kor & Zarei 2016). In this study a novel electrochemical sensor based on poly (methacrylic acid) (PMAA)-co-poly(3,4-ethylenedioxythiophene) (PEDOT) film on gold electrodes, for the selective detection of 17β-estradiol is proposed.

5.1 Experimental

5.1.1 Chemicals

3,4-ethylenedioxythiophene (EDOT) ($\geq 97\%$) and methacrylic acid (MAA) ($\geq 99\%$) monomers, polyvinyl chloride (PVC), tetrahydrofuran (THF), 17β -estradiol (E2) ($\geq 98\%$), 17α -ethynylestradiol (EE2) ($\geq 98\%$), Estrone ($\geq 99\%$), Estriol ($\geq 97\%$), 17α -estradiol ($\geq 98\%$), potassium hexacyanoferrate (III) ($K_3[Fe(CN)_6]$) (ACS reagent, $\geq 99.0\%$), potassium hexacyanoferrate(II) trihydrate ($K_4[Fe(CN)_6]$) (ACS reagent 98.5-102.0%), acetic acid (CH_3COOH), sulfuric acid (H_2SO_4), hydrogen peroxide (H_2O_2) methanol (CH_3OH) and acetonitrile (C_2H_3N) were purchased from Sigma-Aldrich. Disodium hydrogen phosphate (Na_2HPO_4) ($\geq 99.5\%$), sodium dihydrogen phosphate (NaH_2PO_4) ($\geq 99\%$) from Sigma-Aldrich were used for the preparation of 0.1 M phosphate buffer pH 7. Ammonium persulfate (APS) ($\geq 98\%$) was purchased from BIO-RAD laboratories. Alumina micro polishing pads were obtained from Buehler LL, USA. Deionized ultra-purified water used throughout these experiments was prepared with a Milli-Q water purification system.

5.1.2 Instrumentation and procedure

A three electrode configuration was used for all electrochemical experiments. A gold electrode with a surface area of 0.0201 cm^2 from Bio Analytical Systems (BAS) was used as the working electrode. A saturated calomel electrode (SCE) as the reference electrode from BAS, and a platinum wire as the counter electrode. All the measurements were carried out at room temperature. All electrochemical measurements were performed on a computer-controlled potentiostat/galvanostat (CH instruments electrochemical workstation) coupled with Model

270/250 Research Electrochemistry Software 4.30. Alumina micro polishing pads were obtained from BAS and used to polish the surface of the gold working electrode before modification. HRSEM images were taken with a Hitachi S3000N scanning electron microscope at an acceleration voltage of 20 kV at various magnifications. All FTIR spectra were recorded on Spectrum 100 FTIR spectrometer (PerkinElmer, USA) at a region of 400-4000 cm^{-1} .

5.1.3 Cleaning of electrodes

Prior to the electrodes being used, they were polished on 1 μm and 0.05 μm alumina slurries and sonicated in Milli Q water for 10 min to remove any adsorbed material on the surface of the electrode. A very mild version of a piranha clean was prepared from 50 mM H_2SO_4 and 25% hydrogen peroxide. Gold samples spent 10 min in this treatment before being rinsed with Milli-Q. Lastly the electrodes were cleaned by cycling the electrode potential in a weak sulfuric acid solution 0.5 M until a stable CV scan was achieved. Sample potential was cycled from -400 to 1400 mV (vs. Ag/AgCl) at a rate of 100 mV/s in 50 mM sulfuric acid until a stable CV was achieved (approximately 12 cycles).

5.1.4 Preparation of NIP and MIP electrodes

1.6 mL MAA, 1.6 mL of EDOT and 100 mL ammonium persulfate (APS) solution were added in a 250 mL round bottom flask under stirring. An estradiol solution was prepared by dissolving 17 β -estradiol (0.27 g) in acetonitrile and was added to the stirred mixture. The pre-solution was purged with nitrogen for 15 min to drive out oxygen, and then was sealed rapidly. Afterwards, the reaction flask was put in a pre-heated oil bath at 60 $^{\circ}\text{C}$ for polymerization for 24 h under moderate stirring. A black precipitate was formed and collected using vacuum filtration,

washed with methanol and dried in a vacuum oven for 24 h. The obtained precipitate was mixed with poly vinyl chloride (PVC) and dissolved in tetrahydrofuran (THF). 20 μL of the solution was then drop-coated onto the surface of a gold working electrode and dried for 24 h. For estradiol removal the electrode was immersed in a container filled with a methanol/acetic acid (9:1 v/v) mixture under stirring for 3 h. NIP was prepared using the same procedure but in the absence of estradiol.

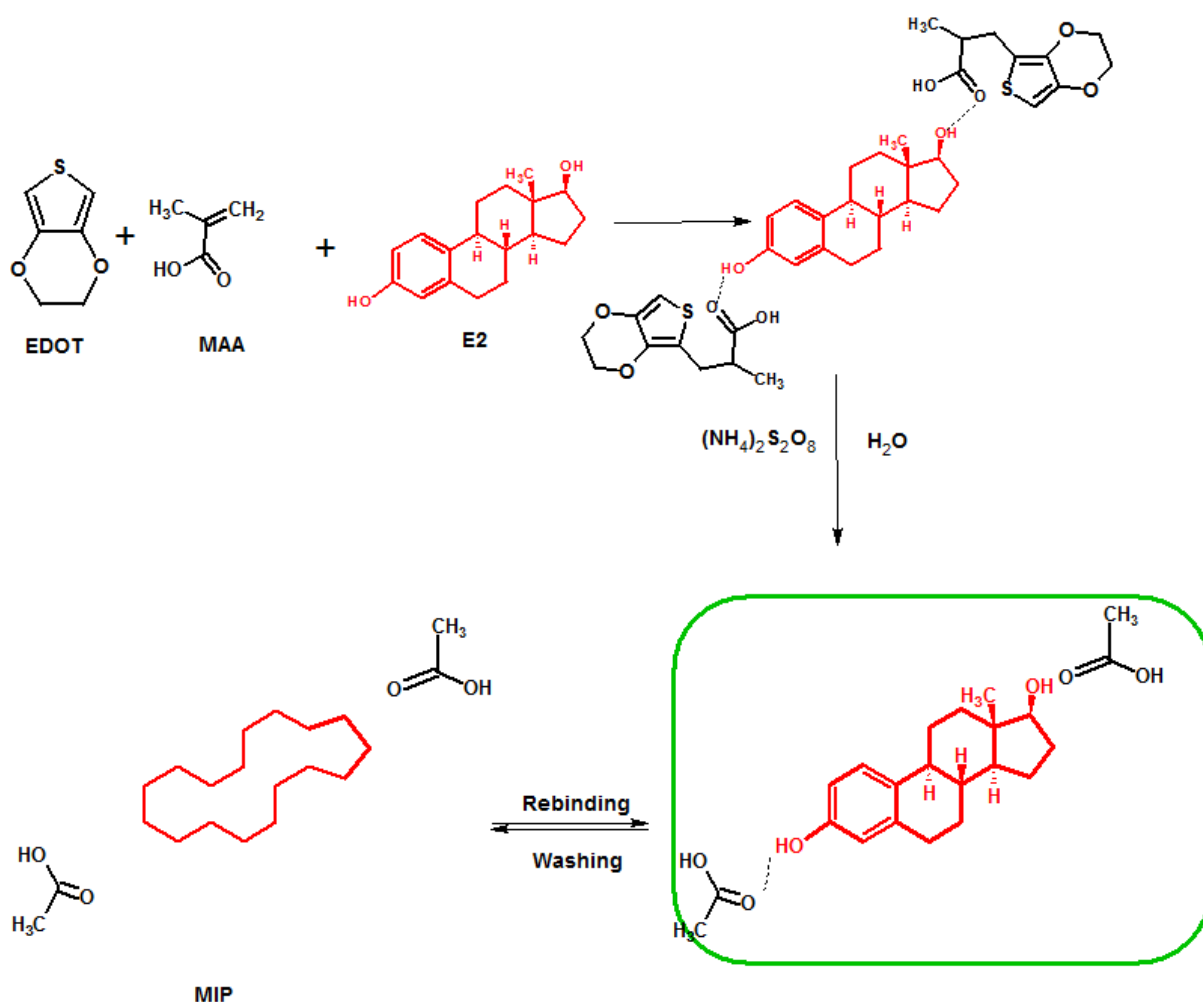


Figure 5. 1: Preparation of molecularly imprinted polymer sensor.

Illustrated in fig 5.1 is the preparation of molecularly imprinted polymer sensor from the reaction of MA and EDOT monomers with 17β -estradiol the analyte of interest in the presence of an oxidising agent ammonium persulfate. The analyte of interest E2 bonds to the PMAA moiety of the copolymer by hydrogen bond through the H from the OH group of E2 and O from the carbonyl group of PMAA. E2 is removed from the copolymer by 3 consecutive washes with a mixture of Acetic acid/methanol (90:10 v/v). Washing of E2 results in the formation of a cavity that is of similar structure to E2, this in turn results in the formation of a MIP which is used for the detection of the imprinted E2 analyte.

5.2 Results and discussion

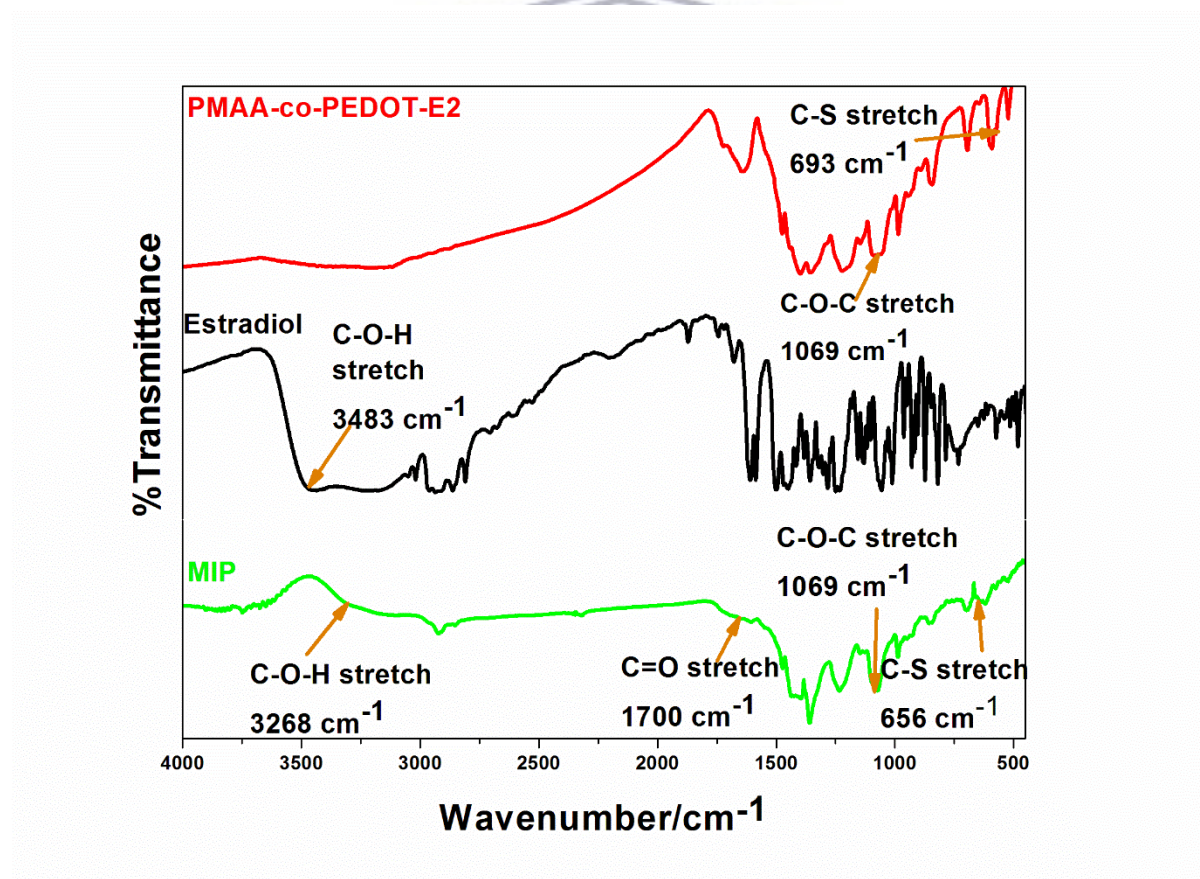


Figure 5. 2: FTIR spectra of (a) P(MAA-co-EDOT)-E2 (Red line), (b) 17β Estradiol (Black line) and (c) MIP (Green line).

The FTIR spectra shown in (**red line, Fig 5.2**) was attributed to the successful binding of E2 on to the PMAA-co-PEDOT copolymer, this is confirmed by disappearance of the C-O-H broad band stretch which is normally found at approximately 3163 cm^{-1} indicating the formation of a hydrogen bond between the OH group of E2 and the carboxyl group of PMAA. The absorption band at 1069 cm^{-1} is attributed to C-O-C band of the ethylenedioxy ring of PEDOT. While the band at 693 cm^{-1} is associated with C-S from the thiophene ring of PEDOT (Alvi, F. *et al.*, 2011). The broad band at 3483 cm^{-1} observed in (**black line Fig 5.2**) is due to the C-OH stretch of the estradiol molecule. A decrease and shift in C-O-H stretch from 3483 cm^{-1} to 3268 cm^{-1} is observed in (**green line, Fig 5.2**), this phenomenon can be attributed to the effect of the removal of the analyte molecule (E2) from the PMAA-co-PEDOT copolymer resulting in formation of cavities with structures that are similar in shape and size of the imprinted molecule.

Depicted in fig 5.3 (A) and (B) are the SEM micrographs of NIP and MIP material respectively prepared with EDOT and MAA at the same magnification levels. The images highlight the extraordinary differences in the morphology of the imprinted material MIP and its non-imprinted counter-part NIP. While the non-imprinted polymer had a completely inhomogeneous rigid structure, the imprinted polymer is porous, thus indicating that there is presence of recognition sites in MIP which could be ascribed to the removal of template molecules.

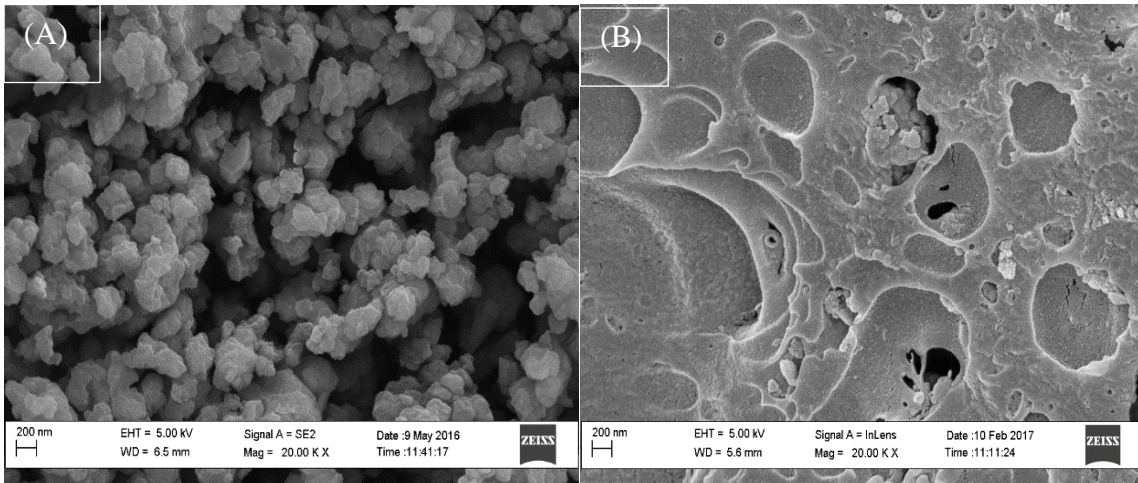


Figure 5. 3: HRSEM images of A) NIP and B) MIP.



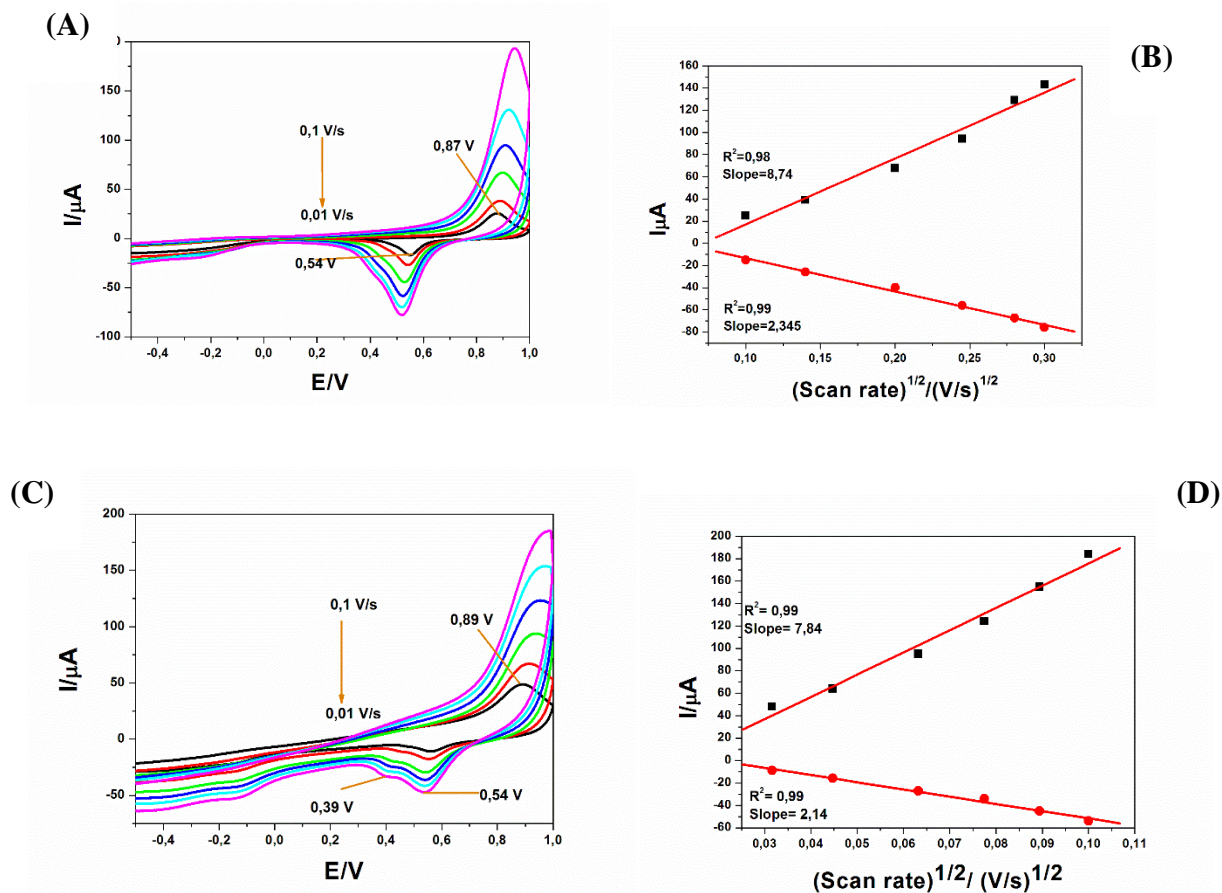


Figure 5. 4: (A) and (C) Cyclic voltammograms of NIP/Au and MIP/Au electrodes respectively (0.01 V/s – 0.1 V/s) and (B) and (D) Randle Sevčik plots of NIP/Au and MIP/Au respectively in 0.1 M phosphate buffer at (0.01 V/s – 0.1 V/s) for the determination of the diffusion co-efficient.

Fig 5.4 (A) is a plot of the cyclic voltammograms of P(MAA-co-EDOT)/Au in 0.1 M pH 7.4 phosphate buffer at the potential window of (-0.4 V to 1 V). There are two peaks that are observable in the voltammograms where the anodic peak at 0.87 V is due to the oxidation of the pyrrole while the cathodic peak at 0.54 V is due to the deposited pyrrole onto the electrode surface. There is a shift of the cathodic potential towards more negative potentials with an increase in scan rate from 0.54 V to 0.45 V showing a more readily reduced species. There is

an observable linear increase in the anodic peak current with an increase in scan rate which indicates the occurrence of the electrochemistry of surface confined species. There is no shift in the anodic peak current indicative of a surface bound species. $\Delta E_p = [E_{pa} - E_{pc}]$ was calculated for the polymer film grown at different scan rates resulted in a value of ΔE_p greater than 65 mV. Fig 5.4 (B) indicates an oxidation reaction that was occurring at E_{pa} which was seen to be diffusion controlled with a correlation co-efficient of $R^2 = 0.98$ and a diffusion co-efficient of $D_o = 1.52 \times 10^{-5} \text{ cm}^2/\text{s}$; indicating a faster electron transfer kinetics within the diffusion layer. The reduction current peak (E_{pc}) had a correlation coefficient of $R^2 = 0.99$ linearity in the Randle Sevčik plots obvious case was that this reductive reaction that was occurring at that potential was diffusion controlled, and a diffusion co-efficient of $3.528 \times 10^{-5} \text{ cm}^2/\text{s}$ indicating a slower electron transfer compared to the anodic electron transfer.

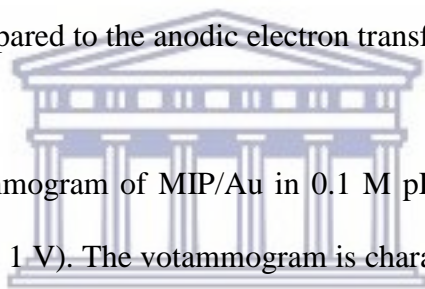


Fig 5.4 (C) is a cyclic voltammogram of MIP/Au in 0.1 M pH 7.4 phosphate buffer at the potential window of (-0.4 V to 1 V). The voltammogram is characterized by the appearance of three peaks where the anodic peak at 0.87 V present in NIP has shifted due to the introduction of 17 β -estradiol into the NIP system while the peak at 0.54 V remains unchanged. In comparison to the NIP voltammogram there is an additional cathodic peak at 0.39 V in the MIP voltammogram which can be attributed to be due to the presence of a certain amount of 17 β -estradiol after its removal from the polymer matrix. There is a shift of the cathodic potential towards more negative potentials with an increase in scan rate showing a more readily reduced species. There is an observable linear increase in the anodic peak current with an increase in scan rate which indicates the occurrence of the electrochemistry of surface confined species. Fig 5.4 (D) indicates an oxidation reaction that was occurring at E_{pa} which was seen to be diffusion controlled with a correlation co-efficient of $R^2 = 0.99$ and a diffusion co-efficient of $D_o = 1.98 \times 10^{-5} \text{ cm}^2/\text{s}$; indicating a faster electron transfer kinetics within the diffusion layer.

The reduction current peak (E_{pc}) had a correlation coefficient of $R^2 = 0.99$ linearity in the Rendle Sevčik plots obvious case was that this reductive reaction that was occurring at that potential was diffusion controlled, and a diffusion co-efficient of $5.528 \times 10^{-5} \text{ cm}^2/\text{s}$ indicating a slower electron transfer compared to the anodic electron transfer.

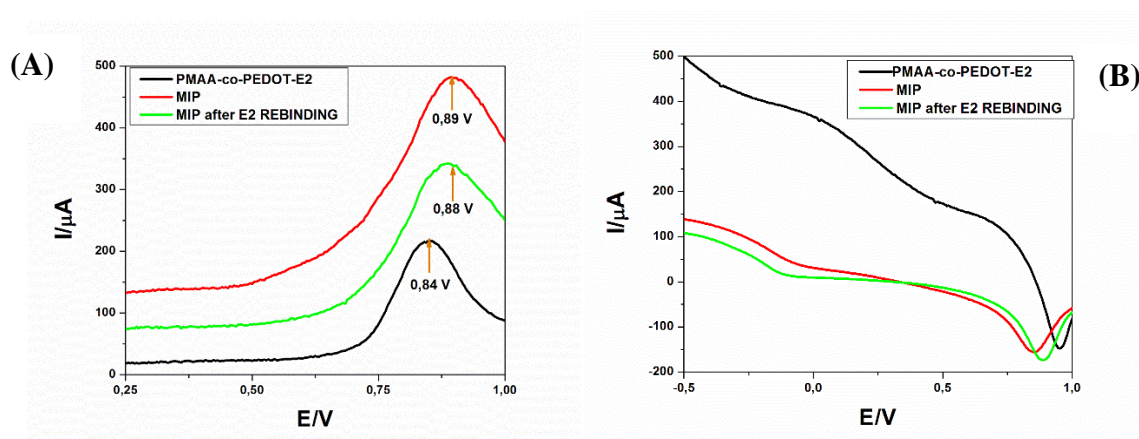


Figure 5. 5: (A) DPV and (B) SWV of P(MAA-co-PEDOT)-E2 (black line), MIP (red line) and MIP after detection of E2 at a concentration of 0.01 nM at a potential of 0.25-1 V.

Fig 5.5 (A) and (B) show the DPV and SWV respectively of PMAA-co-PEDOT-E2 (black line) representing the copolymer with 17β -estradiol incorporated into it, MIP (red line) copolymer after removal of 17β -estradiol and MIP after detection of E2 at a concentration of 0.01 nM at a potential of 0.25-1 V. The behaviour of the modified electrodes was studied using DPV for the detection of E2 analyte. It was the technique of interest as opposed to other electrochemical techniques due to the fact that it has the ability to clearly show the peaks of interest. There is an observed decrease in the current produced when the MIP electrode was immersed into a cell containing 0.01 nM of E2. This indicates that E2 was able to rebind to the copolymer.

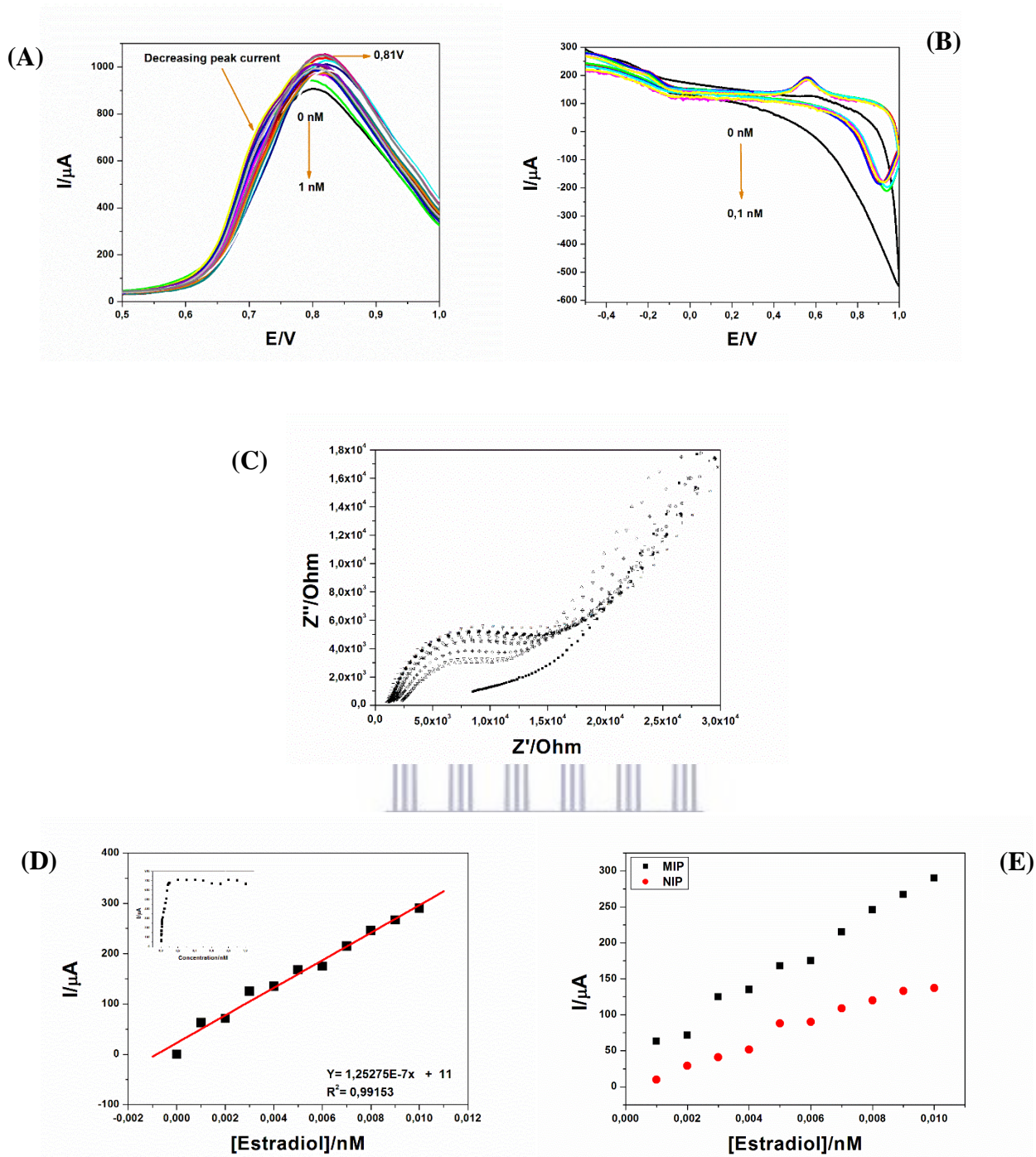
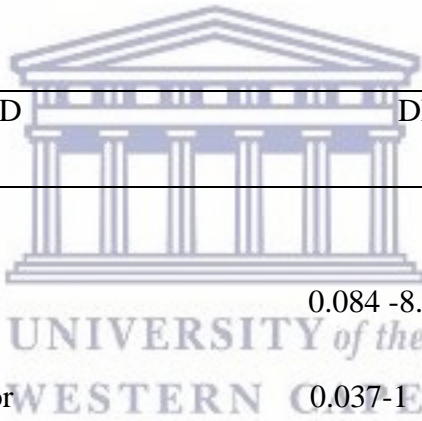


Figure 5. 6: (A) DPV and (B) CV from 0.5-1 V (C) Nyquist plots for the Faradaic impedance measurements in the presence of 5.0 mM $[\text{Fe}(\text{CN})_6]^{3-/4-}$ for the detection of 17β-estradiol from 0 nM-1 nM (D) Calibration curve and linear range of the calibration for the detection of 17β-estradiol using MIP (0-0.01 nM) (E) linear range of the non-imprinted polymer (NIP) (red line) and MIP (black line) sensors.

A MIP electrode was prepared and used for the detection of E2 using DPV as the detection method, DPV was used as the detection method of choice compared to other electrochemical techniques such as CV because it showed more sensitivity and generated a more noticeable change in current response to changes in concentration. The prepared MIP electrode was immersed in a phosphate buffer solution containing different concentrations of the analyte. Fig 5.6 (A) and (B) depicts the DPV and CV response in 0.1 M phosphate buffer solution, pH 7. DPV was scanned from 0.5-1 V. At 0 nM of analyte there is a peak at 0.81 V. With each successive addition of E2 there was a decrease in peak current resulting from the occupation of the E2 imprinted cavities by the E2 molecule. There is a shift in potential towards the negative potentials which can be attributed to a fast electron transfer. The linear range and limit of detection of the P(MAA-co-PEDOT) MIP sensor towards 17β estradiol was determined by the construction of a calibration curve fig 5.6 (D), representing the analytical signal expressed as current against concentration of 17β -estradiol. The calibration curve was derived from the DPV current response with successive additions of various concentrations of the analyte. The relationship between concentration and current is linear with an R^2 value of 0.99, LOD was determined to be 0.006 nM, DLR of 0.001-0.01 nM and sensitivity of $1, 25 \times 10^{-7} \mu\text{A/nM}$. Fig 5.6 (C) depicts the EIS response of the P(MAA-co-EDOT) MIP in sensing 17β -estradiol. The MIP film was exposed to varying concentrations of 17β -estradiol, i.e from 0-0.01 nM. From the Nyquist plots fig 5.6 (C) it can be observed that there is a linear decrease in the semi-circle radii with an increase in concentration of the analyte. This observation can be derived from the assumption that the template molecules were able to penetrate and bind with the cavities present within the imprinted polymer network. The efficient binding of the template molecules in the cavities caused the decrease in electrochemical response which results from the impediment in the flow of the electrons. The imprinted molecule is assumed to block the

surface of the electrode which is dependent on the concentration of 17 β -estradiol. To investigate the affinity of the MIPs electrode and NIPs electrode to 17 β -estradiol measurement of MIPs and NIPs electrodes were carried out. Under the optimized conditions, the determination of 17 β -estradiol at different concentrations was performed. The results of the detection were shown in fig 5.6 (E) showing that there is a strong affinity to 17 β -estradiol when using the MIP sensor than the NIP sensor which is shown by the low current response in the NIP curve.

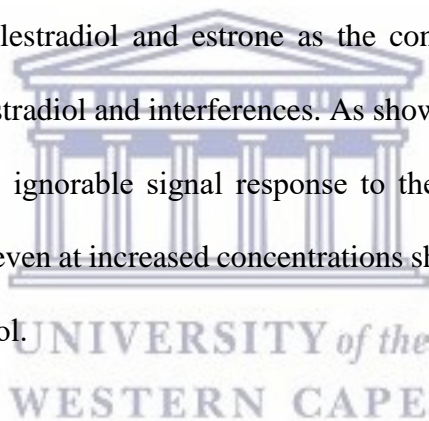
Table 5.1: Comparison of the MIP with other sensors

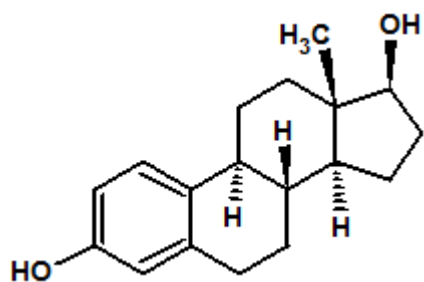


REFERENCES	METHOD	DLR (nM)	LOD (nM)
(Gadzała-kopciuch 2016)	HPLC	0.084 -8.4	0.21
(Li <i>et al.</i> 2016)	Biosensor	0.037-1E	0.037
(Rao <i>et al.</i> 2013)	GC-MS	0.057- 0.059	0.025
(Ben <i>et al.</i> 2017)	Immunosensor	0.027- 0.9	0.01
(Le Noir <i>et al.</i> 2007)	MIP	0.1-0.6	0.009
This study	MIP	0.001- 0.01	0.006

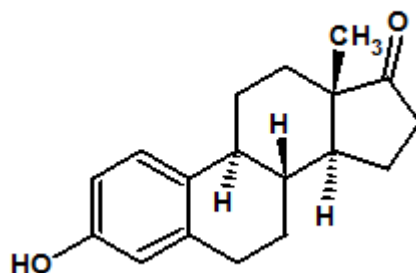
5.2.1 Selectivity and reproducibility of MIP sensor

Selectivity is a fundamental parameter for molecularly imprinted polymer technology as it evaluates its performance. In general, when eEDCs are present in water samples, they are a cocktail of different types of estrogens including estrone, estriol, 17 α -ethynylestradiol making it difficult to detect a specific eEDC in the sample. For the selectivity study, the 17 β -estradiol sensor was exposed to increasing concentrations of estriol, 17 α -ethynylestradiol and estrone. Where in the reaction vessel consisting of phosphate buffer pH 7 and a constant concentration of 0.05 nM while varying the concentrations of estriol, 17 α -ethynylestradiol and estrone creating the conditions in which the estrogenic endocrine disruptors coexist in nature. The chemical structures of these molecules are very similar to that of the imprinted molecule as shown in fig 5.7. The signal response was assessed in samples containing no estrogen i.e 17 β -estradiol, estriol, 17 α -ethynylestradiol and estrone as the control samples and also in the presence of the analyte 17 α -estradiol and interferences. As shown in fig 5.8 the prepared MIP displayed a small and thus ignorable signal response to the interferences (estriol, 17 α -ethynylestradiol and estrone) even at increased concentrations showing selectivity towards the analyte of interest 17 β estradiol.

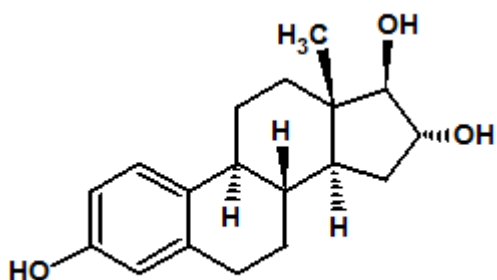




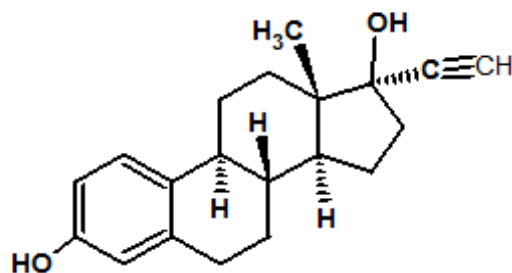
17β-Estradiol



Estrone



Estriol



17α-ethynylestradiol

Figure 5. 7: Chemical structures of the competing molecules.

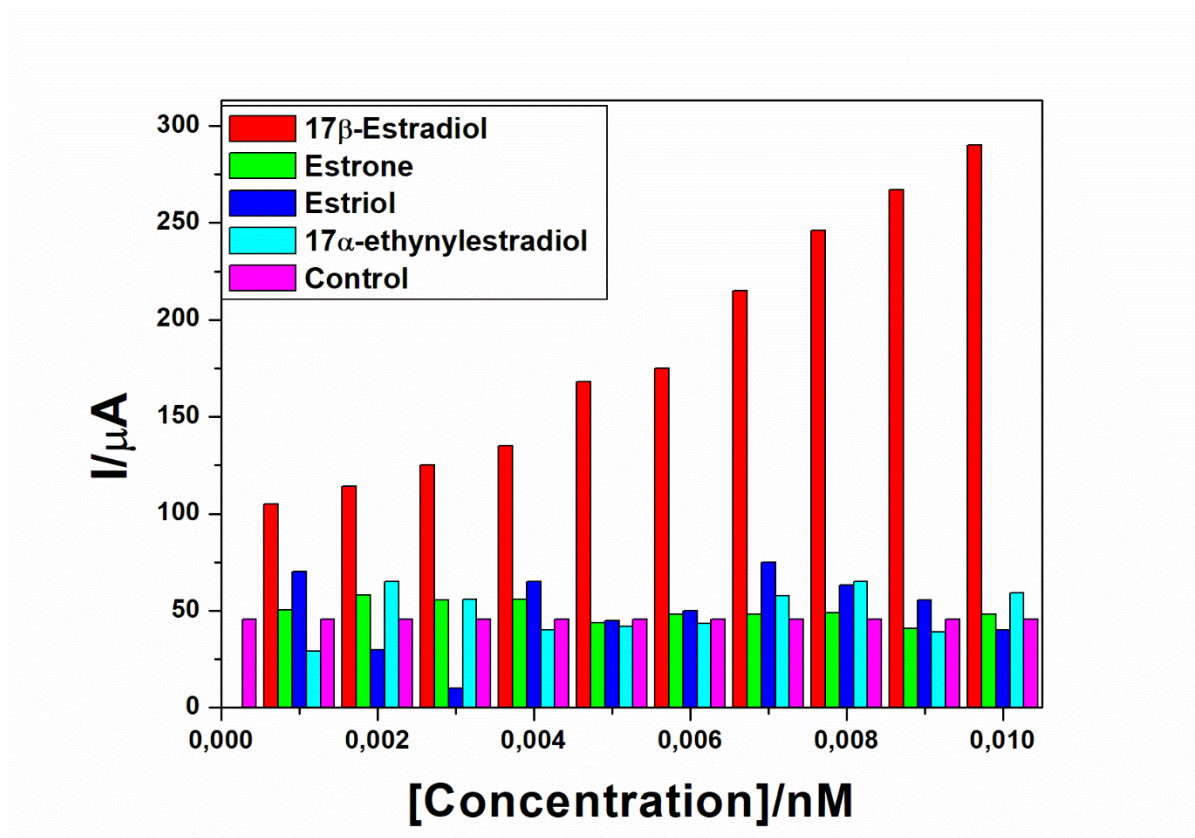


Figure 5. 8: Interference studies using MIP based on 17 β-estradiol (0-0.01 nM).

5.3 Conclusion

This study was aimed at the fabrication and characterization of sensors based on molecularly imprinted polymers (MIPs) for the detection of an estrogenic endocrine disrupting compound 17 β-estradiol. FTIR data was successfully used for assessing the presence of functional groups of the polymer matrix. According to morphological features determined by SEM the MIP exhibited cavities attributed to the removal of 17 β-estradiol used as the template molecule. It was observed that the molecularly imprinted polymer showed a higher retention and better selectivity towards 17 β-estradiol in comparison to NIP. We believe that the PMAA-co-PEDOT molecularly imprinted polymer prepared for the first time can be a useful candidate for future studies involving the detection and entrapment of 17β-estradiol using MIPs and electrochemical methods in water samples than other conventional methods shown in table 1

which shows that the lowest concentrations they can detect is lower than the lowest concentration the proposed method used in this study can detect. It is imperative to detect 17 β -estradiol at low concentrations since there are no guidelines set in place in terms of the minimal quantities that could be rendered harmful when individuals are exposed to them.

5.4 References

Afzal, M., Khan, Q.M. & Sessitsch, A., 2014. Endophytic bacteria: Prospects and applications for the phytoremediation of organic pollutants. *Chemosphere*, 117(1), pp.232–242.

Ben, W. et al., 2017. Transformation and fate of natural estrogens and their conjugates in wastewater treatment plants: Influence of operational parameters and removal pathways. *Water Research*, 124, pp.244–250.

Bronowicka-Kłys, D.E., Lianeri, M. & Jagodziński, P.P., 2016. The role and impact of estrogens and xenoestrogen on the development of cervical cancer. *Biomedicine and Pharmacotherapy*, 84, pp.1945–1953.

Corral, S.A. et al., 2017. Cognitive impairment in agricultural workers and nearby residents exposed to pesticides in the Coquimbo Region of Chile. *Neurotoxicology and Teratology*, 62(June), pp.13–19. Available at: <http://dx.doi.org/10.1016/j.ntt.2017.05.003>.

Dodson, R.E. et al., 2012. Endocrine disruptors and asthma-associated chemicals in consumer products. *Environmental Health Perspectives*, 120(7), pp.935–943.

El-Hefnawy, T., Hernandez, C. & Stabile, L.P., 2017. The endocrine disrupting alkylphenols and 4,4'-DDT interfere with estrogen conversion and clearance by mouse liver cytosol. *Reproductive Biology*, 17(3), pp.185–192.

Esther, M. et al., 2014. Microextraction Techniques Coupled to Liquid Chromatography with Mass Spectrometry for the Determination of Organic Micropollutants in Environmental Water Samples. , pp.10320–10349.

Figueiredo, L. et al., 2015. Talanta Applications of molecularly imprinted polymers to the analysis and removal of personal care products : A review. *Talanta*, pp.1–12.

Florea, A. et al., 2015. Electrochemical sensor for the detection of estradiol based on electropolymerized molecularly imprinted polythioaniline film with signal amplification using gold nanoparticles. *Electrochemistry Communications*, 59, pp.36–39.

Gadzała-kopciuch, R., 2016. Isolation and determination of estrogens in water samples by solid-phase extraction using molecularly imprinted polymers and HPLC in water samples by solid-phase extraction using molecularly imprinted polymers and HPLC. , (July 2013).

Garfí, M. et al., 2016. Life cycle assessment of drinking water: Comparing conventional water treatment, reverse osmosis and mineral water in glass and plastic bottles. *Journal of Cleaner Production*, 137, pp.997–1003.

Gutendorf, B. & Westendorf, J., 2001. Comparison of an array of in vitro assays for the assessment of the estrogenic potential of natural and synthetic estrogens, phytoestrogens and xenoestrogens. *Toxicology*, 166(1–2), pp.79–89.

Iwanowicz, L.R. & Blazer, V.S., 2009. An Overview Of Estrogen-Associated Endocrine Disruption In Fishes : Evidence Of Effects On Reproductive And Immune Physiology. , pp.266–275.

Janegitz, B.C. et al., 2014. Electrochemical determination of estradiol using a thin film containing reduced graphene oxide and dihexadecylphosphate. *Materials Science and Engineering C*, 37(1), pp.14–19.

Jo, M. et al., 2011. Development of Single-Stranded DNA Aptamers for Specific Bisphenol A Detection. *Oligonucleotides*, 21(2), pp.85–91.

Kim, T. et al., 2009. Preparation and characterization of poly(3,4-ethylenedioxythiophene) (PEDOT) using partially sulfonated poly(styrene-butadiene-styrene) triblock copolymer as a polyelectrolyte. *Current Applied Physics*, 9(1), pp.120–125.

Kim, Y.S. et al., 2007. Electrochemical detection of 17 β -estradiol using DNA aptamer immobilized gold electrode chip. *Biosensors and Bioelectronics*, 22(11), pp.2525–2531.

Koç, I. et al., 2011. Selective removal of 17 β -estradiol with molecularly imprinted particle-embedded cryogel systems. *Journal of Hazardous Materials*, 192(3), pp.1819–1826.

Kor, K. & Zarei, K., 2016. Talanta Development and characterization of an electrochemical sensor for furosemide detection based on electropolymerized molecularly imprinted polymer. *Talanta*, 146, pp.181–187.

Li, J. et al., 2016. Sensing Estrogen with Electrochemical Impedance Spectroscopy. *Journal of Analytical Methods in Chemistry*, 2016, pp.1–6.

Lizano-Fallas, V. et al., 2017. Removal of pesticides and ecotoxicological changes during the simultaneous treatment of triazines and chlorpyrifos in biomixtures. *Chemosphere*, 182, pp.106–113.

Migheli, M., 2017. Land ownership and use of pesticides. Evidence from the Mekong Delta. *Journal of Cleaner Production*, 145, pp.188–198.

Le Noir, M. et al., 2007. Selective removal of 17beta-estradiol at trace concentration using a molecularly imprinted polymer. *Water research*, 41(12), pp.2825–2831.

Ohno, S. et al., 2002. Effects of flavonoid phytochemicals on cortisol production and on activities of steroidogenic enzymes in human adrenocortical H295R cells. *Journal of Steroid Biochemistry and Molecular Biology*, 80(3), pp.355–363.

Oliva, J. et al., 2017. Disappearance of six pesticides in fresh and processed zucchini, bioavailability and health risk assessment. *Food Chemistry*, 229, pp.172–177.

Öpik, A., 2009. Molecularly imprinted polymers : A new approach to the preparation of Functional materials. , (October 2016).

Panagiotopoulou, M. et al., 2015. Initiator-free synthesis of molecularly imprinted polymers by polymerization of self-initiated monomers. , 66, pp.43–51.

Pinson, A. et al., 2017. Neuroendocrine disruption without direct endocrine mode of action: Polychloro-biphenyls (PCBs) and bisphenol A (BPA) as case studies. *Comptes Rendus - Biologies*.

Pinto, P.I.S. et al., 2014. Effects of estrogens and estrogenic disrupting compounds on fish mineralized tissues. *Marine Drugs*, 12(8), pp.4474–4494.

Rachkov, A. et al., 2000. Fluorescence detection of B -estradiol using a molecularly imprinted polymer. *Analytica Chimica Acta*, 405(January), pp.23–29.

Rao, K. et al., 2013. Determination of estrogens and estrogenic activities in water from three rivers in Tianjin, China. *Journal of Environmental Sciences (China)*, 25(6), pp.1164–1171.

Rgens, M.D.J. et al., 2002. the Potential for Estradiol and Ethinylestradiol Degradation in English Rivers. *Environmental Toxicology and Chemistry*, 21(3), pp.480–488.

Roszko, M., Szymczyk, K. & Renata, J., 2015. Talanta Simultaneous separation of chlorinated / brominated dioxins , poly- chlorinated biphenyls , polybrominated diphenyl ethers and their

methoxylated derivatives from hydroxylated analogues on molecularly imprinted polymers prior to gas / liquid chrom. , 144, pp.171–183.

Singh, K. & Chan, H.M., 2017. Persistent organic pollutants and diabetes among Inuit in the Canadian Arctic. *Environment International*, 101, pp.183–189.

Socas-Rodríguez, B. et al., 2017. Multiresidue determination of estrogens in different dairy products by ultra-high-performance liquid chromatography triple quadrupole mass spectrometry. *Journal of Chromatography A*, 1496(November 2016), pp.58–67.

Tahboub, Y.R., Zaater, M.F. & Khater, D.F., 2017. Semi-volatile organic pollutants in Jordanian surface water. *Arabian Journal of Chemistry*, 10, pp.S3318–S3323.

Terui, N., Fugetsu, B. & Tanaka, S., 2006. Voltammetric behavior and determination of 17 beta-estradiol at multi-wall carbon nanotube-Nafion modified glassy carbon electrode. *Analytical sciences : the international journal of the Japan Society for Analytical Chemistry*, 22(6), pp.895–8.

Tun, P., 2004. Electrochemical sensors based on molecularly imprinted polymers. , 23(1).

Uygun, Z.O., Deniz, H. & Uygun, E., *Molecularly Imprinted Sensors — New Sensing Technologies*.

Wang, J. et al., 2014. Assessment of estrogen disrupting potency in animal foodstuffs of China by combined biological and chemical analyses. *Journal of environmental sciences (China)*, 26(10), pp.2131–2137.

Wong, K.H. & Durrani, T.S., 2017. Exposures to Endocrine Disrupting Chemicals in Consumer Products—A Guide for Pediatricians. *Current Problems in Pediatric and Adolescent Health Care*, 47(5), pp.107–118.

Yildirim, N. et al., 2012. Aptamer-based optical biosensor for rapid and sensitive detection of 17β -estradiol in water samples. *TL - 46. Environmental science & technology*, 46 VN-r(6), pp.3288–3294.



CHAPTER SIX

Electrochemical molecularly imprinted polymer sensor using a 96-well screen-printed microplate for 17 α -estradiol detection.



UNIVERSITY *of the*
WESTERN CAPE

Summary

This chapter describes the preparation of gold nanoparticles and their use in the preparation of a gold-polymer nanocomposite. The use of the composite in the modification of working electrodes for enhancing the properties of a sensor based on the molecularly imprinted polymer technology for the detection of estrone an estrogen. This chapter also presents the novel determination of estrogens by using a multichannel 96-well carbon screen printed microplate.



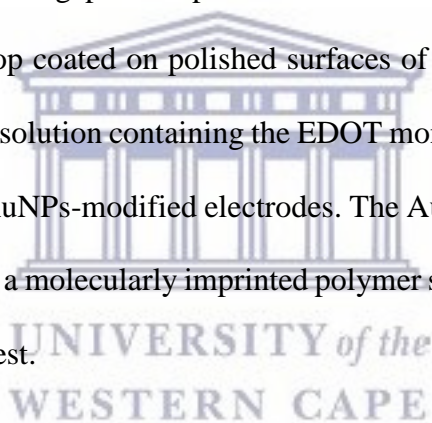
UNIVERSITY of the
WESTERN CAPE

Abstract

A novel analytical molecularly imprinted sensor based on a multichannel electrochemical detection (MED) system using cyclic voltammetry technique for the detection of 17α -estradiol is proposed. The electrochemical behaviour and electroanalytical performance of the 12 carbon sensors (designed as screen printed electrodes) incorporated in the multichannel electrochemical plate were first evaluated. Then the 96-well screen-printed microplate was modified using a copolymer poly(methacrylic-co-3,4-ethylenedioxythiophene) based molecularly imprinted polymer sensor imprinted with 17α -estradiol. The detection of the analyte using CV showed a decrease in current response with an increase in concentration of target analyte. From this phenomenon a calibration curve was constructed and the linear range extrapolated. From the variations in concentration and respective current responses a calibration curve was constructed and linear range was deduced with a DLR of 0.01 nM – 0.14

nM. The LOD of the sensor was determined to be 0.056 nM thus showing that the sensor can be able to detect concentrations of 17 α -estradiol even at as low concentrations as 0.056 nM of analyte and sensitivity of 0.54 μ A/nM.

This study also presents the modification of glassy carbon electrodes with AuNPs and AuNPs/PEDOT nanocomposite. AuNPs were prepared by reduction with sodium borohydride and the produced nanoparticles were characterised using HRSEM and HRTEM which determined that the nanoparticles shapes ranged from spherical to nanoparticles ranging between spherical and pseudo-triangular particles with particle sizes ranging between 51.37-56.48 nm. UV-Vis was used to determine the energy band gap of the nanoparticles. Using the $E = h \times C/\lambda_{\text{onset}}$ equation, the band gap of the particles was 1.98 eV typical of semiconducting material. The AuNPs were drop coated on polished surfaces of GC electrodes, thereafter the electrodes were immersed in a solution containing the EDOT monomer for the electrochemical deposition of PEDOT on the AuNPs-modified electrodes. The AuNPs/PEDOT nanocomposite was used for the preparation of a molecularly imprinted polymer sensor imprinted with estrone, which was the analyte of interest.



6.0 Introduction

Over the years research scientists have investigated and developed synthetic and tailor-made receptors capable of selectively recognizing and binding specific target molecules with high affinity (Rachkov *et al.* 2000; Yuan *et al.* 2015). These receptors have more stability and are easier to fabricate at low costs (Fuchs *et al.* 2012; Shoravi *et al.* 2010; Y. Li *et al.* 2017). One-way of preparing these synthetic receptors is the preparation of molecularly imprinted polymers. Molecularly imprinted polymer sensors are developed in order to try to overcome the challenges that are faced in biosensors which make use of biological elements such as

enzymes and antibodies (Tokonami *et al.* 2009). Although these biological receptors are perfectly fitting with their natural targets, they have a tendency of being unstable when they are not in their natural environment, they are not easy to obtain for a given target and may be difficult to fine-tune for a specific application. Molecularly imprinted polymers commonly referred to as MIPs imitate the receptor-ligand (Zhou *et al.* 2015), antibody-antigen or enzyme-substrate biorecognition (Sassolas 2012) making them applicable in technologies relying on selective molecular binding (Sharma *et al.* 2012). The concept of MIPs was first proposed in the year 1931 by Polyakov (Jenkins *et al.* 2001). The technique requires functional monomers, template molecules and cross-linkers. The procedure for the preparation of MIPs involves three steps (Vasapollo *et al.* 2011; Shoravi *et al.* 2010; Y. Li *et al.* 2017; Haginaka & Kagawa 2002). In the first step, a template molecule (i.e. an imprinting compound) creates a prepolymerization complex with selected functional monomer (s). Then, the prepolymerization complex is cross-linked during the polymerization process. In the final stage, the template is removed from the polymeric matrix, ideally leaving well-defined three-dimensional cavities or binding sites behind. In this procedure, the commonly used template is a small molecule such as pharmaceuticals and chemicals (Zahedi *et al.* 2016).

6.1 Methodology

6.1.1 Chemicals

3,4-ethylenedioxythiophene (EDOT) ($\geq 97\%$) estrone ($\geq 98\%$), potassium hexacyanoferrate (III) ($\text{K}_3[\text{Fe}(\text{CN})_6]$) (ACS reagent, $\geq 99.0\%$), potassium hexacyanoferrate(II) trihydrate ($\text{K}_4[\text{Fe}(\text{CN})_6]$) (ACS reagent 98.5-102.0%), acetic acid (CH_3COOH), methanol (CH_3OH) and acetonitrile ($\text{C}_2\text{H}_3\text{N}$) were purchased from Sigma-Aldrich. Tetrachloroauric acid trihydrate and sodium boron hydride. Disodium hydrogen phosphate (Na_2HPO_4) ($\geq 99.5\%$), sodium dihydrogen phosphate (NaH_2PO_4) ($\geq 99\%$) from Sigma-Aldrich were used for the preparation

of 0.1 M phosphate buffer pH 7. Alumina micro polishing pads were obtained from Buehler LL, USA. Deionized ultra-purified water used throughout these experiments was prepared with a Milli-Q water purification system.

6.1.2 Instrumentation and procedure

A three electrode configuration was used for all electrochemical experiments. A glassy carbon electrode with a diameter of 3 mm from Bio Analytical Systems (BAS) was used as the working electrode. A saturated calomel electrode (SCE) as the reference electrode from BAS, and a platinum wire as the counter electrode. All measurements were carried out at room temperature. Electrochemical measurements were performed on a computer-controlled potentiostat/galvanostat (CH instruments electrochemical workstation) coupled with Model 270/250 Research Electrochemistry Software 4.30 and on multichannel robotic system from . Alumina micro polishing pads were obtained from BAS and used to polish the surface of the glassy carbon working electrode before modification. HRSEM images were taken with a Hitachi S3000N scanning electron microscope at an acceleration voltage of 20 kV at various magnifications. All FTIR spectra were recorded on Spectrum 100 FTIR spectrometer (PerkinElmer, USA) at a region of 400-4000 cm^{-1} .

6.1.3 Cleaning of electrodes

Prior to the electrodes being used, they were polished on 1 μm and 0.05 μm alumina slurries and sonicated in mili Q water for 10 min to remove any adsorbed material on the surface of the electrode. A very mild version of a piranha clean was prepared from 50 mM H_2SO_4 and 25% hydrogen peroxide. Gold samples spent 10 min in this treatment before being rinsed with Milli-Q. Lastly the electrodes were cleaned by cycling the electrode potential in a weak sulfuric acid

solution 0.5 M until a stable CV scan was achieved. Sample potential was cycled from -400 to 1400 mV (vs. Ag/AgCl) at a rate of 100 mV.

6.1.4 Synthesis of gold nanoparticles

AuNPs were firstly synthesized according to the procedure described in the literature (Florea, Cristea, Vocanson, Săndulescu, et al. 2015). For a typical preparation of gold nanoparticles, 0.316 mg of tetrachloroauric (III) acid trihydrate was dissolved in 300 μ L of methanol in a 10 mL round bottom flask and stirred. After 10 min, 0.30 mg of NaBH₄ dissolved in 200 μ L of water was added dropwise to the mixture under vigorous stirring. After 10 min, a red solution was obtaining after which stirring was stopped and the solution was kept in darkness in the refrigerator at 4° C for 1 h.

6.1.5 Electrochemical polymerization of PEDOT

Polished glassy carbon working electrodes were immersed in 50 mM solution containing monomer 3,4-ethylenedioxythiophene for 12 h at 4° C. After the self-assemble of EDOT, electropolymerization of EDOT was performed in a solution containing EDOT monomer in supporting electrolyte comprising of 10 mM 10mM [Fe(CN)₆]^{-3/-4} in phosphate buffer pH 6 containing acetone (4:1 v/v) by cycling between -0.4 V and 1 V for 6 cycles at a scan rate of 0.1 V/s.

6.1.6 Preparation of PEDOT/Au MIP

Onto polished glassy carbon working electrodes 30 μ L AuNP solution was drop coated and dried at 4° C for 12 h. The Au modified electrodes were immersed in a solution containing EDOT monomer and estrone in supporting electrolyte comprising of 10 mM 10mM [Fe(CN)₆]^{-3/-4} in phosphate buffer pH 6 containing acetone (4:1 v/v) by cycling between -2 V

and 2 V for 6 cycles at a scan rate of 0.1 V/s. To confirm the imprinting process, a control experiment, non-imprinted polymer modified electrode (NIP), was prepared under the same experimental conditions but without the addition of 17 α -estradiol (Jiang et al. 2009)k. The modified electrodes were then washed with a solution of acetone:PBS pH=7 (1:1) for 30 min to remove the template molecules embedded in the film and to form the selective recognition cavities.

6.3.1 Preparation of molecularly imprinted polymers by electropolymerization

The estrone imprinted polymer was obtained by electrodeposition on gold electrodes using CV for 9 cycles in a solution containing EDOT monomer and estrone on a glassy carbon electrode modified with AuNPs in the supporting electrolyte of 10mM [Fe(CN) $_6$] $^{-3/-4}$ in phosphate buffer pH=6 containing acetone. The use of acetone, an organic solvent, was to make certain that estrone was dissolved since it is soluble in it and to decrease the surface tension and limit hydrophobic interactions, since MIPs are usually hydrophobic. During electropolymerization the molecules of estrone are trapped in the polymer matrix through non-covalent interactions between H-groups of the polymer and O atoms in the structure of estrone. The formation of the polymeric film is investigated through its permeability, using [Fe(CN) $_6$] $^{-3/-4}$ redox probe. The peak current for the oxidation/reduction of the redox probe decreases with each cycle, due to the continuous formation of a polymer film that hinders the electron transfer to the surface of the electrode. The presence of AuNPs in the polymeric film enhances the number of accessible complementary cavities, the catalytic activity of the surface and the fast equilibration with the analyte. Fig 6.4 shows the (A) CV and (B)EIS of the detection of estrone using [Fe(CN) $_6$] $^{-3/-4}$ redox probe in PBS pH 7. There was a decrease in both the semi-circle of the Nyquist plot and in the oxidation peaks of [Fe(CN) $_6$] $^{-3/-4}$ this was attributed to the filling of the cavities by

estrone as the concentration was increased. The occupation of the cavities by estrone results in the reduction of the exposure of the electrode surface thus decreasing electron-transfer between the surface and electrolytes.

6.3 Results and discussion

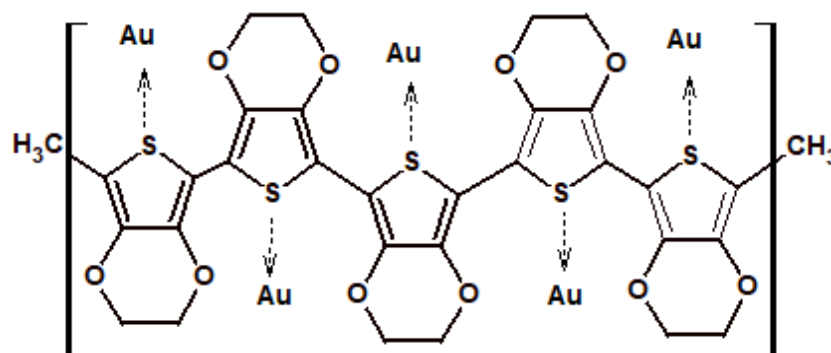
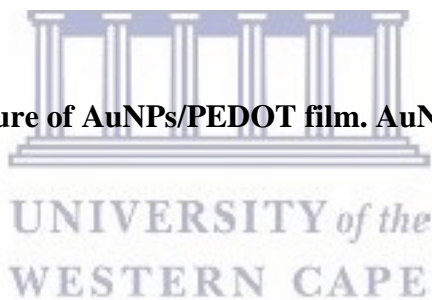


Figure 6.1: Structure of AuNPs/PEDOT film. AuNPs/PEDOT/GCE



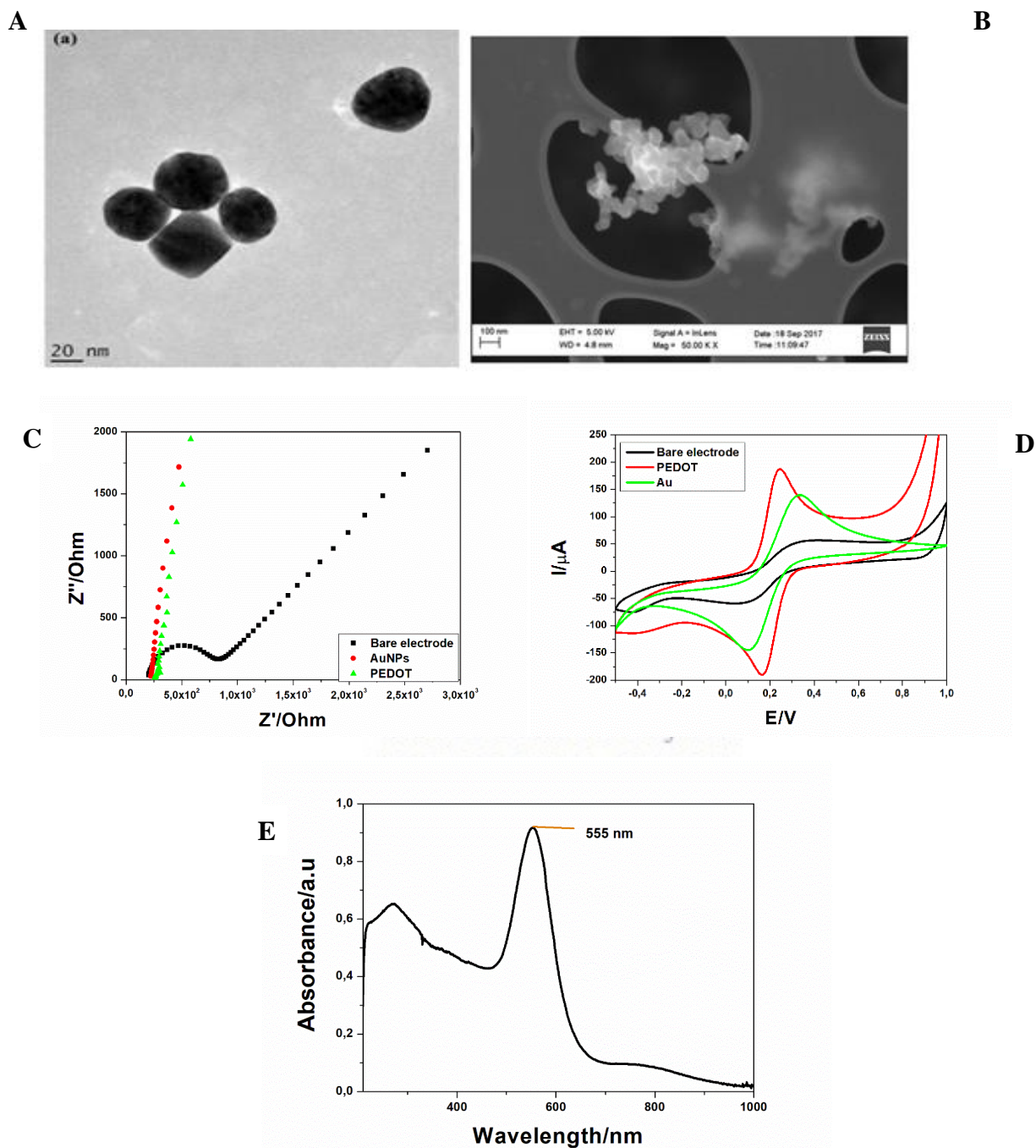


Figure 6.2: (A) TEM of AuNPs and (B) SEM of AuNPs, (C) EIS of bare electrode (Black), AuNPs (red) and PEDOT (green) and (D) bare electrode (Black), AuNPs (red) and PEDOT (green) using $[\text{Fe}(\text{CN})_6]^{3-/4-}$ redox probe in PBS.

As in the study by (T. H. Tsai *et al.* 2011), the gold nanoparticles were incorporated within the polymer backbone through possible gold-sulfur (thiophene) interactions (as shown in fig 6.1). The morphologies of AuNPs samples were investigated by HRSEM and HRTEM. The typical SEM and TEM images in fig 6.2 (A) and (B) revealed the shapes of the nanoparticles ranging from spherical and pseudo-triangular particles with particle sizes ranging between 51.37-56.48 nm (Malarkodi *et al.* 2017). The spherical shaped nanoparticles are formed at the beginning of the reaction and after that, the spherical shaped nanoparticles are aggregated with each other and form triangle and undefined prism-like structure (T. Tsai *et al.* 2011). Furthermore, the optical absorption spectrum of AuNPs is shown in fig 6.2 (E). As shown, the intrinsic band at about 528.5 nm corresponds to other reported literature (Duan *et al.* 2013) which further indicates the successful fabrication of dispersed AuNPs. The narrow band demonstrates the excellent dispersed state of gold nanoparticles. From the absorbance spectrum, the $E = h \times C/\lambda_{\text{onset}}$ equation was used to determine the band gap of the particles and it was found that the energy band gap was 1.98 eV.

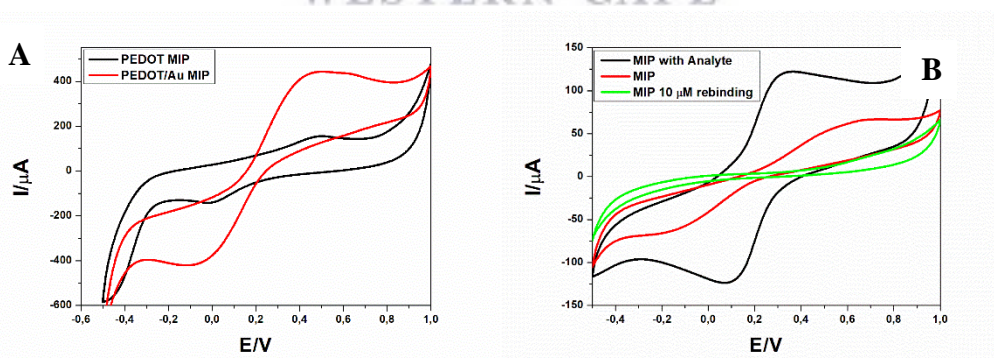
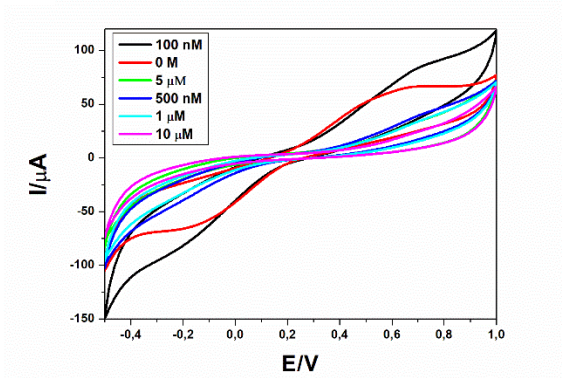


Figure 6.3: CV of (A) MIP fabricated with PEDOT polymer on the surface of the electrode and MIP fabricated using the AuNPs/PEDOT composite and (B) Cyclic voltammograms of Nanocomposite with analyte (Black voltammogram), MIP after removal of analyte (Red voltammogram), and MIP after rebinding of analyte (estrone) using $[\text{Fe}(\text{CN})_6]^{-3/-4}$ redox probe in PBS pH 7.

Fig 6.3 (A) shows the CV of a MIP prepared with PEDOT (black voltammogram) and with PEDOT modified with AuNPs (red voltammogram) and (B) shows the CV PEDOT-E2 (black voltammogram) representing the copolymer with estrone incorporated into it, MIP (red voltammogram) copolymer after removal of estrone and MIP after detection of estrone (green voltammogram) at a concentration of 10 μM at a potential of 0.4-1 V. The voltammogram shown in fig 6.3 (A) shows that the incorporation of AuNPs in the preparation of the MIP was important as it enhanced the current response compared to when PEDOT was used. This can be attributed to the fact that both the polymer and the AuNPs are conductive material, thus their properties were enhanced and they became more conductive once combined. The behaviour of the modified electrodes fig 6.3 (B) was studied using CV for the detection of estrone analyte and using $[\text{Fe}(\text{CN})_6]^{-3/-4}$ as the redox probe. It was used as the technique of interest as opposed to other electrochemical techniques due to the fact that it has the ability to clearly show the peaks of interest (Carvalho *et al.* 2015). There is an observed decrease in the current response produced when the MIP electrode was immersed into a cell containing 10 μM of estrone. This indicates that estrone was able to rebind to the copolymer onto the cavities produced after the analyte molecule was removed from the polymer matrix (Rezaei *et al.* 2014). Thus showing that the MIP sensor was suitable for the detection of estrone as the analyte of interest. Fig 6.4 (A) and (B) show the CV and EIS obtained for the detection of various concentrations of estrone using $[\text{Fe}(\text{CN})_6]^{-3/-4}$ as the redox probe in PBS pH 7. From the results obtained, given by the decrease in analytical signal in CV and a decrease in the semi-circle on the EIS with an increase in concentration of estrone was indicative of estrone molecules occupying the cavities left by the imprinting of estrone onto the polymer matrix.

A



B

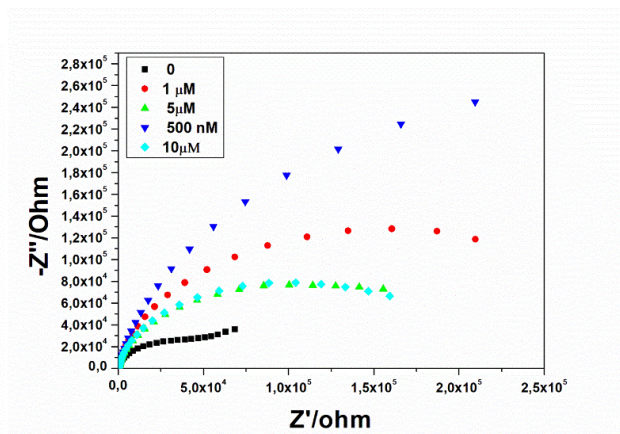


Figure 6.4: (A) CV and (B) EIS AuNPs/PEDOT MIP for the detection of estrone using $[\text{Fe}(\text{CN})_6]^{-3/-4}$ as the redox probe in PBS pH 7.

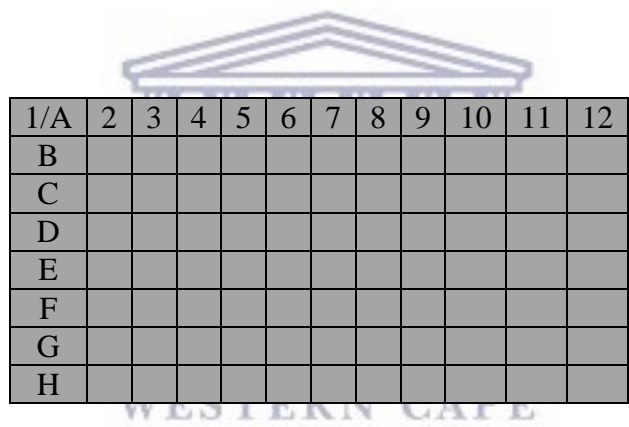


Figure 6.5: Representation of the multichannel 96-well system.

6.3.2 Measurement of 17α -estradiol using multichannel electrochemical system.

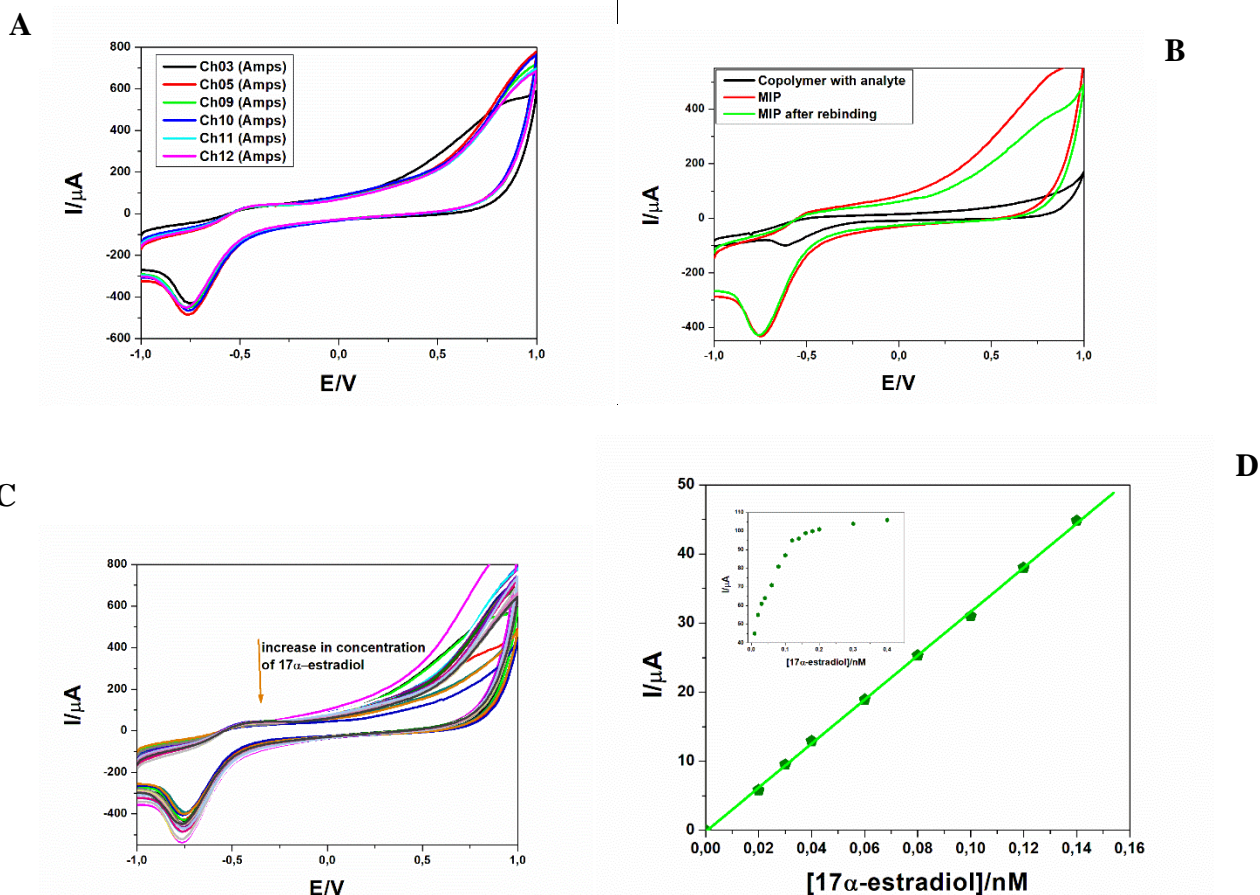


Figure 6.6: (A) CV of comparison between 6 electrodes of the 12 electrodes of the screen printed carbon microplate, (B) CV of PMAA-co-PEDOT-E2 (black line), MIP (red line) and MIP after detection of E2 at a concentration of 0.2 nM, (C) detection of 17α -estradiol in PBS and (D) linear range of the calibration curve inset.

The wells similar to that represented in fig 6.5 were filled with different concentration of 17α -estradiol in phosphate buffer (Matsue *et al.* 1990). A carbon screen printed electrode consisting of 12 individual electrodes was used to measure the response of each of the 12 electrodes to determine their behaviour (Pires *et al.* 2012). Only 6 of the 12 electrodes showed similar responses as shown in fig 6.6 (A). The 12 electrodes were then modified with P(MAA-co-EDOT) MIP. The modified electrodes were each immersed in the 12 wells as shown in fig 6.5 which shows columns marked with numbers 1 to 12 which accommodate the 12 electrodes used

for the electrochemical studies, while the rows marked with letters from A to H represents the electrochemical cells filled with various concentrations of the analyte. The analytical signal was measured using CV. After the measurement before moving to the next row of 12 wells the electrodes were washed with distilled water and the electrode proceeded to the consecutive wells consisting of another concentration of the analyte. This continued until all 96 wells were measured. As the concentration of the analyte increased on the surface of the electrodes and the cavities of the MIP were filling with the analyte there was difficulty in transferring electrons thus resulting in decrease in the current produced fig 6.6 (C). From the variations in concentration and respective current responses a calibration curve was constructed and linear range was deduced as shown in fig 6.6 (D) with a DLR of 0.01 nM – 0.14 nM. The LOD of the sensor was determined to be 0.056 nM thus showing that the sensor can be able to detect concentrations of 17 α -estradiol even at as low concentrations as 0.056 nM of analyte and sensitivity of 0.54 μ A/nM.

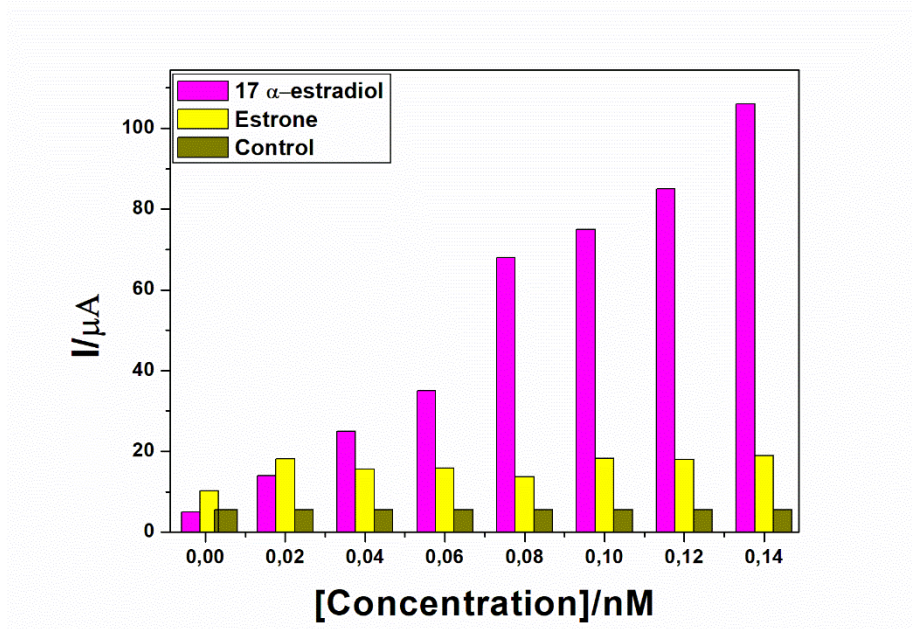
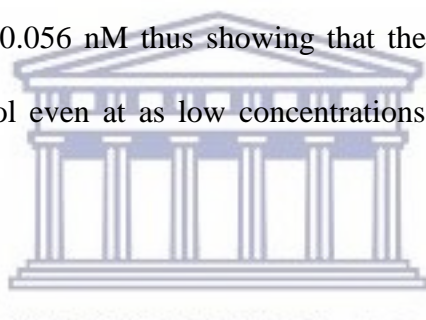


Figure 6.7: Interference studies using MIP based on 17 α -estradiol (0-0.14 nM)

6.3.3 Selectivity of MIP sensor

Selectivity is a fundamental parameter for molecularly imprinted polymer technology as it evaluates of the sensors. In general when eEDCs are present in water samples, they are a cocktail of different types of estrogens including Estrone, Estriol, 17 α -ethynylestradiol making it difficult to detect a specific eEDC in the sample. The selectivity of the 17 α -estradiol sensor was exposed to increased concentrations of estrone. The signal response was assessed in samples containing no estrogen i.e 17 β -estradiol, estriol, 17 α -ethynylestradiol and estrone as the control samples and also in the presence of the analyte 17 α -estradiol and interferences. As shown in fig 6.7 the prepared MIP displayed a small at and thus ignorable signal response to the interferences (estrone) even at increased concentrations showing selectivity towards the analyte of interest 17 α estradiol.



6.4 Conclusion

The aim of this study was to synthesis AuNPs, use the AuNPs for the preparation of an AuNPs/PEDOT on glassy carbon electrodes. MIPs were prepared electrochemically using the nanocomposites and estrone as the imprint molecule. The optical properties of AuNPs showed that the NPs are conductive. Making them compatible in the fabrication of sensors. The novel use of a multichannel as a detection method for 17 α -estradiol in conjunction with molecularly imprinted polymer brings about advantages that other techniques don't have including ease of fabrication, ease of detection with repeatability achieved since there are 12 individual channels used in the detection which means 12 sensors produced at the same time and measured at the same time. The MIP sensor for the detection of 17 α -estradiol was characterized by a good DLR, a low detection limit and good sensitivity. The interference studies show the selectivity

of the sensor towards the analyte of interest when other molecules of similar structure, shape and size are present in the matrix.

6.5 References

Carvalho, A.R.M. et al., 2015. Occurrence and analysis of endocrine-disrupting compounds in a water supply system. *Environmental Monitoring and Assessment*, 187(3).

Duan, J. et al., 2013. Glassy carbon electrode modified with gold nanoparticles for ractopamine and metaproterenol sensing. *Chemical Physics Letters*, 574, pp.83–88.

Florea, A. et al., 2015. Electrochemical sensor for the detection of estradiol based on electropolymerized molecularly imprinted polythioaniline film with signal amplification using gold nanoparticles. *Electrochemistry Communications*, 59, pp.36–39.

Fuchs, Y., Soppera, O. & Haupt, K., 2012. Photopolymerization and photostructuring of molecularly imprinted polymers for sensor applications-A review. *Analytica Chimica Acta*, 717, pp.7–20.

Haginaka, J. & Kagawa, C., 2002. Uniformly sized molecularly imprinted polymer for Evaluation of retention and molecular recognition properties in an aqueous mobile phase. *Journal of Chromatography A*, 948, pp.77–84.

Jenkins, A.L., Yin, R. & Jensen, J.L., 2001. Molecularly imprinted polymer sensors for pesticide and insecticide detection in water. *Analyst*, 126(6), pp.798–802.

Jiang, T. et al., 2009. Molecularly imprinted solid-phase extraction for the selective determination of 17 β -estradiol in fishery samples with high performance liquid chromatography. *Talanta*, 78(2), pp.442–447.

Li, Y. et al., 2017. Tyramine detection using PEDOT:PSS/AuNPs/1-methyl-4-mercaptopyridine modified screen-printed carbon electrode with molecularly imprinted polymer solid phase extraction. *Biosensors and Bioelectronics*, 87, pp.142–149.

Malarkodi, C., Rajeshkumar, S. & Annadurai, G., 2017. Detection of environmentally hazardous pesticide in fruit and vegetable samples using gold nanoparticles. *Food Control*, 80, pp.11–18. Available at: <http://dx.doi.org/10.1016/j.foodcont.2017.04.023>.

Matsue, T. et al., 1990. Multichannel electrochemical detection system for flow analysis. *Analytical Chemistry*, 62(4), pp.407–409.

Pires, L. et al., 2012. Multichannel Impedimetric Biosensor Platform for Label-Free Affinity Assays Using Electrically Conductive Functional Polymers. *16th International Conference on Miniaturized Systems for Chemistry and Life Sciences*, pp.1348–1350.

Rachkov, A. et al., 2000. Fluorescence detection of B -estradiol using a molecularly imprinted polymer. *Analytica Chimica Acta*, 405(January), pp.23–29.

Rezaei, B., Khalili Boroujeni, M. & Ensafi, A.A., 2014. Caffeine electrochemical sensor using imprinted film as recognition element based on polypyrrole, sol-gel, and gold nanoparticles hybrid nanocomposite modified pencil graphite electrode. *Biosensors and Bioelectronics*, 60, pp.77–83.

Sassolas, A., 2012. Biosensors for Pesticide Detection: New Trends. *American Journal of Analytical Chemistry*, 3(3), pp.210–232.

Sharma, P.S. et al., 2012. Electrochemically synthesized polymers in molecular imprinting for chemical sensing. *Analytical and Bioanalytical Chemistry*, 402(10), pp.3177–3204.

Shoravi, S. et al., 2010. On the influence of crosslinker on template complexation in molecularly imprinted polymers: A computational study of prepolymerization mixture events

with correlations to template-polymer recognition behavior and nmr spectroscopic studies. *International Journal of Molecular Sciences*, 15(6), pp.10622–10634.

Tokonami, S., Shiigi, H. & Nagaoka, T., 2009. *Analytica Chimica Acta Review* : Micro- and nanosized molecularly imprinted polymers for high-throughput analytical applications. , 641, pp.7–13.

Tsai, T., Lin, K. & Chen, S., 2011. Electrochemical Synthesis of Poly (3 , 4-ethylenedioxythiophene) and Gold Nanocomposite and Its Application for Hypochlorite Sensor. , 6, pp.2672–2687.

Tsai, T.H., Lin, K.C. & Chen, S.M., 2011. Electrochemical synthesis of poly(3,4-ethylenedioxythiophene) and gold nanocomposite and its application for hypochlorite sensor. *International Journal of Electrochemical Science*, 6(7), pp.2672–2687.

Vasapollo, G. et al., 2011. Molecularly imprinted polymers: Present and future prospective. *International Journal of Molecular Sciences*, 12(9), pp.5908–5945.

Yuan, Y. et al., 2015. Ionic liquid-molecularly imprinted polymers for pipette tip solid-phase extraction of (Z) -3- (chloromethylene) - 6-flourothiochroman-4-one in urine. *Journal of Chromatography A*, 1408, pp.49–55.

Zahedi, P. et al., 2016. Biomacromolecule template-based molecularly imprinted polymers with an emphasis on their synthesis strategies : a review. , 2016(November 2015).

Zhou, Y. et al., 2015. Talanta Rapid and selective extraction of multiple macrolide antibiotics in foodstuff samples based on magnetic molecularly imprinted polymers. *Talanta*, 137, pp.1–10.



UNIVERSITY *of the*
WESTERN CAPE

CHAPTER SEVEN

Conclusion and recommendations



Summary

This chapter gives an overview of the main objectives and the achievements of the study. It also outlines the future investigations required for (i) the optimization of the performance of the MIP sensor and (ii) the application of the sensor in determination of endocrine disruptors in real samples (waste water)

7.1 Conclusions

This study reported the successful synthesis of a conductive molecularly imprinted polymer-polyrrole sensor prepared electrochemically for the determination of dimethoate organophosphorus pesticide. Electrochemical studies show that the prepared MIP was compatible for the detection of dimethoate. The electrochemical signal obtained from the sensor in the detection of the analyte showed a decrease, signifying that the analyte was

rebound on the cavities of the MIP. These cavities are formed by electropolymerization of pyrrole monomer in the presence of dimethoate. The analyte was then washed off and removed from the polymer matrix thus leaving cavities that are complimentary to the analyte in both size and shape. The MIP sensor based on polypyrrole for the selective detection of dimethoate had a dynamic linear range (DLR) of 0.01 nM – 0.14 nM. The limit of detection (LOD) of the sensor was found to be 0.035 nM, thus showing that the sensor can detect concentrations of acetylthiocholine chloride (ATCl) even at low concentration as 0.035 nM dimethoate that may be present and showed good sensitivity of 0.32 $\mu\text{A/nM}$. This study also presents the successful preparation of a composite formed between AuNPs and PEDOT and a copolymer P(MAA-co-PEDOT), the copolymer was synthesized by chemical polymerization using ammonium persulfate as the oxidising agent. The monomers used in the study were selected on the basis of their properties and their structures. Poly methacrylic acid was selected since it possess the functional groups that makes it possible to covalently bond with the analytes of interest, 17β -estradiol, 17α -estradiol, estrone, 17β -ethynylestradiol and estriol. Poly(3,4-ethylenedioxythiophene) was important in the enhancement of the conductivity of the copolymer (non-imprinted polymer). The success of the synthesis of the copolymer was determined using various techniques; HRSEM was used for the determination of the surface morphology in combination with EDS which showed all the functional groups through composition determination of the material (C, O, H and S) present in the individual polymers and in the copolymers formed. Optical properties were investigated by UV-Vis, the wavelengths obtained were used for the determination of the energy band gaps which were found to be 4.96 eV, 4.32 eV and 4.92 eV for PMAA, PEDOT and P(MAA-co-EDOT) respectively. The copolymer was then used in the preparation of a molecularly imprinted polymer (MIP) sensor used for the determination of estrogenic endocrine disrupting compounds. The prepared MIP was prepared by polymerization of functional monomers in the

presence of the analyte of interest. FTIR was used to determine the structural properties of all materials. There was presence of a broad band at 3483 cm^{-1} attributed to the C-OH stretch of the estradiol molecule, a decrease and shift in C-O-H stretch from 3483 cm^{-1} to 3268 cm^{-1} is observed in, this phenomenon can be attributed to the effect of the removal of the analyte molecule (E2) from the P(MAA-co-PEDOT) copolymer resulting in formation of cavities with structures that are similar in shape and size of the imprinted molecule. The MIP showed good results in detection of analytes and excellent selectivity of the analytes which was deduced by performance of interference studies. The MIP sensor based on P(MAA-co-EDOT) had a limit of detection (LOD) of 0.006 nM , a dynamic linear range (DLR) of $0.001\text{-}0.01\text{ nM}$ and sensitivity of $1,25\times 10^{-7}\text{ }\mu\text{A/nM}$ with a good selectivity for $17\text{ }\beta$ -estradiol detection, it also demonstrated good selectivity towards the target analyte even in the presence of molecules of similar characteristics and structural fetures. Based on a study done by the world health organization (WHO) there are about 800 chemicals suspected and known to be capable of being endocrine disruptors, however as much as there are a number of such chemicals known only a small fraction of them have been investigated and tested to determine the overt endocrine effects on organisms. Thus it is important to fabricate a sensor with a low LOD and a wide DLR such as the one in this study. So that even at lowest concentrations estrogens can be detected in samples.

7.2 Recommendations and future work

Preparation of composites based on conducting polymers such as gold nanoparticles/poly(3,4-ethylenedioxythiophene(AuNPs/PEDOT) takes advantage of the properties of the metal and

the remarkable properties of conducting polymers such as excellent conductivity, making them interesting material for the application in molecularly imprinted polymers. Electrochemical polymerization of polymers offers ease of fabrication, less preparation times and low costs. The prepared molecularly imprinted polymer sensor for the detection of estrone will be applied in real samples, where water samples from waste water treatment plants especially those who get water from industrial waste as those are most likely to receive water that consists of estrogenic endocrine disruptors. In these samples the MIP will be used to selectively detect the presence of estrone as it will be tailor-made specifically for estrone. This sensor will also have to be applied in detecting interferences since these estrogenic endocrine disruptors usually coexists in samples. Thus it would be paramount to determine if the sensor will be sensitive only to the molecule used in the fabrication of the sensor even in the presence of molecules that are of similar structure to it. Essentially it is of importance to apply all the sensors prepared in this study (P(MAA-co-EDOT)) sensor for the detection of 17β -estradiol and 17α -estradiol in real samples. They will also be used in the detection of pesticides that are used in South Africa in the production of maize, a crop that is produced in abundance in the country. The presence of large quantities of pesticides in Maize samples poses a great risk to those who work in harvesting as they have to handle the crops. It is therefore important to fabricate a device that will be able to detect selectively the pesticides that are used during crop production and detect them even at low concentrations. As the main purpose of the fabrication of each of the sensor is so that they can be used in detection of target analytes in real samples. Thus it is important to determine the behaviour of the sensors in the samples they will be potentially applied on. The use of multichannel robotic electrochemical system as the detection method makes the detection of these analytes in samples less complex and less time consuming. As it gives the opportunity to fabricate 12 sensors and use the 12 sensors to detect samples in 96 wells, each well consisting of samples that are 300 μ L, thus generating less waste while it gives

you reproducibility of 12 sensors. The results obtained from the sensors that are detected using the multichannel robotic electrochemical system will then be compared to other conventional techniques to determine the advantages of using the MIP sensors in conjunction with the multichannel as the detection technique as opposed to techniques such as the enzyme-linked immunosorbent assay (*ELISA*).

